

SIMPLIFICATION OF 3D COOLED TURBINE BLADE MODELS FOR EFFICIENT DYNAMIC ANALYSES

AROKIA LOURDU MARSHALL, AROKIA



**KTH Industrial Engineering
and Management**

Master of Science Thesis
Stockholm, Sweden 2013

Turbomachinery Aeromechanics University Training
THRUST

SIMPLIFICATION OF 3D COOLED TURBINE BLADE MODELS FOR EFFICIENT DYNAMIC ANALYSES

AROKIA LOURDU MARSHALL, AROKIA

MSc Thesis 2013

Department of Energy Technology
Division of Heat and Power Technology
Royal Institute of Technology
100 44 Stockholm, Sweden



**KTH Industrial Engineering
and Management**

**Master of Science Thesis, EGI 2013: 113MSC
EKV974**

**SIMPLIFICATOIN OF 3D COOLED TURBINE
BLADE MODELS FOR EFFICIENT DYNAMIC
ANALYSES**

AROKIA LOURDU MARSHALL, AROKIA

Approved	Examiner BJÖRN LAUMERT	Supervisor MARIA MAYORCA NENAD GLODIC
	Commissioner	Contact person

ABSTRACT

In gas turbines, the temperature behind the combustors is the highest, meaning that the blades in the first stage of the turbine require cooling air. This makes the structural blade model very detailed due to the presence of the cooling pattern. For aeromechanical design, one of the first steps is to perform a modal frequency check by using 3d Finite Element models and the Campbell diagram to establish if the design is acceptable with respect to resonance margins. If the 3d detailed geometry (including all the cooling details) is used the model becomes extremely large. In order to perform various loops between structural dynamics and aerodynamics in an early stage, the dynamic model of cooled blades should be simplified. The simplified model should be accurate enough in terms of predicting correct frequencies but much lighter in size.

The objective of this thesis is to perform parametric studies of different 3d simplified cooled turbine blade models. Various models with different geometrical features are created from the history of the CAD software (NX). Different FE meshes are produced in the Hypermesh software and the modal analyses are solved in Abaqus. The results are compared with the fully detailed model. The influence of the cooling features for each test case is summarized and this will be useful for creating reduced order models. Explanation and guidelines with respect to the mesh generation and loading conditions in Hypermesh software are also included in the appendix section.

For quick frequency checks during the intial stages of the design, the solid blade model can be used which has the modal frequencies within 10 percent range from the fully detailed model. The cooling core features that are important with respect to dynamics are cooling matrix, the ribs and the trailing edge cutback which contribute to the stiffness of the blade.

ACKNOWLEDGEMENTS

I would like to thank Professor Damian Vogt for giving me the opportunity to be selected in this program and teaching me the basics of Turbomachinery through which I was enlightened and inspired.

Thanks to Maria Mayorca, my local supervisor at Siemens Industrial Turbomachinery AB, Sweden for her constant guidance and also the opportunity to perform the thesis. Her positive thoughts and encouragement gave me an insight into the industrial atmosphere. Special thanks to Dr. Ronnie Bladh for his expertise and experience for my thesis work.

Thanks to my supervisor Nenad Glodic at KTH, Sweden for his support and in organizing the project meetings. I would like to thank Björn Laumert for assessing my thesis work.

To my colleagues UtkuDeniz Ozturk, Bengt Johansson, Oleg Rojkov, Patrick Rasmusson, Yong Lee and Qingyuan Zhuang, for helping me during this thesis work and their hospitality has made my work enjoyable.

Thanks to my classmates in Thrust program who have made it a memorable and life changing experience.

Finally, I would like to thank my family, my Appa Michael, my Amma Sophia and my Anna Rex for their unconditional love, support and prayers. Thanks to my friends back in Sweden, Belgium, South Africa and back home in India. Special thanks to Magdaleen for her support and love.

TABLE OF CONTENTS

ABSTRACT	II
ACKNOWLEDGEMENTS	III
TABLE OF CONTENTS	IV
LIST OF FIGURES	VI
NOMENCLATURE	8
1 INTRODUCTION	10
2 BACKGROUND.....	12
2.1 GAS TURBINE OVERVIEW	12
2.1.1 Compressor Section.....	13
2.1.2 Combustor Section	14
2.1.3 Turbine Section.....	14
2.2 COOLED TURBINE.....	15
2.3 TURBINE COOLING DESIGN	15
2.3.1 Cooling Trend History.....	15
2.3.2 Cooling Techniques.....	16
2.4 MODAL ANALYSIS.....	19
2.5 TURBINE BLADES STRUCTURAL DYNAMICS	20
2.5.1 Natural Frequency and Mode shape	20
2.5.2 Excitation Forces	21
2.5.3 Campbell Diagram	22
2.5.4 SAFE Diagram	23
2.5.5 Bladed Disk Mistuning	25
3 OBJECTIVES.....	27
4 METHOD OF ATTACK	28
5 TEST CASE	30
5.1 FIRST STAGE TURBINE BLADE CT1	30
5.1.1 Cooling Features.....	30
5.1.2 NX Models from Detail History.....	31
5.1.2.1 Model 1	32
5.1.2.2 Model 2	32
5.1.2.3 Model 3	33
5.1.2.4 Model 4	34
5.1.2.5 Model 5	34
5.1.2.6 Model 6	35
5.2 SECOND STAGE TURBINE BLADE CT2.....	36
5.2.1 Cooling Features.....	36
5.2.2 NX Models from Detail History.....	37
5.2.2.1 Model 1	37
5.2.2.2 Model 2	38
5.2.2.3 Model 3	38
5.2.2.4 Model 4	39
6 RESULTS AND DISCUSSION	41
6.1 MESH SENSITIVITY ANALYSIS	41
6.1.1 Root Optimization.....	42
6.1.2 Airfoil Optimization.....	43
6.2 CT1 MODAL ANALYSIS	44
6.2.1 Temperature Profile	45
6.2.2 Centrifugal Load	45
6.2.3 Seal Pressure.....	46
6.2.4 Disk Fixation	46
6.2.5 Full Modal Analysis	47

6.2.5.1	Modal Analysis with Only Centrifugal Load	48
6.2.5.2	Mode shape Comparison	48
6.2.6	Mass Scaling	49
6.3	CT2 MODAL ANALYSIS	51
6.3.1	Full Modal Analysis	51
6.3.2	Mode Shape Comparison	52
6.3.3	Mass Scaling	53
7	SUMMARY AND CONCLUSION	55
7.1	FUTURE WORK	57
8	REFERENCES	58
9	APPENDIX A: GUIDELINES IN CREATING MESHERS FOR COOLED TURBINES IN HYPERMESH VER12.0 AND MAKING IT COMPATIBLE FOR ABAQUS VER6.12	60
9.1	STARTING WITH HYPERMESH	60
9.2	IMPORTING GEOMETRY	61
9.3	GEOMETRY CLEANUP	62
9.3.1	Suppress unwanted edges.....	62
9.3.2	Removing Fillets in the geometry.....	63
9.3.3	Splitting Surface or Additional trim	63
9.4	CREATION OF COMPONENTS.....	63
9.4.1	Creating Surfaces.....	64
9.4.2	Mask / Unmask entities.....	64
9.5	2D MESH CREATION.....	66
9.6	ELEMENT CHECK OF 2D MESH	67
9.6.1	Minimum angle check.....	67
9.6.2	Free edges	68
9.6.3	Jacobian	69
9.6.4	Penetration	69
9.7	CREATION OF 3D TETRA MESH	69
9.8	QUALITY TETRA CHECK	70
9.9	CREATION OF ELEMENT / NODE SETS	70
9.10	SCALING	71
9.11	LOADING CONDITIONS AND CONSTRAINT DEFINITION.....	71
9.11.1	Pressure definition.....	73
9.11.2	Centrifugal force definition	74
9.11.3	Temperature profile definition.....	75
9.12	EXPORTING TO ABAQUS.....	75
10	APPENDIX B: RESULTS OF MESH SENSITIVITY ANALYSIS.....	77
10.1	MODE 2 – ROOT OPTIMIZATION	77
10.2	MODE 3 – ROOT OPTIMIZATION	77
10.3	MODE 4 – ROOT OPTIMIZATION	78
10.4	MODE 5 - ROOT OPTIMIZATION.....	78

LIST OF FIGURES

Figure 1.1 Design process with dynamics with full 3d geometry (a); design process with simplified dynamics model (b).	10
Figure 2.1 SGT 750 Gas turbine ; Hellberg (2011)	12
Figure 2.2 Simple Gas turbine Stage; Saravanamuttoo (2001).....	12
Figure 2.3 Compressor flow characteristics; Ganesh.,V (2010).....	13
Figure 2.4 Turbine flow characteristics;Ganesh.,V (2010).....	14
Figure 2.5 Turbine section after the combustion chamber ; Hellberg (2011).....	15
Figure 2.6 Cooling trend history; Lakshminarayana (1996).....	16
Figure 2.7 Schematic of a modern, cooled gas turbine blade; Je-Chin Han (2013)	17
Figure 2.8 Trailing edge cooling in high pressure turbine blade; Horbach (2011).....	18
Figure 2.9 Cooling matrix; Sundberg (2005).....	18
Figure 2.10 Single degree of freedom vibration system	19
Figure 2.11 Different methods of solving multi-degree of freedom systems; Barkanov (2001).....	20
Figure 2.12 Blade first order eigen modes ; Vogt (2005)	21
Figure 2.13 Disk mode shapes and nomenclature; Mayorca (2011)	21
Figure 2.14 Illustration of blade row interaction mechanisms; Mayorca(2011)	22
Figure 2.15 Campbell diagram ; Mayorca (2011)	23
Figure 2.16 SAFE Diagram ; Dello (2013).....	23
Figure 2.17 Producing SAFE diagram from Campbell Diagram ;Dello (2013).....	24
Figure 2.18 3 Nodal diameter mode shape of a tuned bladed disk; Castanier et al(2006) .	25
Figure 2.19 Localized mode shape of a mistuned bladed disk; Castanier et al(2006).....	26
Figure 4.1 Flow chart of the process.....	28
Figure 5.1 Multi flow cooling path in turbine blade	30
Figure 5.2 Rib turbulator and cooling matrix of CT1 blade	31
Figure 5.3 Presence of film cooling holes in CT1 blade.....	31
Figure 5.4 CT1 Model 1(no cooling features)	32
Figure 5.5 CT1 Model 2 (only multi-flow cooling path).....	33
Figure 5.6 CT1 Model 3 (multi-flow path and film cooling holes)	33
Figure 5.7 CT1 Model 4 (multi-flow path and cooling matrix).....	34
Figure 5.8 CT1 model 5 (multi-flow path, film cooling and cooling matrix)	34
Figure 5.9 CT1 Model 6 (all cooling features)	35
Figure 5.10 CT2 cooling features	36
Figure 5.11 CT2 Model 1 (no cooling).....	37
Figure 5.12 CT2 Model 2 (multi-flow cooling path and ribs)	38
Figure 5.13 CT2 Model 3 (multi-flow path, ribs and trailing edge cutback).....	39
Figure 5.14 CT2 Model 4 (complete cooling core)	39
Figure 6.1 Components selected for meshing process.....	41
Figure 6.2 Root mesh convergence; mode 1; CT1	42
Figure 6.3 Airfoil optimization process of Mode 2	43
Figure 6.4 Final model from the mesh sensitivity analysis	44
Figure 6.5 Temperature profile from Abaqus result file.....	45
Figure 6.6 Seal pressure boundary conditions	46
Figure 6.7 Full modal analysis results	47
Figure 6.8 Modal analysis with centrifugal load only	48
Figure 6.9 Mode 1 from the modal analysis	49
Figure 6.10 Mode 2 to Mode 5 from the modal analysis; CT1.....	49
Figure 6.11 Mass scaling on CT1	50

Figure 6.12 Full modal analysis results with respect to model number.....	51
Figure 6.13 Full Modal Analysis result with respect to number of elements	52
Figure 6.14 Mode 1 to 4 from full modal analysis results; models 1 to 4 from left to right.....	52
Figure 6.15 Mode shapes 5 to 7 for CT2; models 1 to 4 from left to right.....	53
Figure 6.16 Mass scaling results of CT2	54
Figure 7.1 Comparison of CT1 turbine blade models.....	56
Figure 7.2 Comparison of CT2 turbine cooled blade models	56
Figure 7.3 Future objectives in a flow chart	57
Figure 9.1 User Profile Option at the start up of Hypermesh	60
Figure 9.2 Import Menu in Hypermesh	61
Figure 9.3 UG part browser menu in Hypermesh.....	62
Figure 9.4 Quick edit option in Hypermesh.....	63
Figure 9.5 Defeature option in Hypermesh.....	63
Figure 9.6 Surface creation in Hypermesh	64
Figure 9.7 Masking entities of a model	65
Figure 9.8 Surface edit option in Hypermesh	65
Figure 9.9 Component creation in Hypermesh	65
Figure 9.10 Automesh option for 2d mesh in Hypermesh.....	66
Figure 9.11 Interactive mesh mode in Hypermesh	67
Figure 9.12 Element check option in Hypermesh.....	67
Figure 9.13 Replacing node with another node by using replace command	68
Figure 9.14 Penetration menu in Hypermesh	69
Figure 9.15 tetramesh option in Hypermesh.....	70
Figure 9.16 Entity set option in Hypermesh	70
Figure 9.17 Scaling option in Hypermesh	71
Figure 9.18 Load collector pop up menu in Hypermesh	72
Figure 9.19 Initial conditions browser in Hypermesh	73
Figure 9.20 Pressure menu browser in Hypermesh	74
Figure 9.21 Centrifugal loading option in Hypermesh	74
Figure 9.22 Export browser in Hypermesh.....	76
Figure 10.1 Mode 2 root optimization process	77
Figure 10.2 Mode 3 root optimization process	77
Figure 10.3 Mode 4 root optimization process	78
Figure 10.4 Mode 5 root optimization process	78

NOMENCLATURE

Latin Symbols

a	Acceleration
C	Damping
K	Stiffness
M	Mass
ND	Nodal Diameter
t	Time
V	Volume
v	Velocity
x	Displacement

Greek Symbols

ρ	Density
ω	Frequency

Subscripts

r	damped
---	--------

Abbreviations

AG	Aktiengesellschaft
AIAA	American Institute of Aeronautics and Astronautics
ASME	The American Society of Mechanical Engineers
CT	Compressor Turbine
FE	Finite Element
TIT	Turbine Inlet temperature

1 INTRODUCTION

Gas turbines play an important role in the industrialized society. Today, the production of power becomes a demand and due to that, the thermal efficiency and power output of the gas turbine becomes significant. One technique that increases the thermal efficiency and power output of a gas turbine is to increase the temperature of the gas entering the turbine. For increasing the temperature, cooling in the first two stages of the turbine has become a significant part.

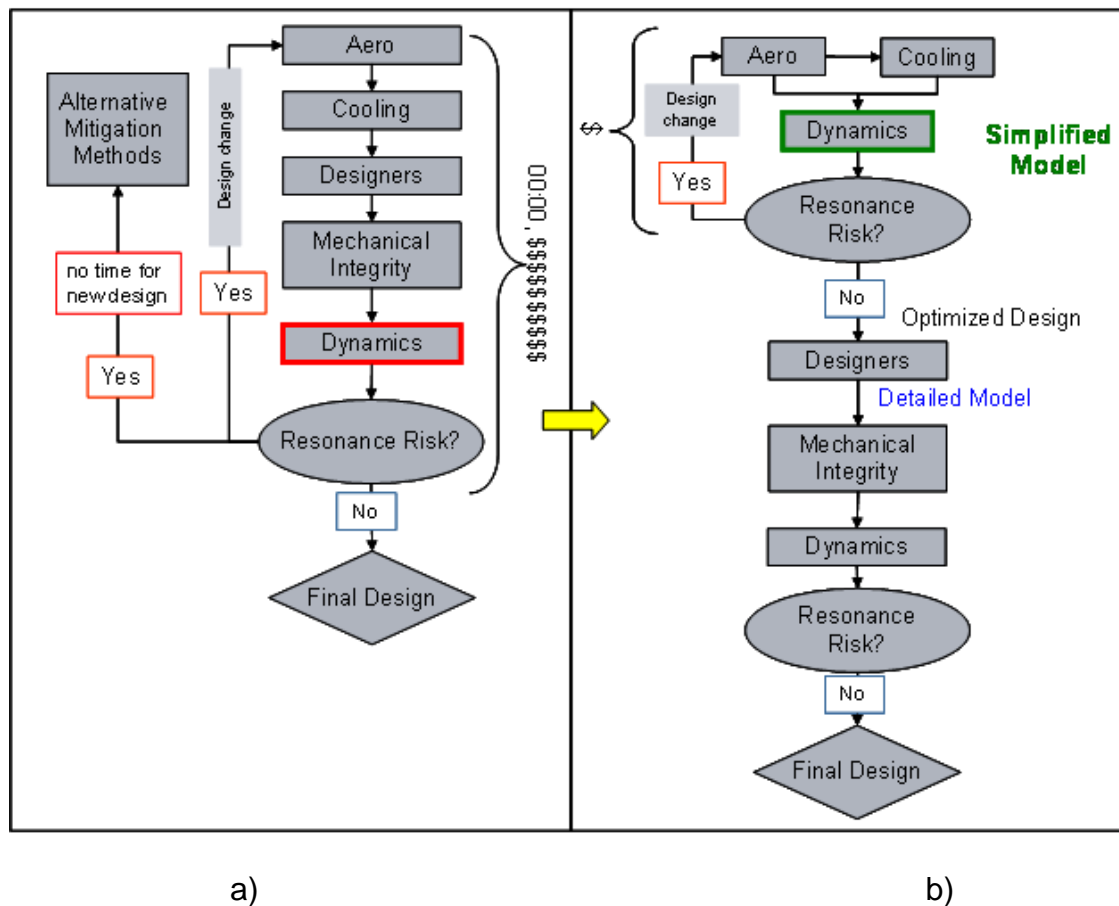


Figure 1.1 Design process with dynamics with full 3d geometry (a); design process with simplified dynamics model (b).

During the design process of the turbine, estimating the natural frequencies is required. The natural modes of a system are those at which the system will vibrate with the highest amplitudes when excited at the corresponding natural frequencies. When the natural modes are excited, it is said that the system is in resonance. In gas turbines, resonance at the lower natural frequencies of the blades becomes a danger when it happens in the operating range. The blade dynamics specialists should then be involved in the estimation of the natural frequencies in the design process. This process generally starts in the aerodynamics group, where the blade is designed optimizing for efficiency. At this stage, definition of the blade profile is assessed. The cooling group will then implement the cooling core details of the blade optimizing for heat transfer and

thermal efficiency. The cooling core changes the properties of the structure (i.e.: mass, stiffness, etc.). Then, the CAD designers will create the 3d geometry to manufacture. This geometry is the basis for the generation of the full 3d Finite Element (FE) mesh by the mechanical integrity group where various analyses are done (i.e.: static analyses, creep, etc). The same mesh could then be used by the dynamics experts who will perform the modal analysis and evaluate the resonance risks. If there is an occurrence of a critical resonance, then a geometrical change is proposed and the iteration loop needs to start from the beginning.

This process is illustrated in Figure 1.1 a. One drawback of this design loop is that the dynamics frequency check appears too late and thus if a resonance risk is encountered, there is not enough time to allow sufficient iterations. Additionally, using the full 3d detailed model in the dynamics analysis makes the time involved in meshing and modal frequencies estimation too long. The cooled turbine blades have intricate geometric details that deal with the cooling of the blade. The meshing involved in these blades is more complex than non-cooled blades. During the meshing process, if the geometric details are intricate, much time in geometry cleaning is required before meshing. The cleaning of geometries before meshing becomes higher with the complexity in the model. On the other hand, including excessive details in the mesh makes the size of the FE model so large that it could limit the dynamics calculations to blade-alone analyses, without the disk influence (e. g.: various nodal diameters).

There is then a need to have a more efficient manner of estimating the modal frequencies in the initial design stage of the cooled turbine blades. The influence of the geometric details in the modal frequencies of a model has to be found so that only relevant features of the geometry are included in a simplified model. The simplified model could then allow having the dynamics check earlier in the design chain as in Figure 1.1 b, reducing costs and time.

As a first step for achieving an efficient calculation, this study will focus on evaluating the influence of the cooling features in the estimation of the modal frequencies.

2 BACKGROUND

2.1 Gas Turbine Overview

A gas turbine is an internal combustion engine that uses air as the working fluid. Saravanamuttoo et al (2001) explain the conversion of chemical energy from the fuel and the working fluid into mechanical energy in the production of power inside a gas turbine. An example of gas turbine is represented in Figure 2.1 where the components are visible through a cross sectional view. Detailed explanation of the important components of the gas turbine is discussed later in this section.

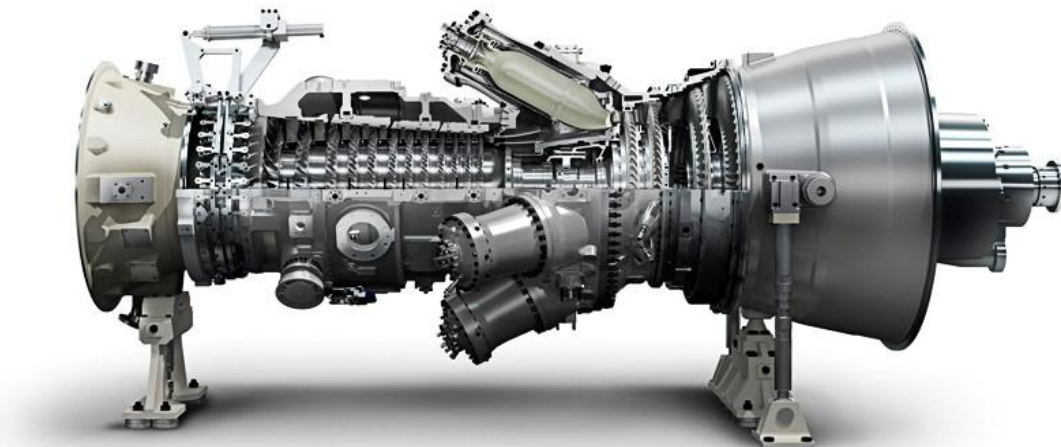


Figure 2.1 SGT 750 Gas turbine ; Hellberg (2011)

The gas turbine consists of three important components: the compressor, the combustion chamber and the turbine. Refer Figure 2.2 to visualize the process of power generation in the gas turbine.

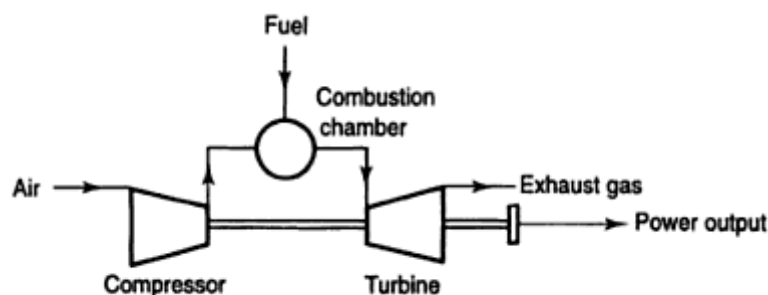


Figure 2.2 Simple Gas turbine Stage; Saravanamuttoo (2001)

The air is drawn from atmosphere pressure through the inlet guide vane to the compressor where the compression of inlet air takes place and then, the

combustion chamber comes into play where the fuel mixes with the inlet air to combust and move further to the turbine to generate power.

2.1.1 Compressor Section

It is the responsibility of the compressor to provide high pressure flow to the combustion chamber with utmost efficiency. A single stage of compression consists of a rotating blade which is connected to a rotating disk (the rotor), followed by a stationary vane (or stator). The flow area in the compressor blade and vanes are divergent. The inlet and the outlet guide vanes of the compressor are neither divergent nor convergent. They are arranged to provide the best orientation for the compressor and the combustor respectively.

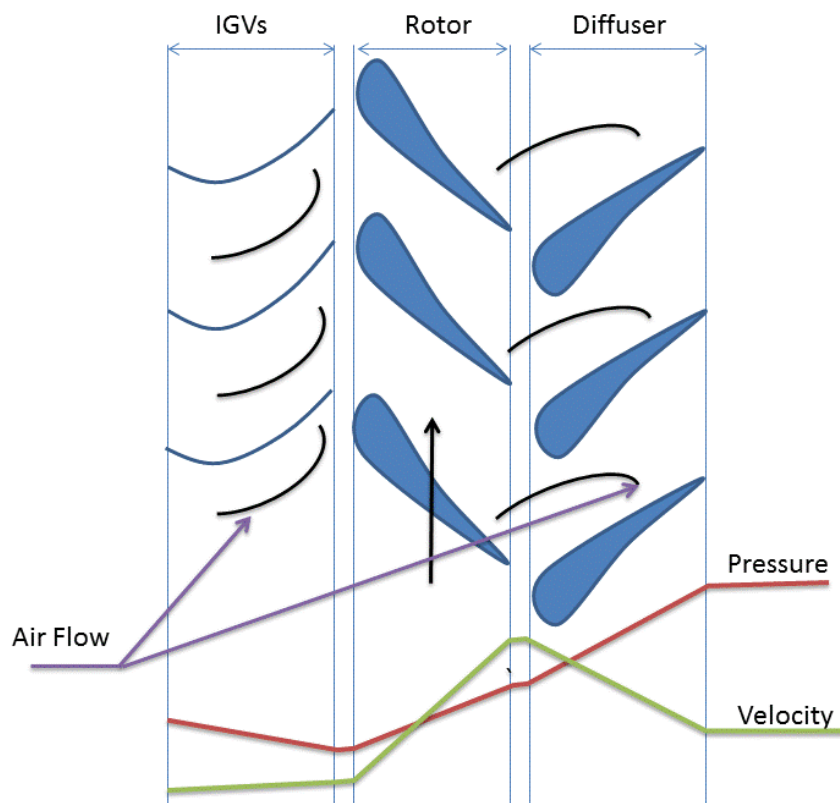


Figure 2.3 Compressor flow characteristics; Ganesh.,V (2010)

Figure 2.3 shows the pressure characteristics of the flow for one stage in the compressor section. The physical mechanism of the compressor is to convert the rotary energy into the gaseous energy. This conversion increases the total pressure (P_t) on which most of the increase is in the velocity of the fluid with a small increase in the static pressure due to the divergence of the blade flow paths.

The efficiency of the compressor depends on the smoothness of the air flow in the section and it is affected due to the occurrences of friction and turbulence. Efforts are made to minimize losses and it is likely to occur due to the high pressure ratio outcomes generated.

The air leaves the compressor through the diffuser into the combustion chamber. The diffuser is critical in converting the velocity increase through the compressor section to static pressure. The static pressure reaches the highest at the outlet of the diffuser or inlet of the combustion chamber.

2.1.2 Combustor Section

The task of the combustor section is controlling of the burning of the large amount of fuel and air in an efficient manner. This must be achieved with minimum pressure loss and maximum heat release. In addition to that the combustion must be orientated in such a manner that overheating of the metal parts is avoided.

The combustion takes place in the primary zone or the front end of the cans/burners. The primary air is used in the combustion process (approximately 25 percent of the inlet air) and the rest of the inlet air in this section is termed as the secondary air or the dilution air. The secondary air controls the flame pattern, cooling of the liner walls and increases mass.

The transition section is the rear end of the combustion liners and it is convergent in shape. The objective is to accelerate the gas stream and reducing the static pressure providing a good platform as an inlet to the turbine section.

2.1.3 Turbine Section

The physical mechanism of the turbine section is to convert the gaseous energy of the burnt fuel into mechanical energy. This is achieved by expanding the hot, high pressure gas from the combustor into lower temperature and pressure. The stator vanes increase the velocity of the gas and the rotor extracts the energy.

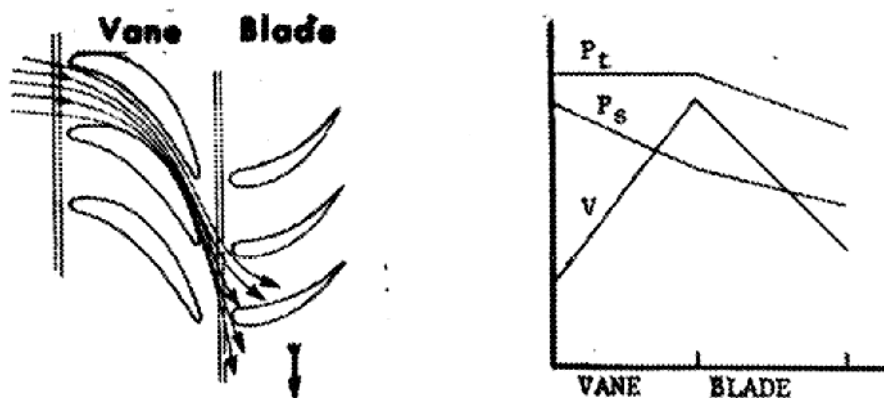


Figure 2.4 Turbine flow characteristics; Ganesh., V (2010)

The stator vanes are convergent ducts that will convert the higher heat and pressure energy into higher velocity gas flow. Velocity, temperature and the pressure are sacrificed in order to rotate the turbine which in turn generates the shaft power.

The efficiency of this section is on maximum conversion of the mechanical energy from the hot and pressure energy of the gases. The seal provided at the base and the shroud available at the rear stages of the turbine contributes to the efficiency.

The Turbine Inlet Temperature (TIT) is a critical factor in the design of a gas turbine.

2.2 Cooled Turbine

In modern gas turbines cooled turbines are the first stages of the turbine in which the cooling arrangements are provided. Cooling is critical at this section because the temperature is closer to or greater than the melting point of the material. In Figure 2.5, the first two stages of the turbine have cooling arrangements and are connected to the compressor. This means that the work done by this turbine is used to move the compressor and thus referred to as the Compressor-Turbine (CT). The next two stages are responsible for the transmission of the power and referred to as Power Turbine (PT).

The turbine inlet temperature is an important factor in the design of the gas turbine and it is strived to maintain it as high as possible to obtain maximum thermal efficiency. In a modern gas turbine, the temperature is close to 1500 degrees Celsius.



Figure 2.5 Turbine section after the combustion chamber ; Hellberg (2011)

2.3 Turbine Cooling Design

The cooling design has to bridge the gap between continuously increasing gas temperature and the pressures and the allowable material temperature, which have increased significantly in the recent years. The gas temperature is influenced by the focus on the turbine inlet temperature and thermal efficiency.

2.3.1 Cooling Trend History

The cooling design in the turbine section has improved the thermal efficiency indirectly by increasing the turbine inlet temperature. The cooling trend history is demonstrated from Lakshminarayana (1996). Initially, the cooling was not of much importance. The urge of increasing thermal efficiency paved way to make hollow blades which have internal flow passages to cool the blades. It began with simple flow path and later on emerged to produce complex cooling structures like ribs, matrix and many more complicated profiles.

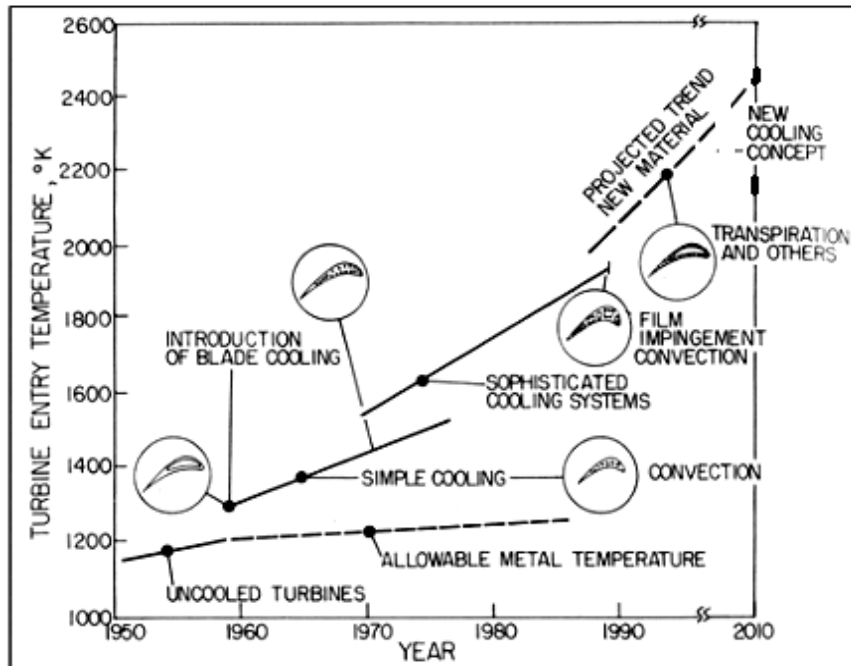


Figure 2.6 Cooling trend history; Lakshminarayana (1996)

As the years passed by, the cooling of the turbine blades have gained significant importance as the criterion of TIT became more critical in the design.

2.3.2 Cooling Techniques

The turbine cooling is divided into internal and external cooling techniques with the same motive. In the internal cooling, the heat is removed by the variation of convection and impingement cooling configurations, where the high velocity air flows and hits the inner surfaces of the turbine vanes and blades. The external blade cooling techniques is provided when the cold air is injected through the film cooling holes on the external blade surface in order to create a thin film cooling layer. The surface heat transfer occurring on the turbine blade is affected by combustor-generated high turbulence, laminar to turbulent transition, acceleration, film cooling flow, platform secondary flow and surface roughness, centrifugal forces and blade tip leakage and clearance.

The blade displayed in Figure 2.7 consists of a zigzag cooling passage lined with the rib turbulators. Jet impingement technique is used to cool the leading edge and pin fin cooling technique with ejection is used near the trailing edge of the blade. The cooling path is different from that of the vanes as the effect of the rotation is considered and the flow of the coolant is altered accordingly.

Rib turbulators are the most commonly used method to enhance the heat transfer in the internal multi flow cooling path. The rib turbulence promoters are typically cast on two opposite walls of the cooling passage.

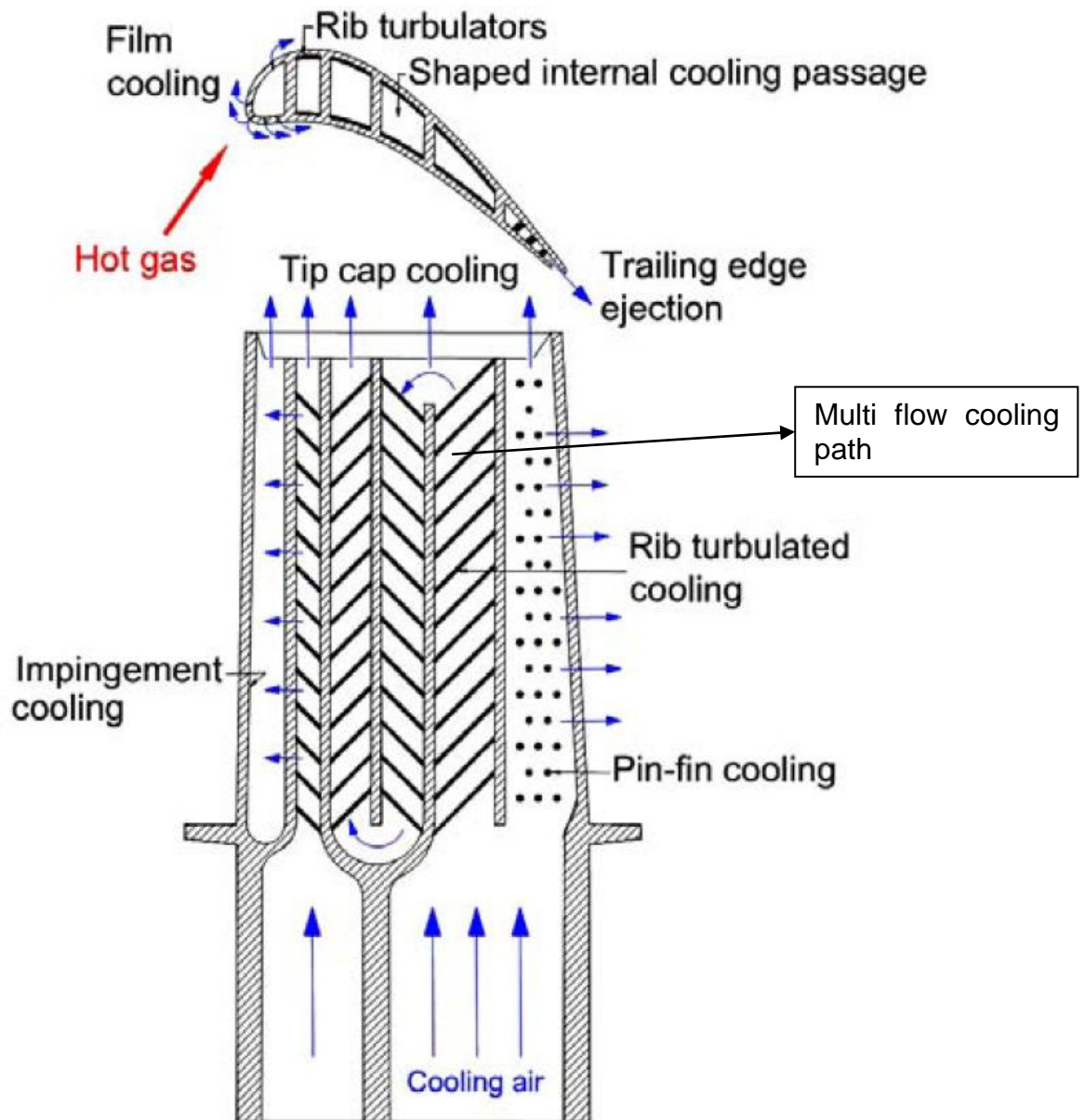


Figure 2.7 Schematic of a modern, cooled gas turbine blade; Je-Chin Han (2013)

The heat transfer performance of the ribbed channel depends on the aspect ratio of the blade, the rib configuration and the Reynolds number of the coolant flow. In the film cooling method, the air is extracted from the compressor and forced through internal cooling passages within the turbine blade and vanes before being ejected through discrete cooling holes on the airfoil surfaces. The air exiting these cooling holes forms a film of cool air on the component surface which protects the components from hot gas exiting the combustor.

The trailing edge film cooling is a technique that gained popularity in the modern gas turbine due to its influence in the film cooling effectiveness and heat transfer. It is subjected to aerodynamic and structural constraints. The objective is to remove heat from the trailing edge region, since it is desirable to keep the trailing edge as thin as possible to minimize aerodynamic losses. The pressure side of the trailing edge is cutback to form the ejection slot (Figure 2.8). The ejected film

cooling acts as an insulating layer to prevent hot gases from impinging in to the wall and also serves as a convective sink for the heat transferred to the suction side. To counteract the structural weakening, the opposing walls forming the trailing edges are connected by arrays of pin-fin arrangement. The additional benefit of this arrangement is to act as turbulators for the flow from the ejection slot.

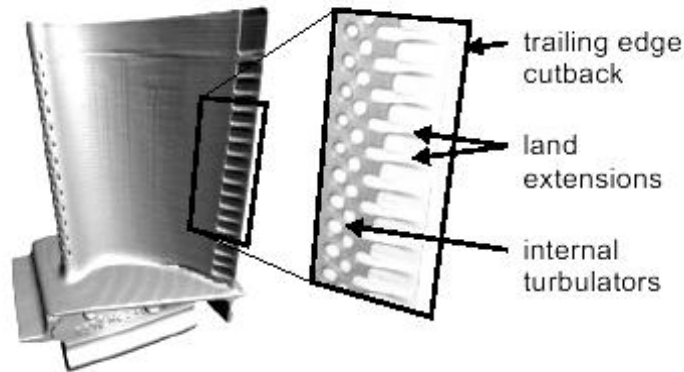


Figure 2.8 Trailing edge cooling in high pressure turbine blade; Horbach (2011)

Sundberg (2005) explains that matrix cooling is a complicated way of cooling but it provides the additional stiffness to the blade which will try to make it close to the blade without any cooling core. A matrix consists of two layers of opposite angled longitudinal ribs (Figure 2.9). The ribs create a system of channels, in which the cooling air changes direction continuously as it changes channel on its path through the airfoil.

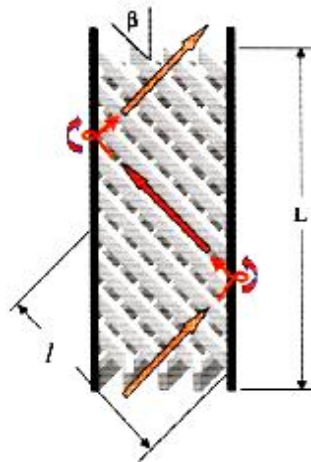


Figure 2.9 Cooling matrix; Sundberg (2005)

A thin boundary layer is developed at each channel and it increases the heat transfer coefficient. The flow passes from one channel to another creating a swirl and increasing the turbulence of the flow. In addition to that, the heat transfer is increased due to the increase in the surface area from the presence of the longitudinal ribs.

2.4 Modal Analysis

The goal of the modal analysis in structural mechanics is to determine the mode shapes and natural frequencies of a structure during free vibration. The single degree of freedom vibration system can be used to illustrate the modal analysis, as shown in Figure 2.10.

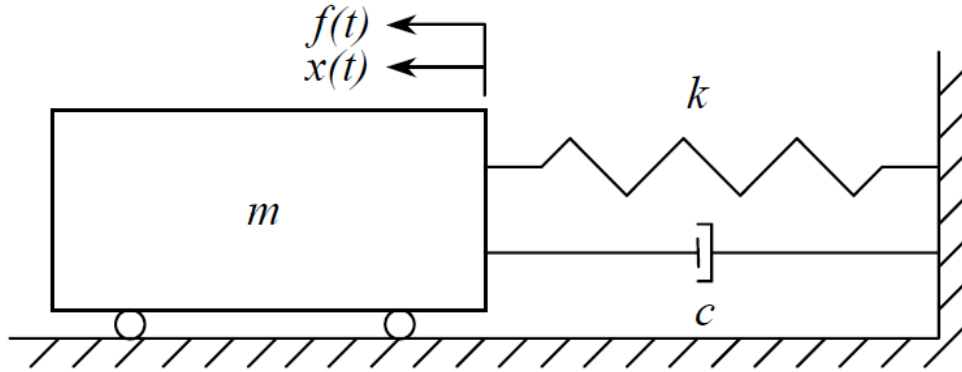


Figure 2.10 Single degree of freedom vibration system

The general idea of the single degree of freedom vibration system is described by the dynamic equation of motion 2.1.

$$m\ddot{x}(t) + c\dot{x}(t) + kx(t) = f(t) \quad (2.1)$$

In the above mentioned form m represents the mass of the system, c represents the damping, k represents the stiffness of the system, f represents the forcing function, \ddot{x} represents the acceleration, \dot{x} represents the velocity, x represents the displacement and t is the time.

Assuming periodic excitation and periodic response, the equation can be mass normalized to determine the modal frequencies and the damping of the system as shown in equation 2.2.

$$\omega_r = \pm \sqrt{\left(\frac{c}{2m}\right)^2 - \left(\frac{k}{m}\right)} \quad (2.2)$$

Where ω_r is the damped natural frequency of the system.

For the modal analysis, the complementary solution is formed by transforming the original differential equation in homogenous form. This can be done by temporarily removing the damping and forcing function in this case. Laplace transforms can be implemented to determine the modal frequencies and modal vectors in the case of time domain. Otherwise, the equation can be transferred to the frequency domain by the Fourier transformation method to find the modal frequencies.

There are several methods for solving multi degree of freedom systems. The classification of the methods is illustrated in Figure 2.11. The numerical solution from FEM is concentrated on in this project.

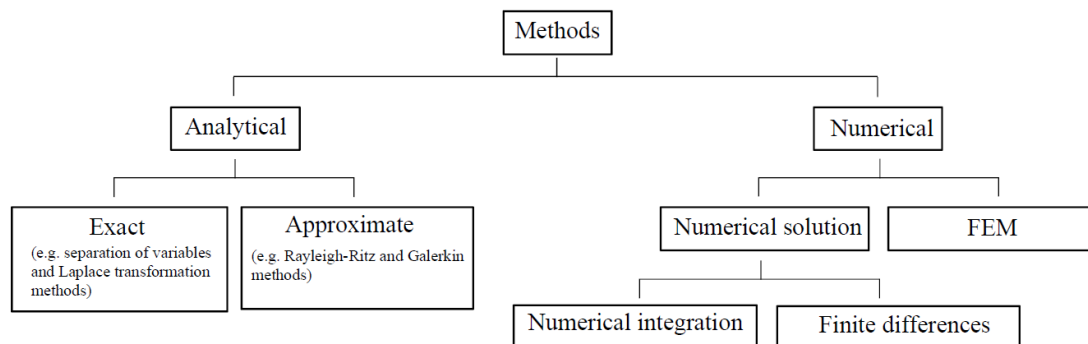


Figure 2.11 Different methods of solving multi-degree of freedom systems; Barkanov (2001)

Assembly of elements with local stiffness and mass descriptions is the basis of constructing computational models in the finite element method. It is assumed that the elements of the model are connected by finite number of nodal points. The field of displacements of each nodal point is determined giving the possibility of using the principle of virtual displacements to write the equilibrium equation for the element assembly.

Barkanov(2001) states and explains the general algorithm of FEM and it consists of:

- Presentation of potential energy for the system from the element assembly
- Determination of boundary conditions present in the system for the analysis
- Initial approximation for the finite element
- Stiffness integration, finite element meshing and building of stiffness are done either analytically or by numerical simulation
- Determination of the minimum potential energy where the solution is stable
- Outputs of displacement and
- Computation and output of stresses

By constructing the finite element mesh, it is possible to obtain the component mass and stiffness matrices of the size of $N \times N$, being N the number of degrees of freedom. The solution of the free response or homogeneous system (zero force) and no damping becomes an eigenvalue problem. The eigenvalues are then the square of the natural frequencies of each mode and the eigenvectors are the mode shapes of each specific mode.

2.5 Turbine Blades Structural Dynamics

2.5.1 Natural Frequency and Mode shape

When the frequency of external forces matches the blade's (or bladed disk's) natural frequencies a resonance condition exists and thus High Cycle Fatigue (HCF) failure of the component might occur. The mode shapes is the way in which

the structure deflects at the natural frequency. For bladed disks, the mode shapes can be divided in to disk dominated and blade dominated mode shapes.

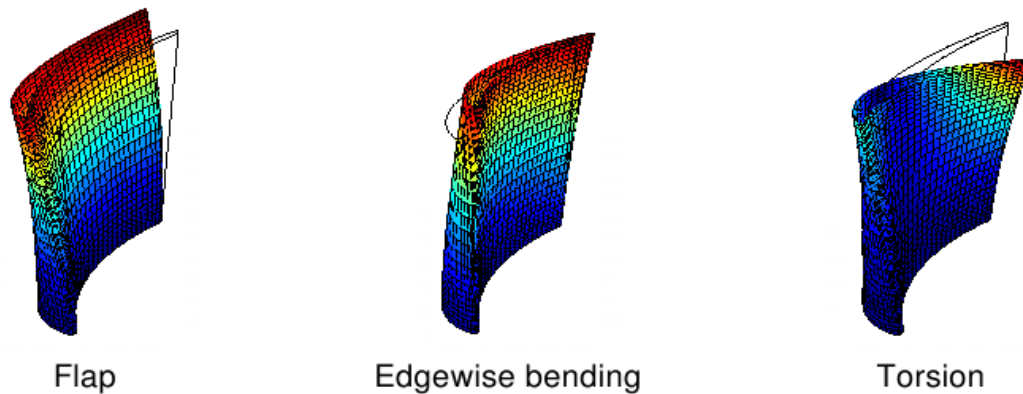


Figure 2.12 Blade first order eigen modes ; Vogt (2005)

Blade dominated mode shapes could be related to beam modes. Generally, the modes with the three lowest frequencies are two bending modes and one torsion mode which are defined by the position of the elastic axes. The two bending modes and the torsion mode are illustrated in Figure 2.12. Additionally, for blades with very high aspect ratio, the edgewise bending modes could be important. However, generally this is not the case for turbine blades. Other mode shapes that could be seen in blades are stripe mode and local deformation modes which are otherwise known as corner modes. The eigen frequencies of different modes vary with the rotational speed due to the effect of centrifugal forces.

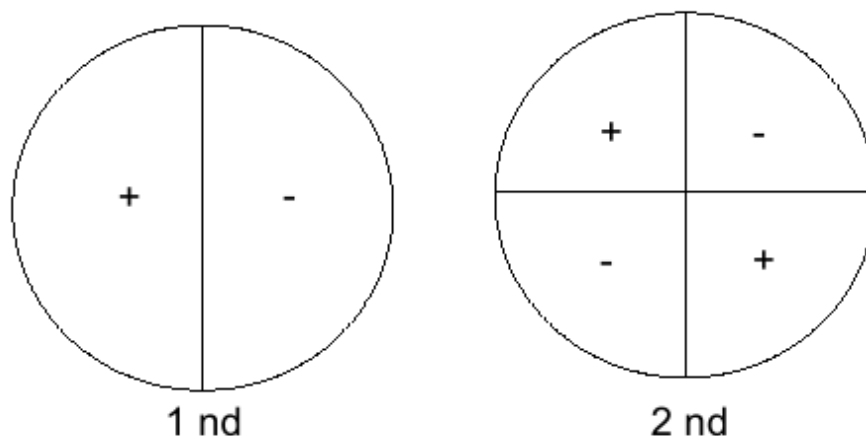


Figure 2.13 Disk mode shapes and nomenclature; Mayorca (2011)

The disk dominated modes are defined with Nodal Diameters (ND) due to the presence of inflexion lines across the disk diameters. It is represented in Figure 2.13.

2.5.2 Excitation Forces

Vibratory forces are the forces that excite the structure to vibrate and the highest resulting displacement amplitudes are obtained at resonance. In the case of gas turbine blades, the most common sources of excitation are vane passing

frequencies and running speed harmonics. Running speed harmonics are due to disruptions in the fluid flow path. The running speed frequencies are the multiples of the rotor operating speed. The multiples of the rotational speed are also referred to as Engine Orders (EO).

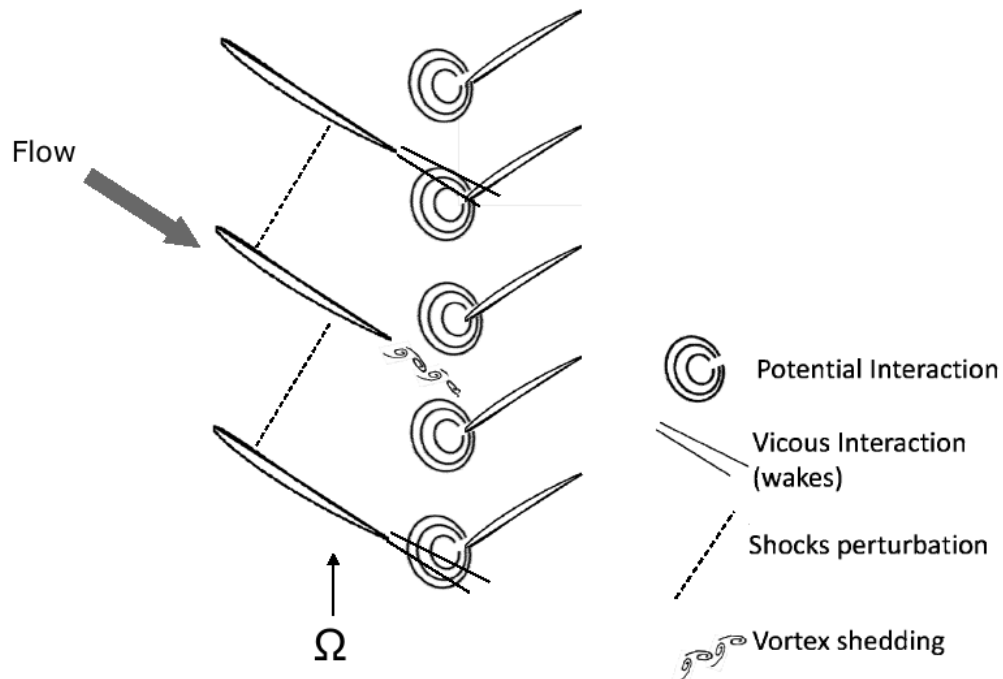


Figure 2.14 Illustration of blade row interaction mechanisms; Mayorca(2011)

Laumert (2002) did an investigation in which the main excitation mechanisms for a turbine stage were determined. In Figure 2.14, the main excitation mechanisms are illustrated. Wakes generated in the blade row interaction are classified as viscous interaction. The passing blades generate a change in the static pressure which is known as potential field perturbations. In the case of wide trailing edge turbine blades, vortex shedding is possible. Shock perturbations are caused by localized unsteady pressure and also due to the static pressure field change. All these mechanism are available in real life conditions resulting in an unsteady pressure distribution on the blade surface.

2.5.3 Campbell Diagram

Campbell diagram illustrates the crossings of the natural frequencies of the structure with the exciting forces.

The possible resonance conditions are highlighted in Figure 2.15 with circles. When the engine orders crosses with the natural frequencies of the structure within the operating range, then it becomes a potential threat for the integrity of the structure.

The difficulty in defining the resonance is that it normally considers only one isolated blade in its analysis. The typical blade-alone case means that the blades are treated as isolated oscillators. The concept of nodal diameter and hence the disk influence is not illustrated in the Campbell diagram.

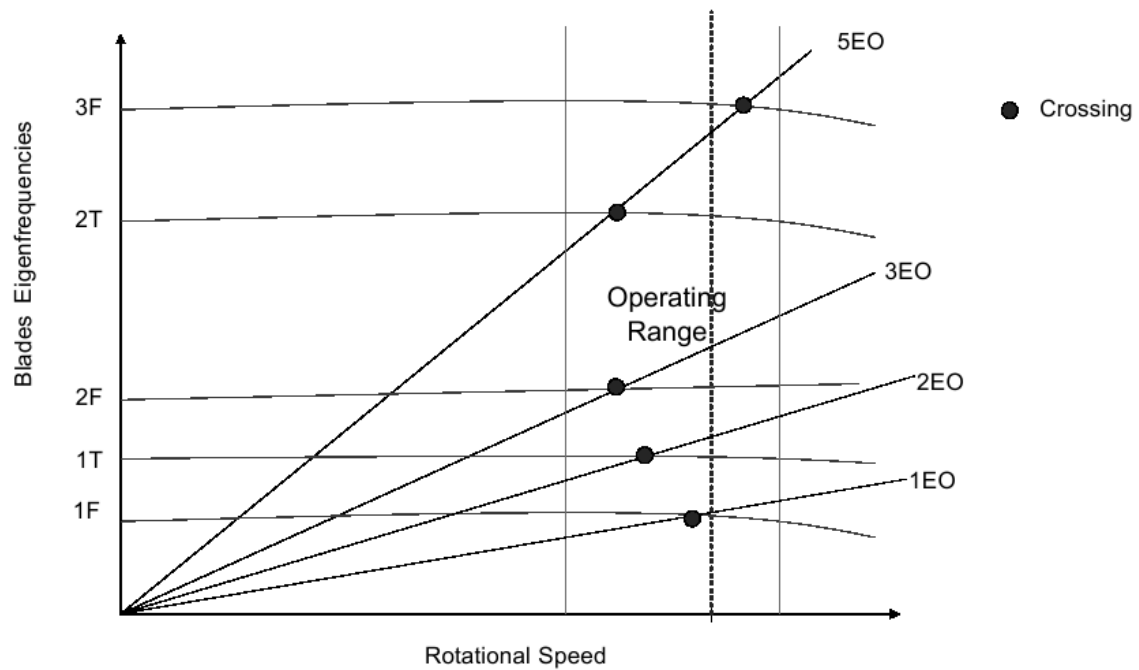


Figure 2.15 Campbell diagram ; Mayorca (2011)

2.5.4 SAFE Diagram

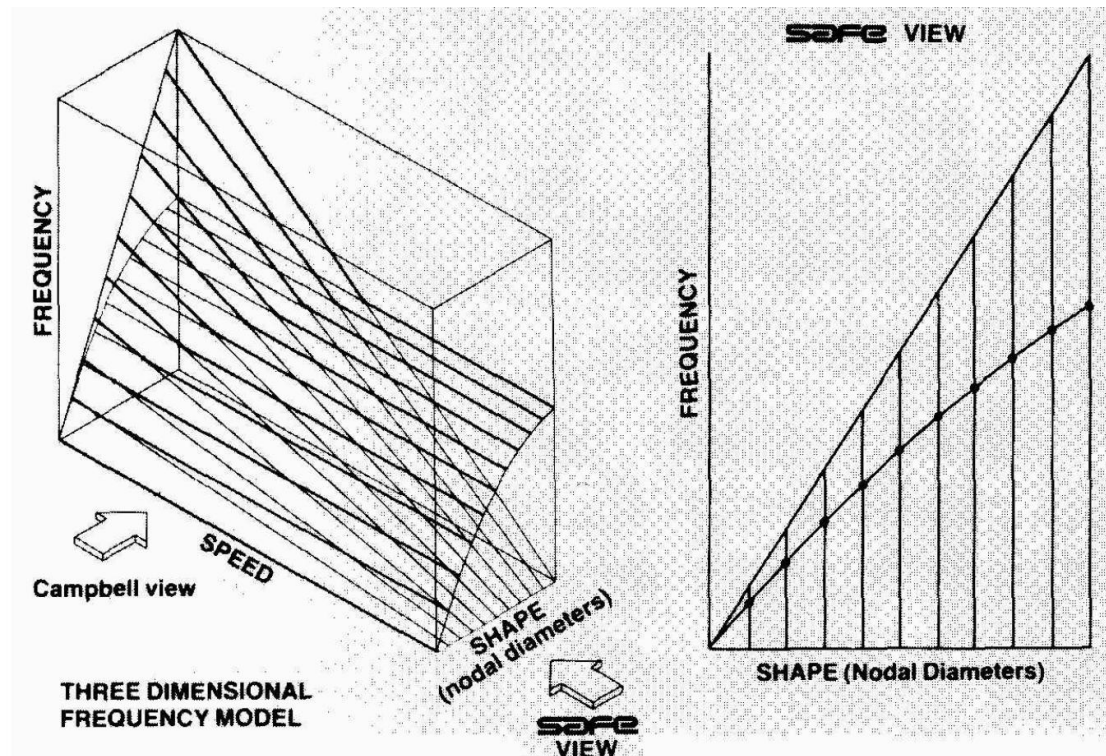


Figure 2.16 SAFE Diagram ; Dello (2013)

The Campbell plane is projected in another manner to show the same information in a clear and concise manner (Figure 2.16). This projected plane is the SAFE plane. The SAFE planes and Campbell diagram shares the same vertical

frequency axis. Instead of the operating speed on the horizontal axis, it is replaced with nodal diameter. Nodal diameter provides an insight to the mode shape of the bladed disk structure and also the shape of the varying force. SAFE diagram will reveal the true resonances. Note however that for many blade designs the conventional Campbell diagram view is sufficient, since the nodal diameter influence is small for designs with stiff disks versus flexible blades (e.g., compressor blades).

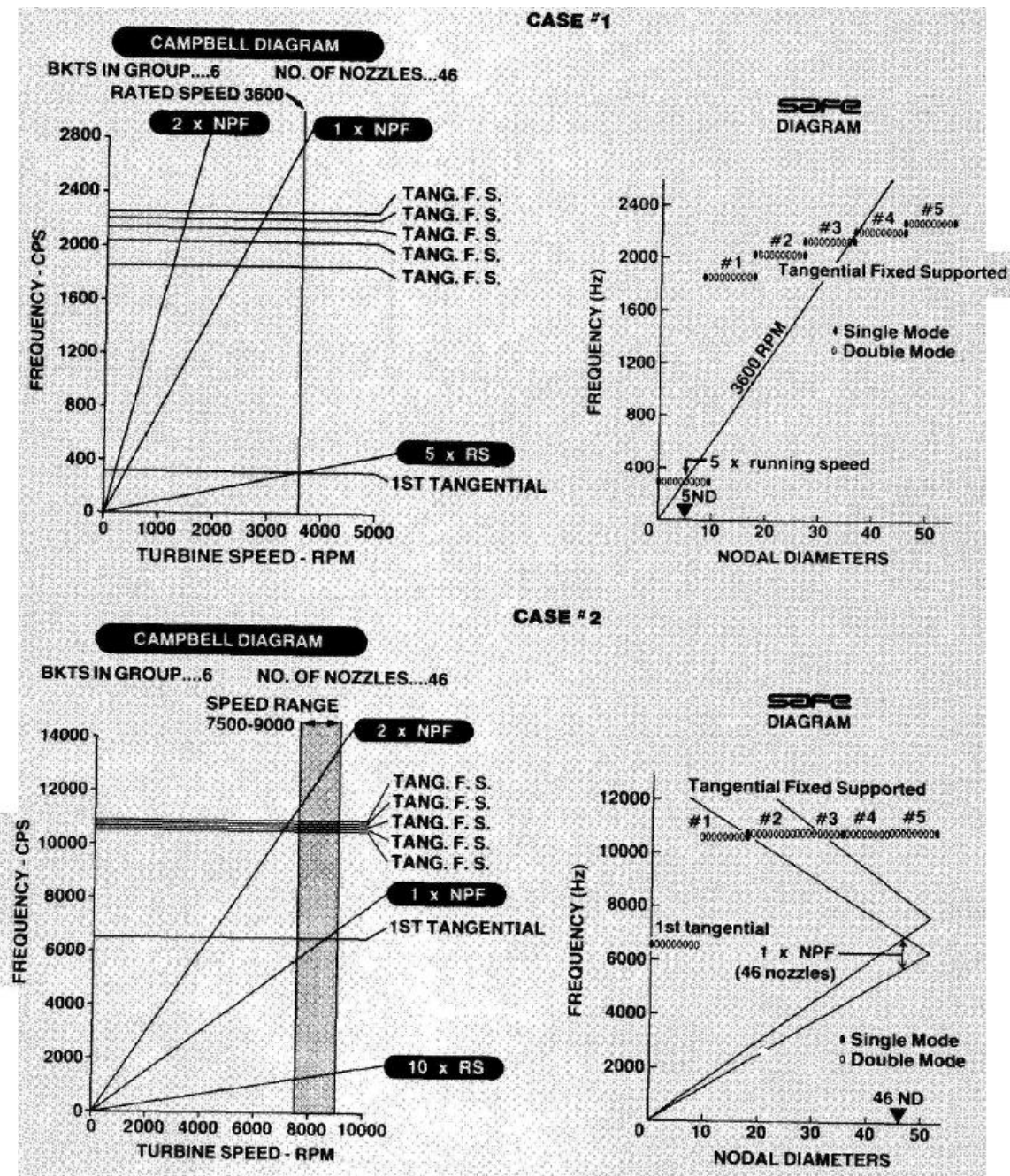


Figure 2.17 Producing SAFE diagram from Campbell Diagram ;Dello (2013)

In Figure 2.17, only the first family of tangential modes is plotted. In order to construct the SAFE diagram from the Campbell diagram, the frequencies at the different nodal diameters need to be known. The case 2 mentioned in Figure 2.17 describes the shortcoming of the Campbell diagram interpretation. The interference of the first tangential mode with the 1 x NPF (Nozzle Passing Frequency) excitation is shown in the Campbell diagram, but the SAFE diagram

does not show this interference. On careful examination of the SAFE diagram, it is shown that the shape of the force at 46 nodal diameter does not match with 0 to 8 nodal diameters. The second case justifies that the SAFE diagram contains enough information to accurately determine the occurrence of the bladed disk resonance.

In the case of the cooled turbine blades, the evaluation of the frequencies for all the nodal diameters is a time consuming process and generally, they are done only for a limited set as the models are complex and large in size. Hence, lighter models are required to evaluate the frequencies at sufficient nodal diameters for a particular mode shape. These calculations imply that a sector of the disk and blade should be included in the FE model and cyclic symmetric boundary conditions should be applied at different nodal diameters.

For the fully detailed cooled turbine blade, most of the elements are concentrated on the blade section, and thus for the simplification studies in this project, the blade alone is considered.

2.5.5 Bladed Disk Mistuning

Castanier et al (2006) investigated mistuned bladed disk vibration and states that there are always small deviation among the blades caused by manufacturing tolerances, wear and other causes. This is called mistuning which is a small deviation relative to the ideally tuned blade. Comprehensive modeling, analysis and understanding of mistuned bladed disk vibrations is critical in reducing the occurrence of HCF and improving the performance and reliability of turbines.

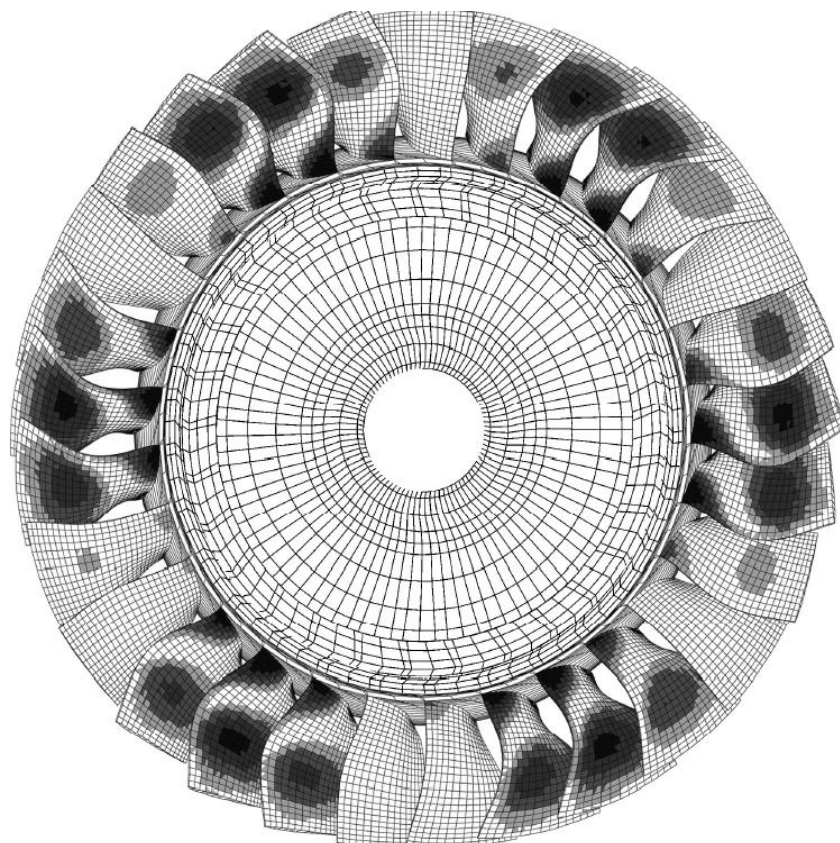


Figure 2.18 3 Nodal diameter mode shape of a tuned bladed disk; Castanier et al(2006)

Figure 2.18 shows the behavior of the mode shape in a tuned bladed disk where the cyclic symmetry models can be used. Figure 2.19 shows the mistuned bladed disk vibration model where the cyclic symmetry cannot be used as it highlights the non uniform displacement amplitude distribution of the mode shape in the bladed disk.

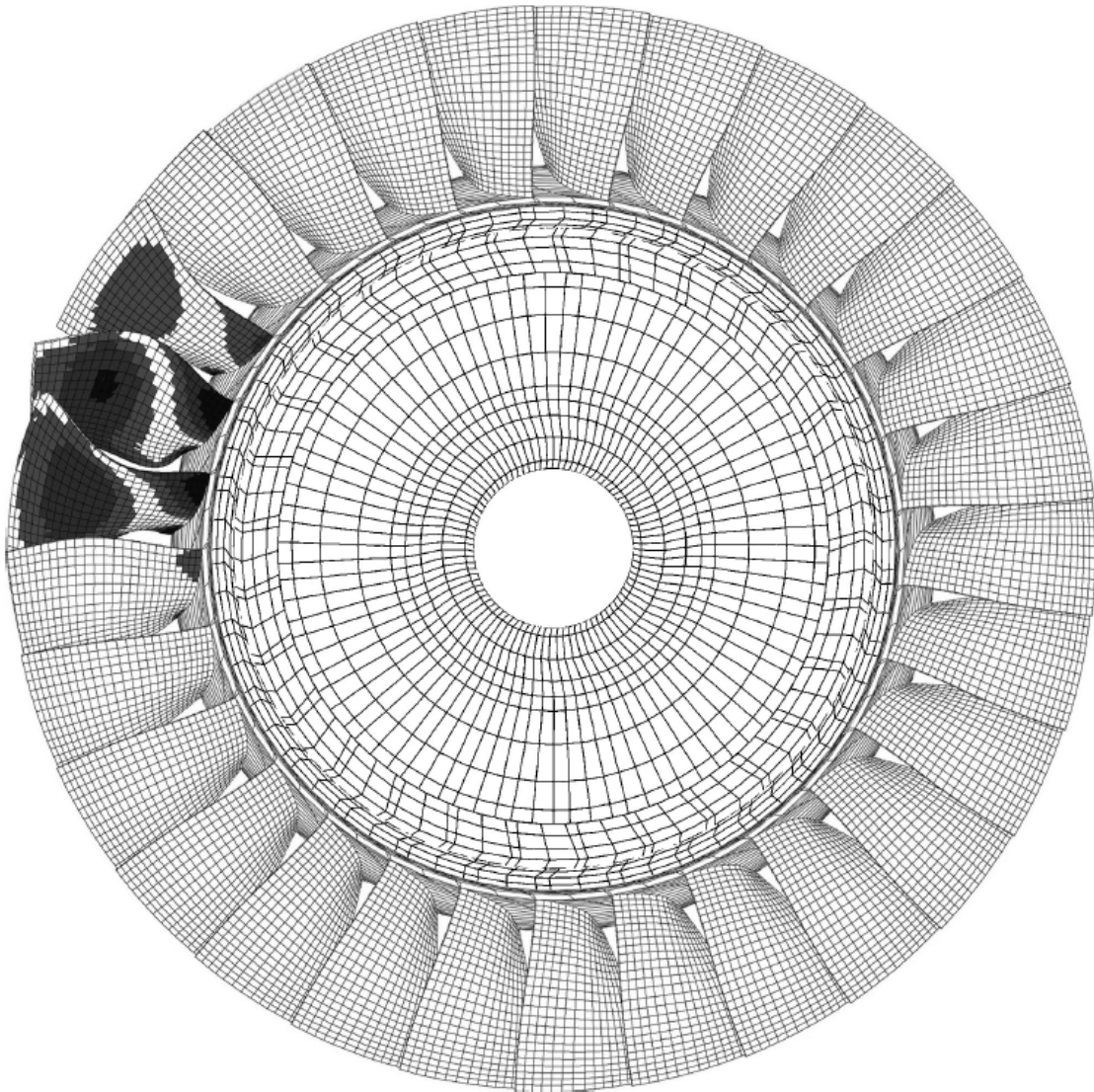


Figure 2.19 Localized mode shape of a mistuned bladed disk; Castanier et al(2006)

In the case of cyclic symmetry models (Figure 2.18), one section of the bladed disk is enough to simulate efficiently the full bladed disk. Mistuning cause a drastic change in the bladed disk dynamics and breaks the cyclic symmetry as well (Figure 2.19). Therefore modeling only one sector is not enough in this case, full bladed disk model is needed. Even with accelerated Monte Carlo simulation, these finite element models are heavy and non-feasible to simulate. Hence, the emergence of reduced order models comes into use for these heavy and complicated analyses.

3 OBJECTIVES

In the initial stages of the aeromechanical design of turbine blades, the modal frequency check of 3d finite element models is important to be within the acceptable range in the Campbell diagram. The cooled turbine models consist of intricate geometric details which make the model heavy and time consuming. It is also difficult to perform for all nodal diameters.

The main objective of this project is to obtain lower size 3d finite element turbine blade models but yet with sufficient accuracy for modal analyses. The following are the sub-objectives to achieve this goal:

- Understand the influence of cooling features in the dynamic analyses for different cooled turbine blades
- Obtaining the mesh detailing impact on the analyses and providing a process for cooled turbine reduced mesh sizes
- Benchmarking the modeling process with the fully detailed model to address the industrial applicability of dynamic analyses with simplified models in terms of computational cost and accuracy

4 METHOD OF ATTACK

To get an insight about the contribution of the cooling features in the estimation of modal frequencies, two representative cooled turbine blade models are assessed. The process of solving and estimation is illustrated in Figure 4.1. The history of the geometry details for the models is available in an NX CAD model. Different models are created depending on the detailing. The finite element mesh of the different models is created. The models do not have the disk in it.

Before doing the modal analysis, a mesh sensitivity study is performed so that the mesh influence in the modal analysis is eliminated. This mesh sensitivity study is done in the model without any cooling core.

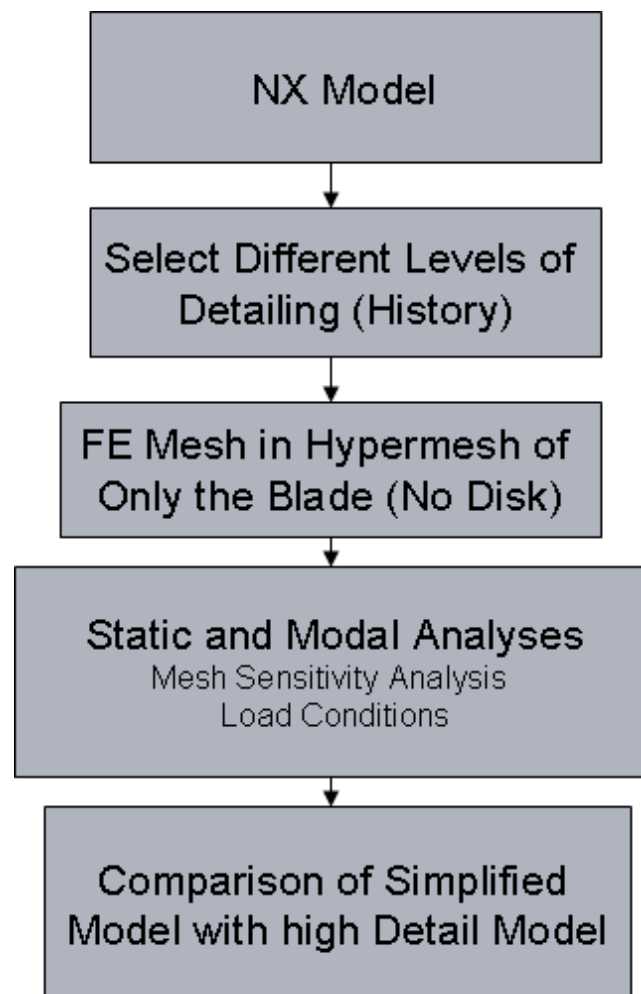


Figure 4.1 Flow chart of the process

Different loading conditions are taken into consideration while doing the modal analysis. These modal analyses are performed to make sure that the difference in the results is only due to geometrical features and independent of boundary conditions.

Finally, the full modal analysis is performed with actual loading conditions and constraints. The different models are compared with the original model with the complete cooling details. The results of the comparison will provide an insight into whether they are dependent on the mass properties or the stiffness properties. The importance of geometric details in the modal analyses of a particular test case is noted and discussed. The possibility of modifying the density on the non-cooled blade to achieve dynamics characteristics of the cooled blade is brought up.

Guidelines are formulated from the results and discussions for future improvements on the estimation of modal frequencies.

5 TEST CASE

The first two stages turbine blades from SGT-750 are considered as test cases. These are part of the Compressor Turbine (CT) as they drive the compressor of the engine. The air that is used in the cooling of these turbine blades is drawn from the compressor section. The first stage blade is referred to as CT1 and the second stage blade is referred to as CT2. These two blades exhibit cooling features that are quite different and thus both of them are studied.

5.1 First Stage Turbine Blade CT1

5.1.1 Cooling Features

The first turbine stage (CT1) is modeled and the cooling features that are of primary importance are cooling matrix, rib turbulator, film cooling holes and multi flow cooling path. The models are developed based on the detailing of the geometry involved in the turbine blade.

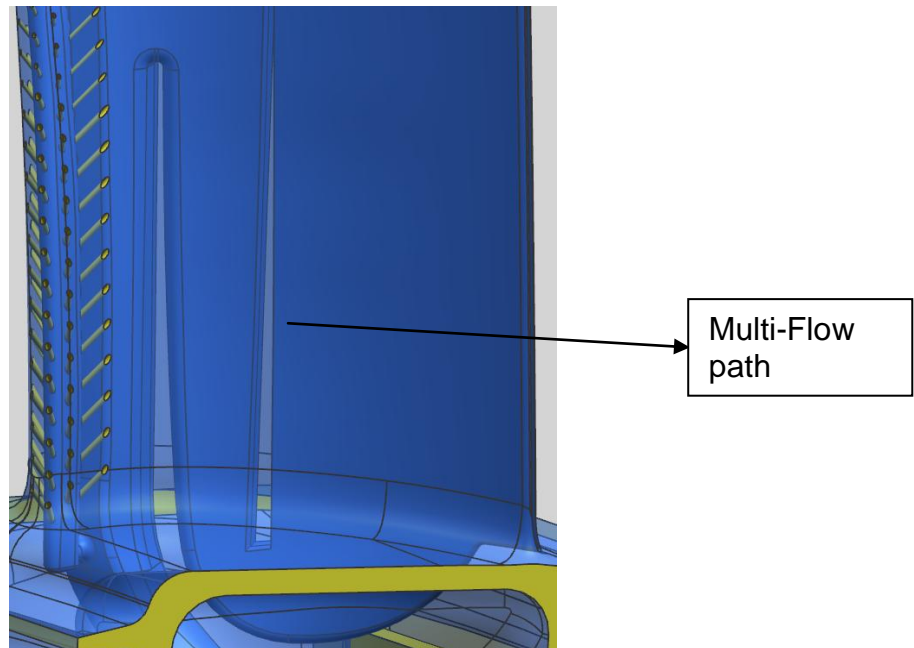


Figure 5.1 Multi flow cooling path in turbine blade

The *multi-flow cooling path* is the flow path for the cooling air in the turbine blade (Figure 5.1). The flow path is designed so that the heat transfer surface area is increased due to the zig-zag shape.

The most complicated cooling feature in this blade is the presence of the cooling matrix (Figure 5.2). It consists of two layers of oppositely angled longitudinal ribs.

The cooling matrix provides the structure with an additional stiffness which is otherwise deprived from the structure due to the removal of material to form the cooling flow path. The rib turbulators are small indentation marked on the surface of the flow path which assists in increasing the turbulence of the flow inside the cooling passage. The turbulence, separation of flow and also the mixing of the flow are the characteristics which contribute to the heat transfer occurring on the flow passage.

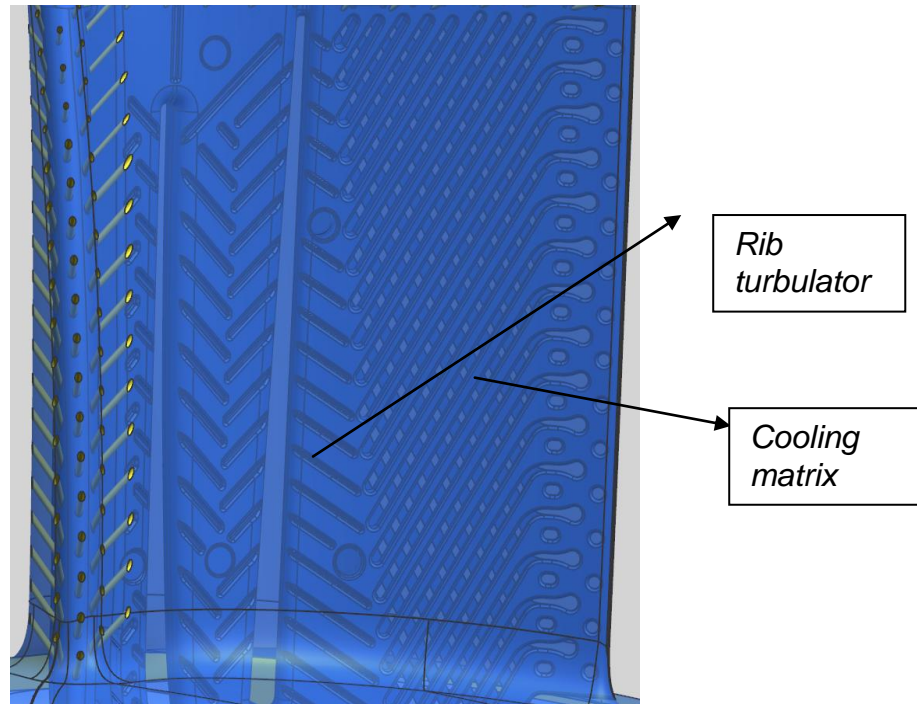


Figure 5.2 Rib turbulator and cooling matrix of CT1 blade

The next important feature of cooling in the blade is the presence of the film cooling holes (Figure 5.3). The film cooling holes are also a complicated feature as they can be skewed relative to the surface of the airfoil. They are present on the leading edge and also on the tip of the turbine blade.

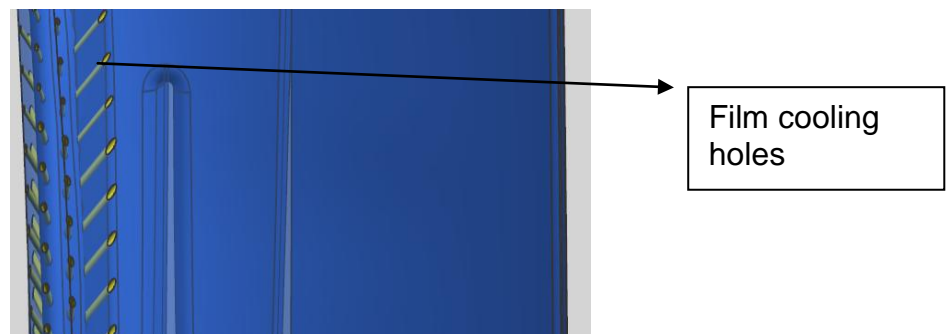


Figure 5.3 Presence of film cooling holes in CT1 blade

In this cooling method, the air is extracted from the compressor section and it maneuvers through the cooling path and as it exits through the film cooling holes, it forms a film of cooling air on the airfoil surface. It protects the surface from the hot gas exiting from the combustor.

5.1.2 NX Models from Detail History

The models are generated from the history of geometric detailing provided in the design of the blade. The models are generated in such a way that the influence of the features with respect to the variation in the modal frequency is identified. From the cooling features mentioned earlier, the models are formulated accordingly.

5.1.2.1 Model 1

The first model that was considered for calculation of modal frequencies had no cooling path or feature in it. It is also referred to as *no cooling model* (Figure 5.4). The model had solid inside and it does not have any hollow structure inside the model.

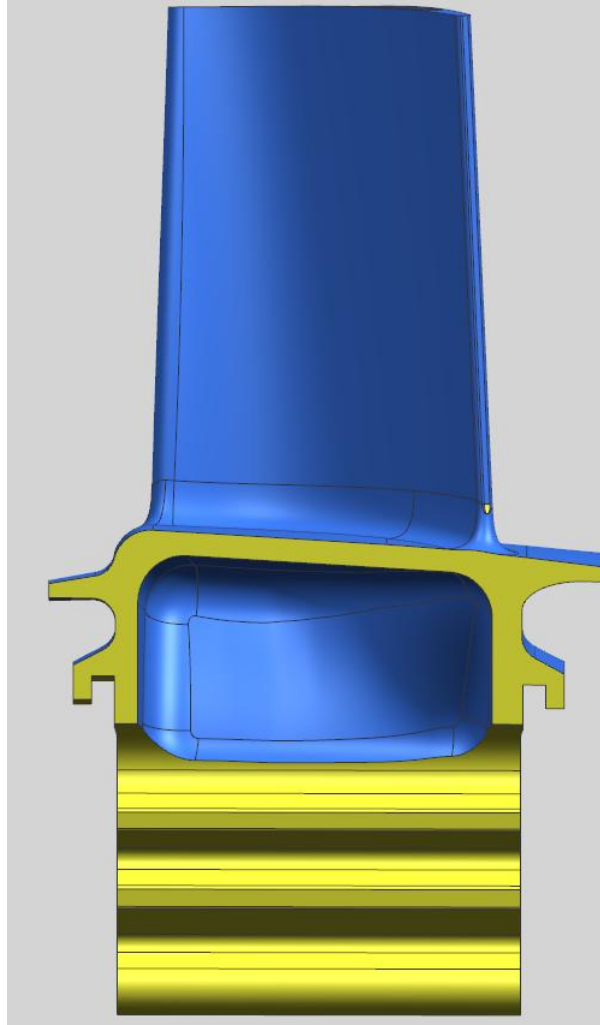


Figure 5.4 CT1 Model 1(no cooling features)

5.1.2.2 Model 2

The second model generated includes the multi flow path only (Figure 5.5). All the other features contributing to the cooling of the turbine were not involved in this model.

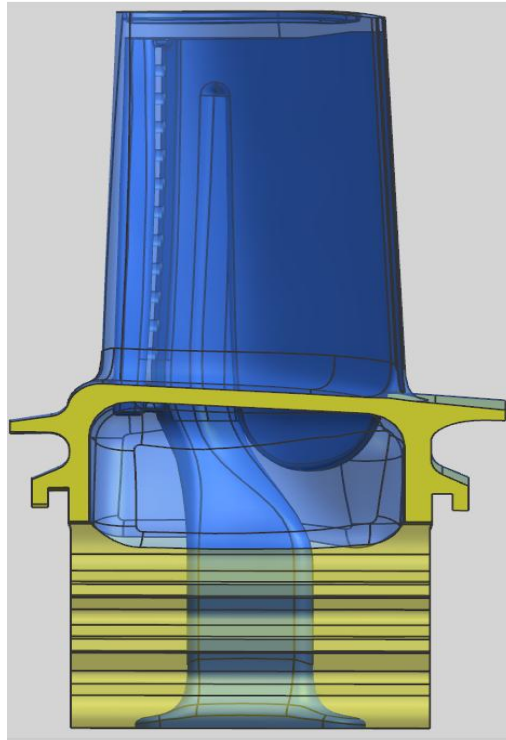


Figure 5.5 CT1 Model 2 (only multi-flow cooling path)

5.1.2.3 Model 3

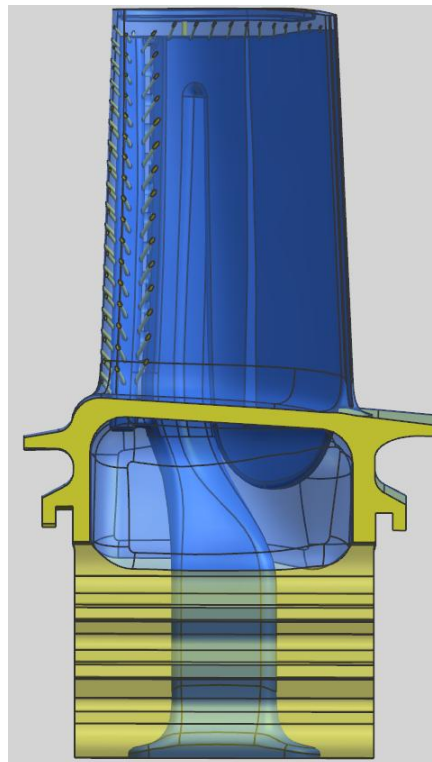


Figure 5.6 CT1 Model 3 (multi-flow path and film cooling holes)

The model 3 has the multi flow path and the film cooling holes at the leading edge and also the tip of the turbine blade (Figure 5.6). This model was generated to find out the influence of film cooling holes and also the multi-flow path with respect to the modal frequencies for different modes.

5.1.2.4 Model 4

The cooling features that are involved in this model are the cooling matrix and multi flow path (Figure 5.7). But, in this model, there was no film cooling holes and no rib turbulators. This model is created to determine the influence of the cooling matrix.

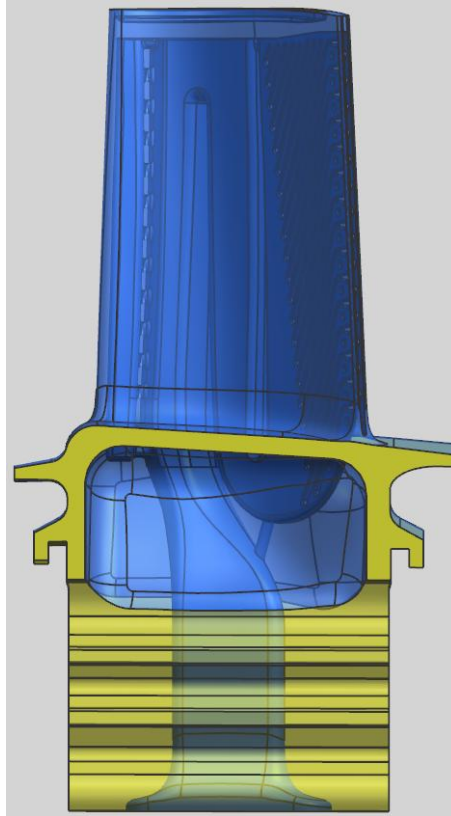


Figure 5.7 CT1 Model 4 (multi-flow path and cooling matrix)

5.1.2.5 Model 5

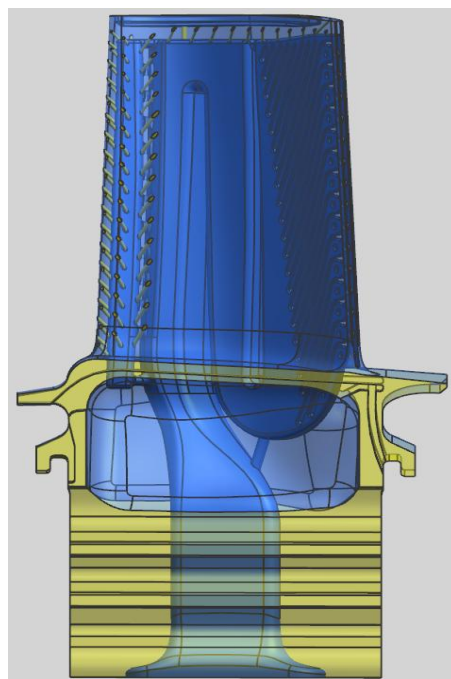


Figure 5.8 CT1 model 5 (multi-flow path, film cooling and cooling matrix)

Figure 5.8 illustrates the cooling features in model 5, which include the cooling matrix, film cooling holes and multi flow path. The only cooling feature that is not present in this model is the rib turbulators. The model was generated to identify the influence rib turbulators with respect to the modal frequencies for different modes.

5.1.2.6 Model 6

The model has the complete cooling features which consist of cooling matrix, rib turbulators, film cooling holes and the multi flow path (Figure 5.9). This model is generated as a benchmark model for the other models to be compared with. The properties used to compare the models are the modal frequencies and mode shapes at the lower modes.

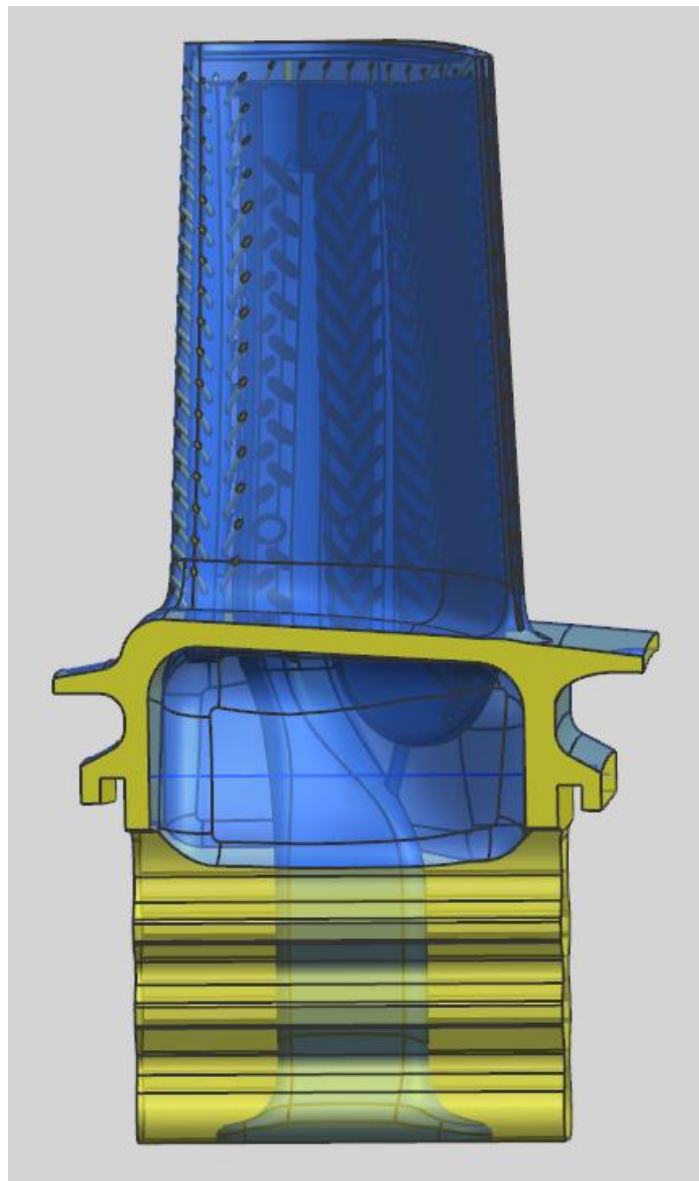


Figure 5.9 CT1 Model 6 (all cooling features)

The loading conditions and constraints are varied for the different models and the modal analyses are solved in Abaqus. The results will be discussed in the subsequent chapters. A mesh sensitivity study will also be presented later.

5.2 Second Stage Turbine Blade CT2

5.2.1 Cooling Features

The cooling features of the second stage turbine blade consist of ribs, rib turbulators and trailing edge cutback (Figure 5.10). The turbine blade in this stage has less intricate geometrical features than the first stage turbine blade. On the other hand, the size and the twist available in this blade are comparatively more pronounced than in the first stage turbine blade.

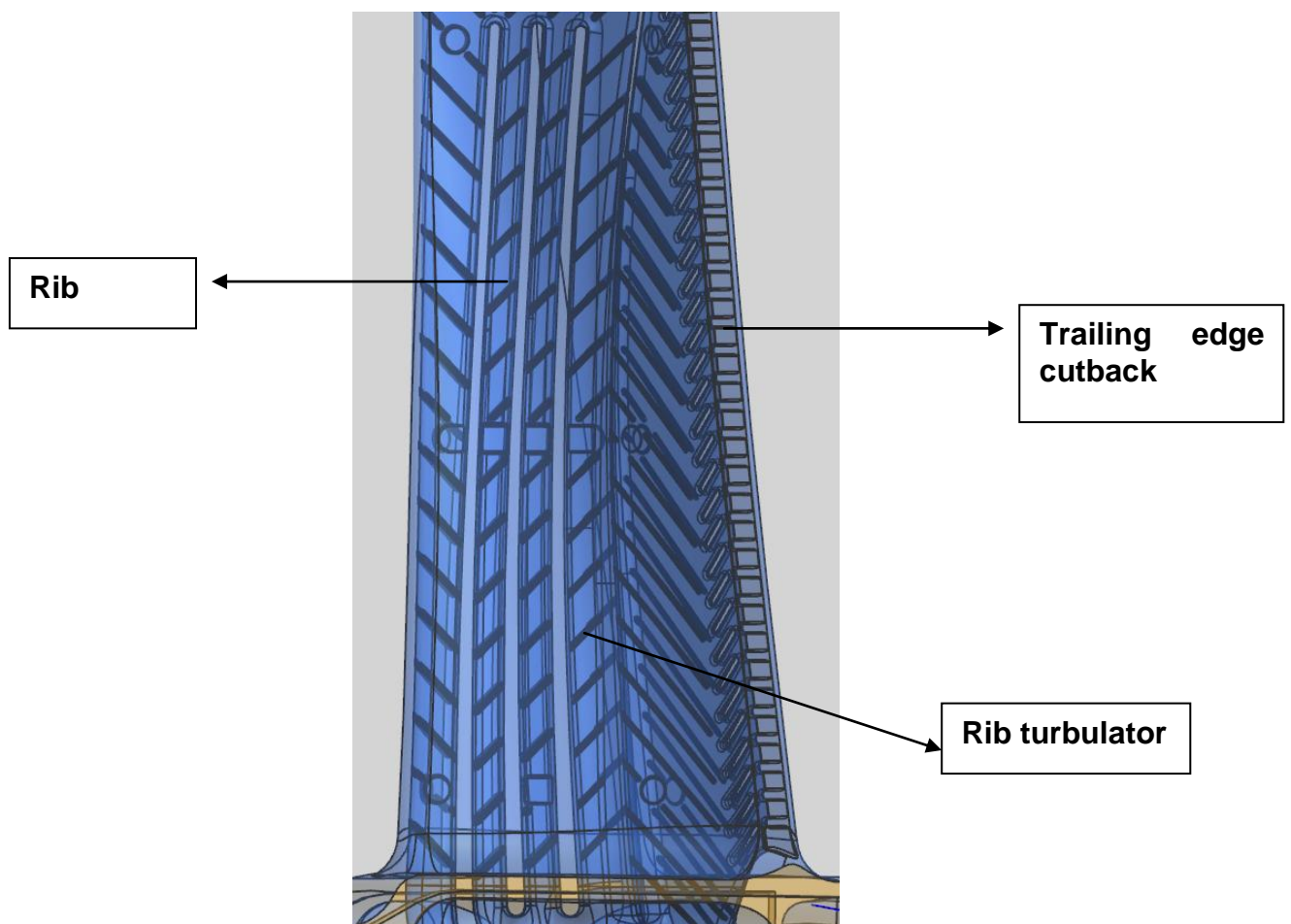


Figure 5.10 CT2 cooling features

The ribs are a very important cooling feature in this blade. The ribs compensate for the structural weakening that is caused by the introduction of the cooling flow path. The trailing edge ejection is the cooling technique that is used in the area where the temperature gradient is high but the transfer surface area is low. This could cause many complications. In that case, the trailing edge cutback profile supports the purpose to compensate the increase of transfer surface area and also increases the structural weakening caused by the trailing edge ejection profile.

The rib turbulator in this model enhances the turbulence of the cooling flow. However, these structures are intricate and have much detailing which makes meshing and solving complicated in this section.

5.2.2 NX Models from Detail History

The NX models are formed according to the history of the detailing created for the cooling path. The ribs, rib turbulator and trailing edge cutback are some of the important cooling features that are involved in this model. The influence of the cooling features on the modal frequencies of different modes is the motive for developing the different models.

5.2.2.1 Model 1

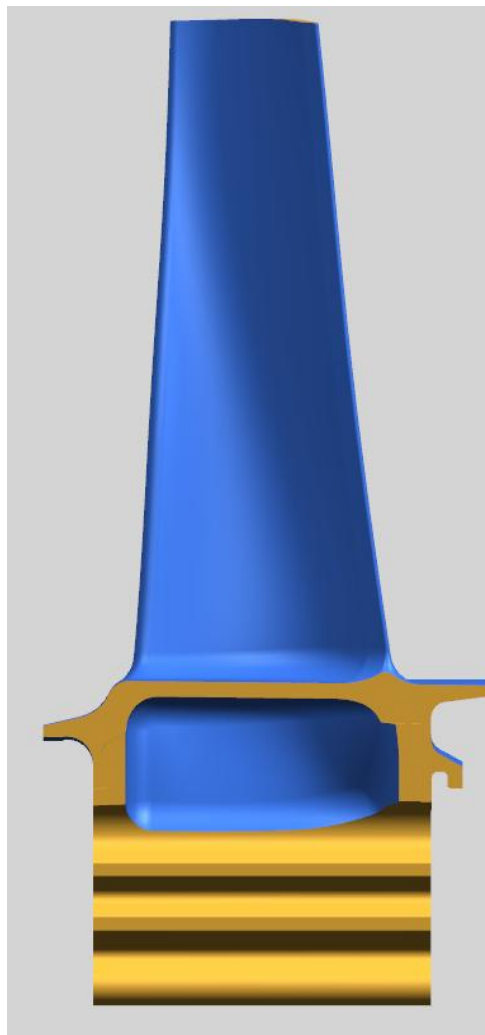


Figure 5.11 CT2 Model 1 (no cooling)

There is no cooling core in this model (Figure 5.11). This is solid in nature and it does not have any holes or hollow partition in it. The trailing edge has the tapered part and the trailing edge is closed. This model is the simplest model to mesh and solve. It is used here to show its deviation with respect to the model with the complete cooling core.

5.2.2.2 Model 2

This model has the multi flow cooling path with ribs introduced to increase the heat transfer surface area and also to increase the effective length of the flow path (Figure 5.12). The ribs are the cooling feature that provides structural strengthening.

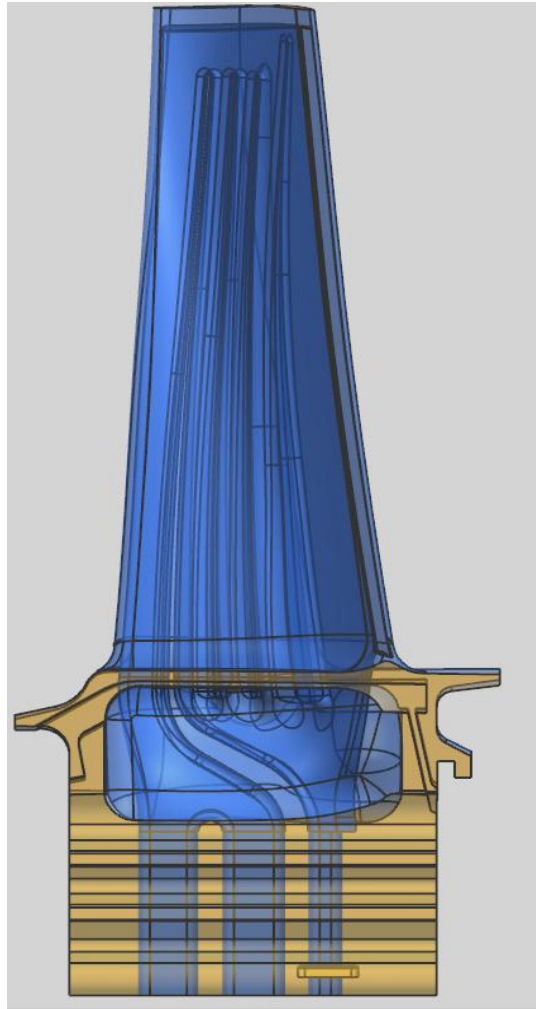


Figure 5.12 CT2 Model 2 (multi-flow cooling path and ribs)

5.2.2.3 Model 3

The cooling features that are available in this model are the ribs, multi flow path and also the trailing edge cutback which are shown in Figure 5.13. The trailing edge cutback is the additional cooling feature that is implemented in this model. The direction of the wedge shaped surfaces in the trailing edge region is perpendicular to the radial direction of the model.

This model is generated in order to investigate the influence of trailing edge cutback with respect to the modal frequencies.

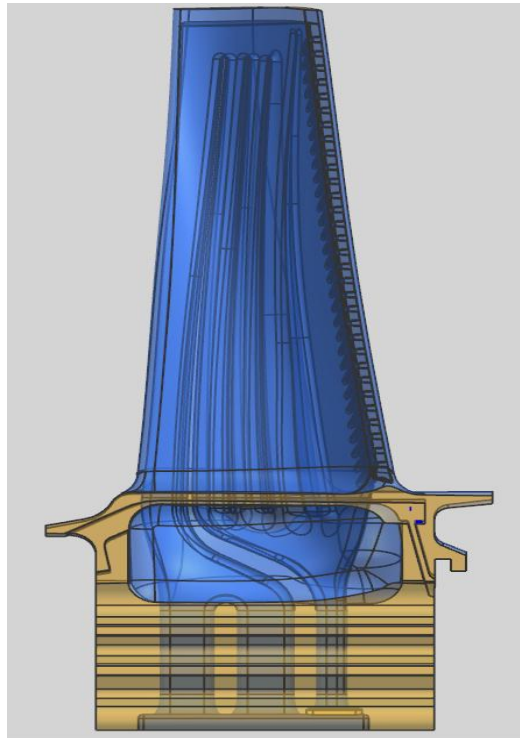


Figure 5.13 CT2 Model 3 (multi-flow path, ribs and trailing edge cutback)

5.2.2.4 Model 4

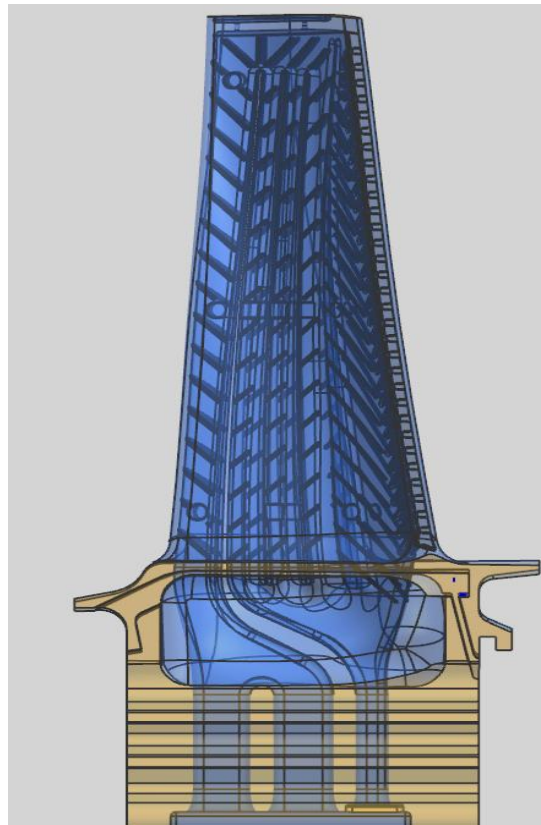


Figure 5.14 CT2 Model 4 (complete cooling core)

This model is the complete cooling core model. In this model (Figure 5.14), all the cooling features are implemented. Ribs, multi flow path, rib turbulators and trailing edge cutback are some of the important cooling features that are available here.

Rib turbulators are small indentation patterns that are present in the multi flow cooling path. This cooling feature creates turbulence for the cooling flow.

6 RESULTS AND DISCUSSION

6.1 Mesh Sensitivity Analysis

The CT1 turbine blade is here used to perform a mesh sensitivity study. The mesh sensitivity study is a process through which a robust mesh optimization is done so that there is no mesh influence or minimum influence towards the modal frequencies. The model that is used for the mesh sensitivity analysis is Model 1 of CT1, i.e., without cooling core.

In this process, Model 1 is divided into three individual components and the components are named as airfoil, root and platform. This is illustrated in Figure 6.1.

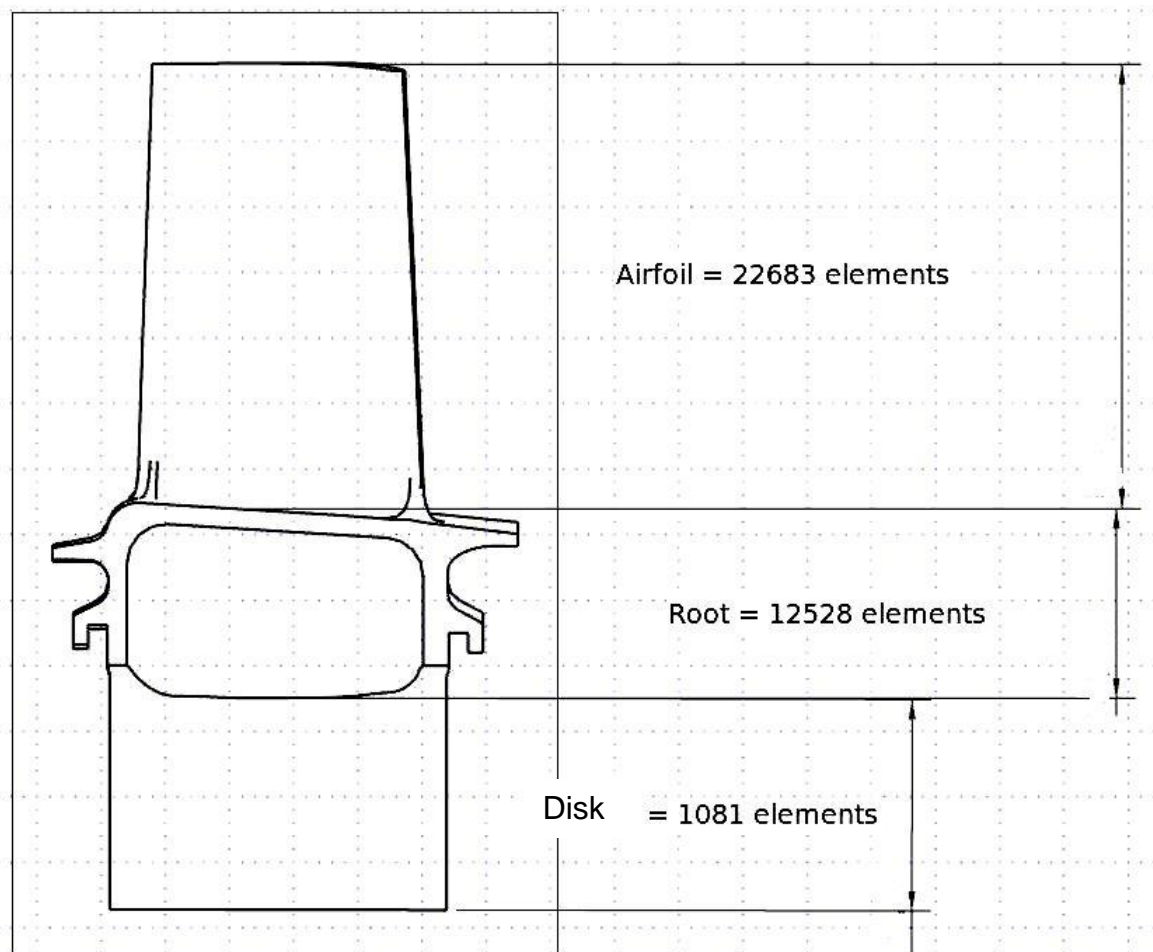


Figure 6.1 Components selected for meshing process

The airfoil region that is developed in the model is from the tip of the blade to the platform of the blade. The root region is from the platform of the blade to the fir tree region of the blade. The disk region is named after the region that has the fir-tree structure and this structure connects the disk with blade. The disk region is the region that is fixed and this constraint is implemented for the modal analysis.

The loading condition that is used is the centrifugal load. The constraint implemented is the fixation of the disk part. The mesh sensitivity analysis starts

with a coarse mesh and progresses towards a fine mesh with smaller size elements.

6.1.1 Root Optimization

The different models are generated from the coarse mesh and it progresses to finer mesh sizes. The convergence criterion that is involved in this process is the modal frequency. Figure 6.2 shows the frequency convergence of mode 1 with increasing mesh size. The highlighted model in red color denotes the model that is the coarser model considered converged. The number of elements in that region is around 50,000 elements. The size and the number of elements are not changed in the disk region which has fixed number of elements. It was found that the graphs followed a similar pattern for higher modes. The graphs are presented in Appendix B. Initially, the number of elements in the root region is varied with the other two regions having fixed number of elements which is displayed in Figure 6.2. After the optimization of the root region, the number of elements in the airfoil region is varied with the optimized number of elements in the root region and the fixed number of elements in the disk region which is displayed in Figure 6.3.

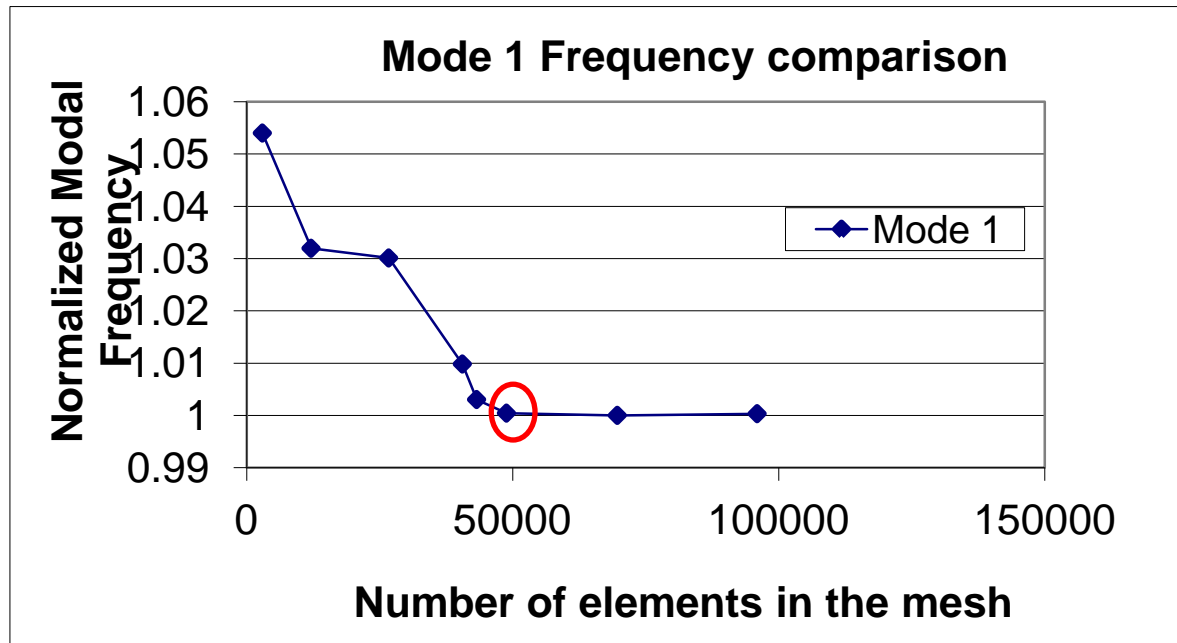


Figure 6.2 Root mesh convergence; mode 1; CT1

6.1.2 Airfoil Optimization

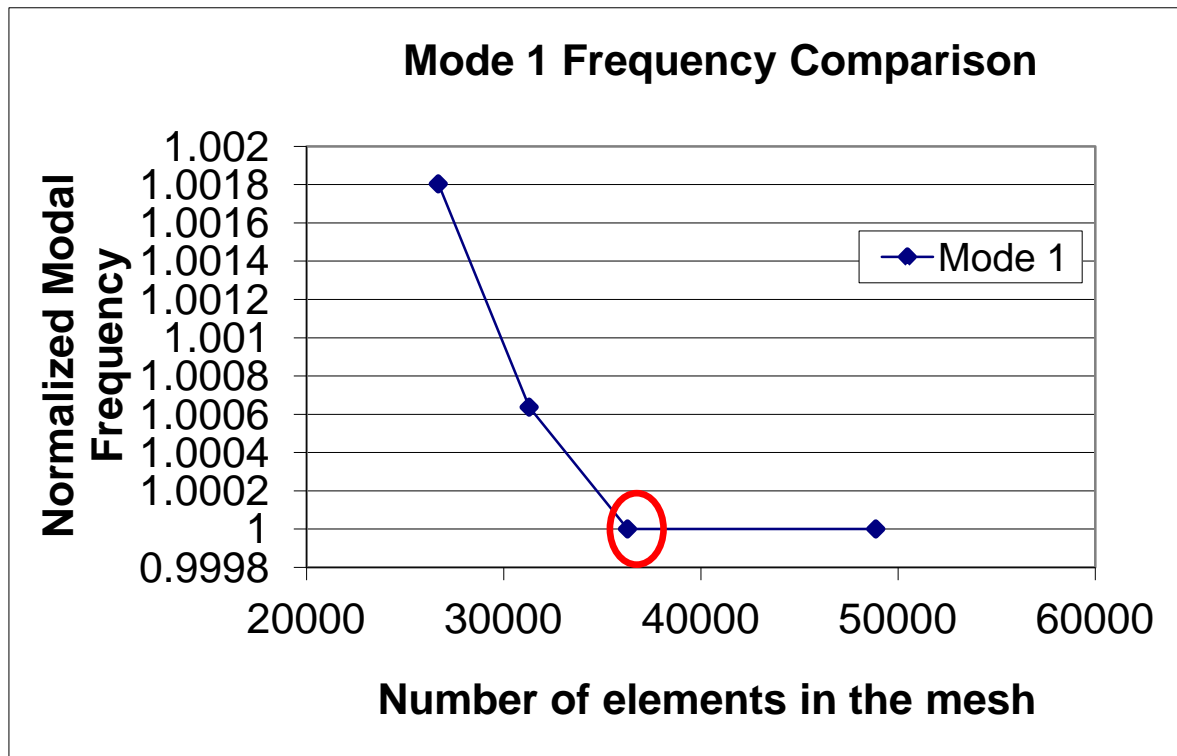


Figure 6.3 Airfoil optimization process of Mode 2

The converged model that is taken from the process of root optimization is used as a base model for optimizing the airfoil mesh (Figure 6.3). In this optimization process, the number of elements is reduced by increasing the size of the elements in the airfoil region. The optimized model is highlighted in Figure 6.3 and considers the optimum mesh density in the airfoil and root. The mesh size of this final model will be kept almost constant for the models with different geometries.

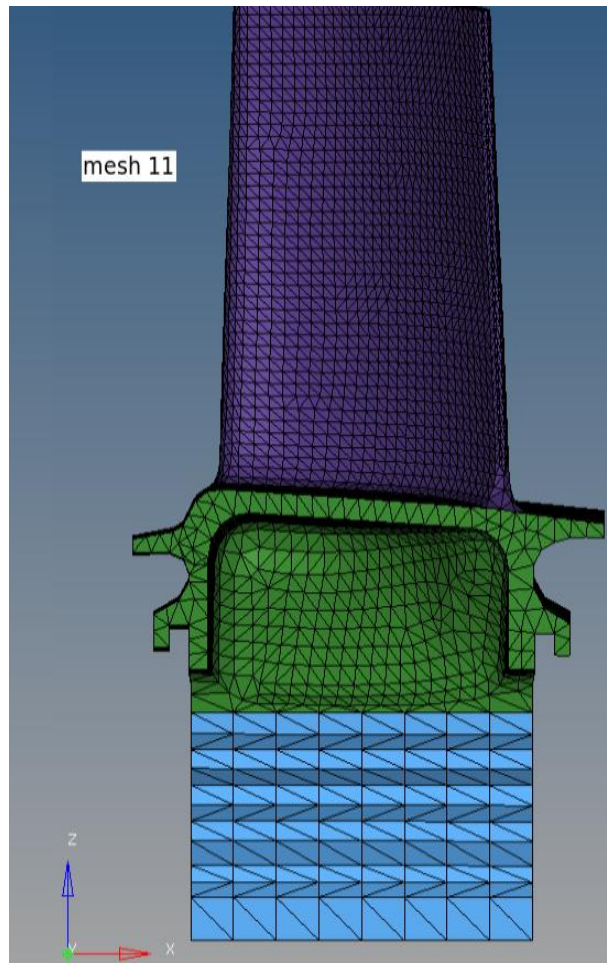


Figure 6.4 Final model from the mesh sensitivity analysis

The final mesh that is optimized from the process is displayed in Figure 6.4. The model is generated using the Hypermesh software and the number of elements, nodes and degrees of freedom are optimized (minimized) with the modal frequencies kept as criteria.

6.2 CT1 Modal Analysis

The 6 different models are taken from NX and imported in to Hypermesh. The meshing is done in Hypermesh with loading conditions and constraints being applied to the model. The solver deck is taken into Abaqus to be solved for modal analysis.

The modal analysis of the CT1 models is performed with different loading conditions and constraints. The loading conditions that are applied are the following:

- Temperature profile
- Seal pressure
- Centrifugal load and
- Fixation of disk

6.2.1 Temperature Profile

The temperature profile is implemented as a loading condition. The temperature profile corresponds to an operating condition ~30 degree higher than nominal temperature (Figure 6.5). The loading condition is obtained from an already existing Abaqus output file (.odb).

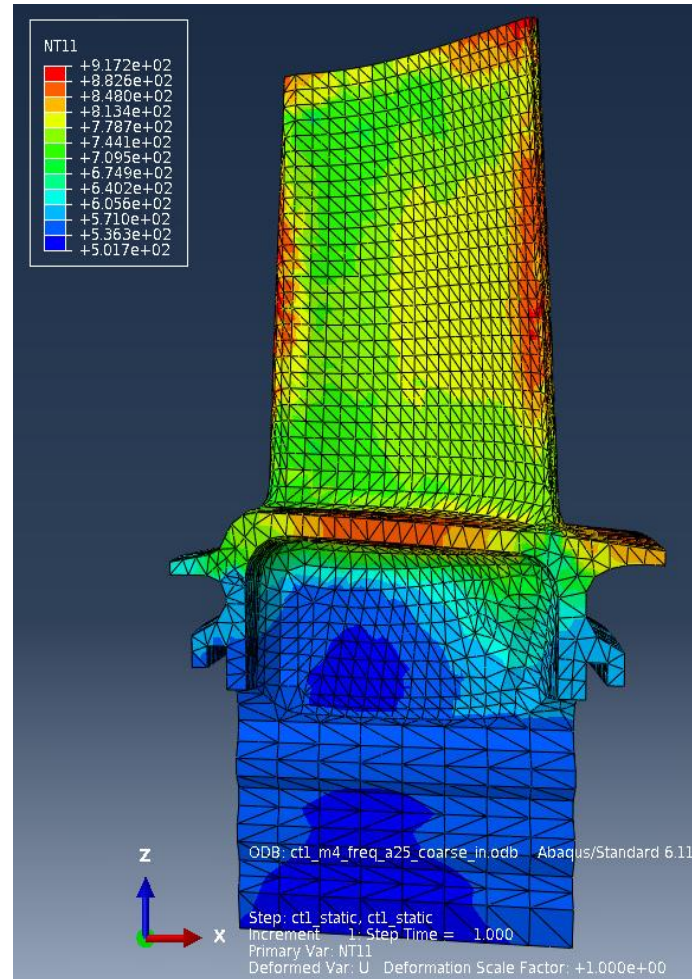


Figure 6.5 Temperature profile from Abaqus result file

The temperature distribution is included as a loading condition directly into the Abaqus solver input file after it is created from Hypermesh. The manner it is implemented is explained in Appendix A.

6.2.2 Centrifugal Load

The centrifugal load is an important loading condition which contributes to the modal frequency. The origin of this loading is due to the rotational effects of the turbine which pulls the structure in the radial direction. The centrifugal load is applied to all the mesh elements.

6.2.3 Seal Pressure

The seal pressure is applied in the platform region where the seals are connected to the blade and the pressure values vary from the leading edge and the trailing edge of the blade (Figure 6.6). The pressure is applied at the radial direction of the rotating blade. The elements at which the pressures are applied are the connecting elements between the blade and the seal plates. It is applied on only one face for the above mentioned elements.

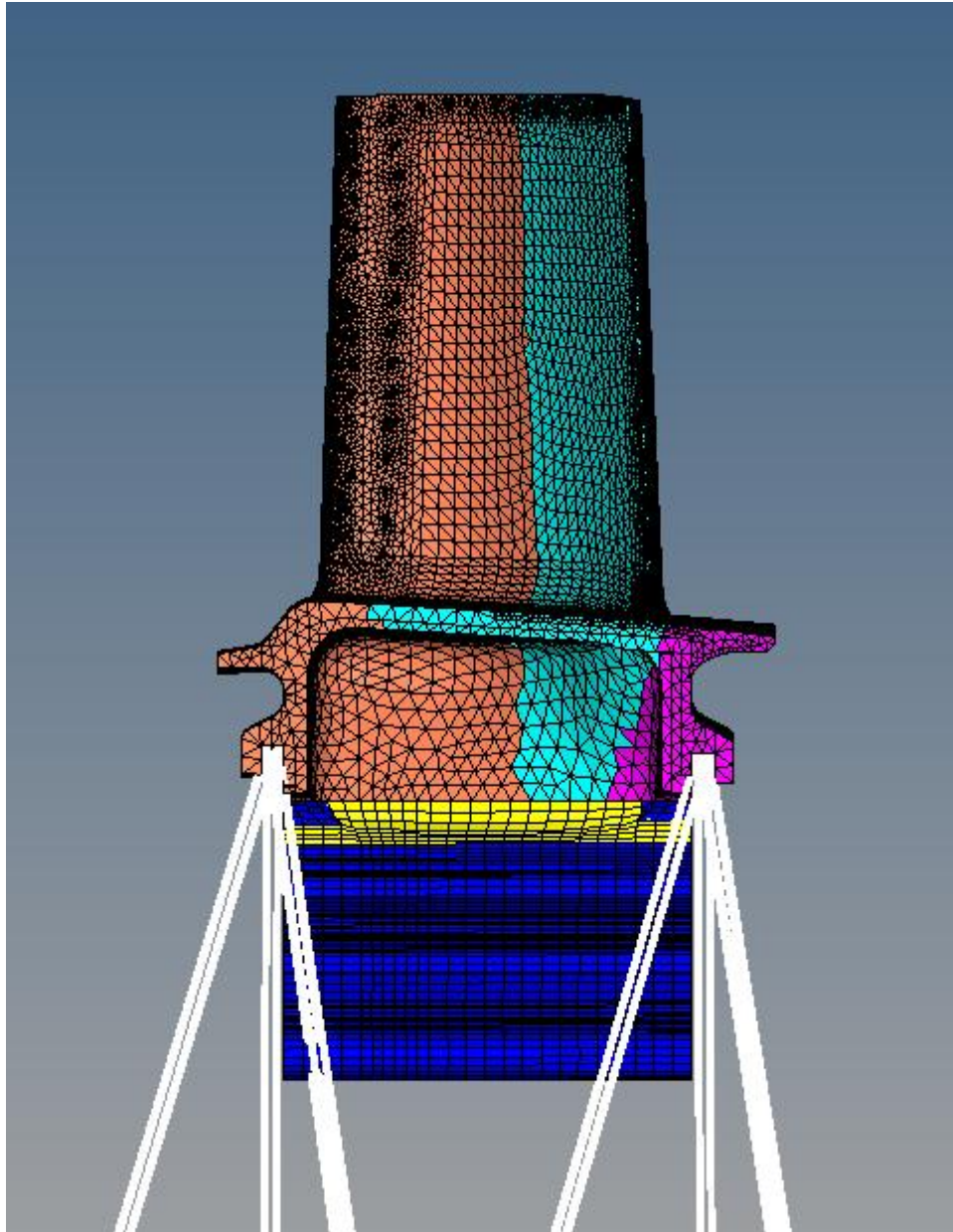


Figure 6.6 Seal pressure boundary conditions

6.2.4 Disk Fixation

Since no disk is included, the main constraint at the fir tree region in the three axes is because in reality, the root flanks are in contact with the disk slot which makes them fullr restrained. The fixation of the disk elements is explained in detail in Appendix A.

6.2.5 Full Modal Analysis

After application of all the loads a static analysis is performed, including large deformation. The pre-stressed matrices are then the basis for the further modal analysis. The normalized modal frequencies of the first five mode frequencies of the 6 different geometries are plotted in Figure 6.7. The normalized modal frequencies are formulated from the ratio of modal frequencies of the different models to the modal frequencies of the converged (full-featured) model.

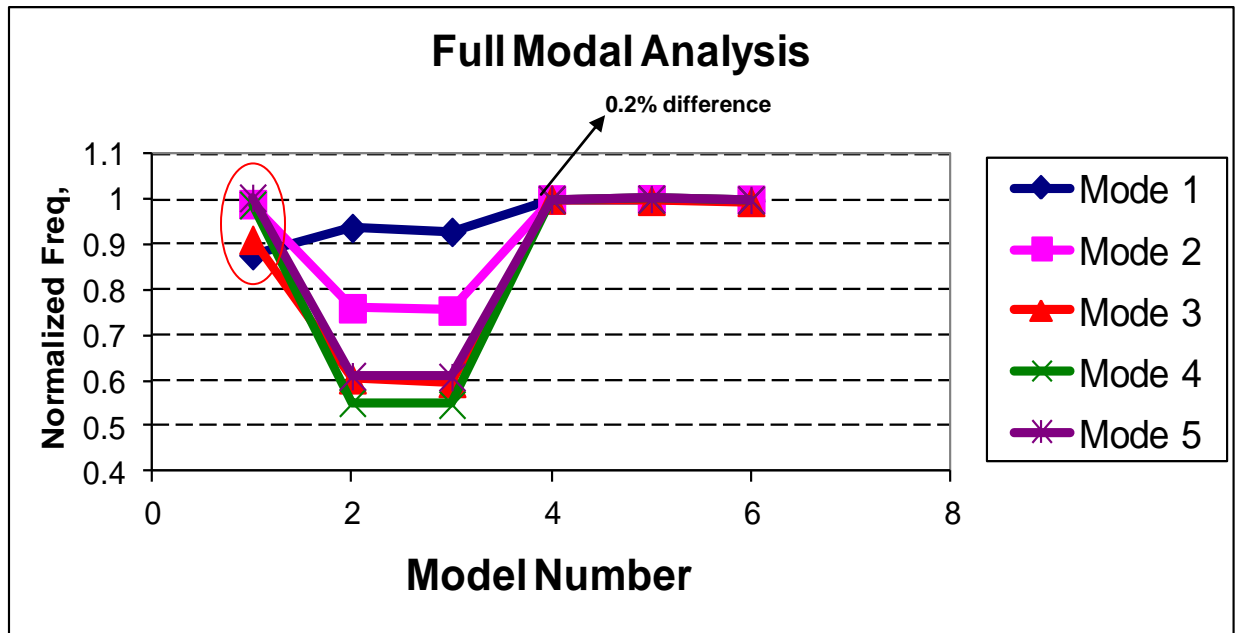


Figure 6.7 Full modal analysis results

From the plot it is inferred that Model 4 could be considered as size optimized model, having only around 0.2% difference compared to the complete cooling core model. Model 4 consists of cooling matrix and multi flow path. However, it does not have film cooling holes and rib turbulators, making it much lighter and easier to model than the fully detailed one.

One important observation is that model 1 (no cooling core) does not show a huge difference to the more detailed models 4-6. The difference is around 12% for modes 1 and 3, but much lower for modes 2, 4 and 5. This is rather surprising, since this model has absolutely no details of the inner cooling core, making this model the easiest model to mesh, and the fastest to compute.

Concerning models 2 and 3 most of the resulting mode frequencies are much lower than the detailed model. This shows the importance of modeling the cooling matrix as none of these two models consider it. This means that the blade is lacking the added stiffness and thus much lower frequencies are obtained.

6.2.5.1 Modal Analysis with Only Centrifugal Load

The modal analysis is done with only centrifugal load as the loading condition and the constraints are fixation of disk and initial temperature. The loading conditions that are not involved in this modal analysis are seal pressure and temperature profile. Even when different set of loads are applied, the results show the same trends as in the actual loading case, as seen in Figure 6.8.

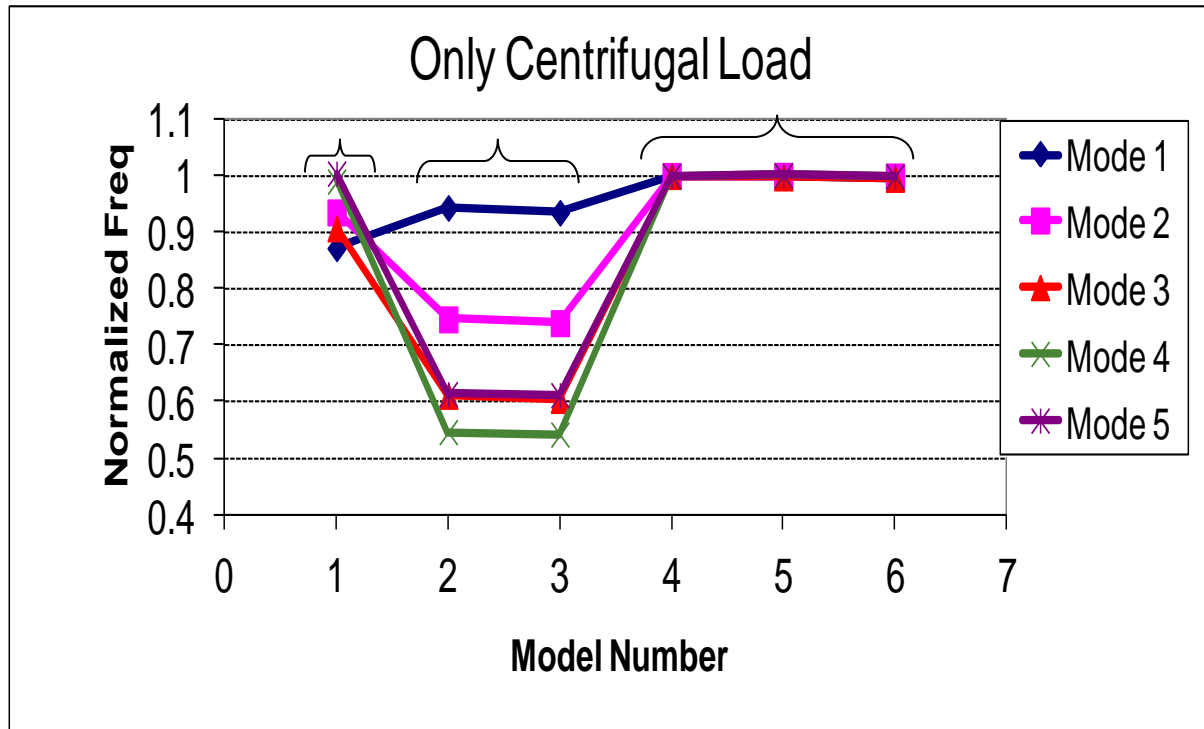


Figure 6.8 Modal analysis with centrifugal load only

The models can be grouped into 3 groups: group 1 is only model 1; group 2 includes models 2 and 3 and group 3 will involve the models with converged modal frequencies (models 4, 5 and 6).

6.2.5.2 Mode shape Comparison

From the results of the modal analysis, three groups are formed. The mode shapes are analyzed to provide further insight to the behavior of models 2 and 3.

It is seen that for mode 1, there is already a difference between group 2 and the rest of the groups (Figure 6.9). For higher modes, the second group is deviating even more from the other two groups with mode shapes localized to the trailing edge. Group 2 (models 2 and 3) is highlighted in Figure 6.10. There is structural weakening due to the absence of the cooling matrix. This creates localized mode shapes at the trailing edge.

In contrast, all the first five mode shapes are predicted accurately with both groups 1 and 3. This means that even the non-cooled model (completely solid core) predicts well the main characteristics of the dynamics of the blade. It can also be noted that details such as rib turbulators and film cooling holes have almost no effect on frequencies and mode shapes for the first five modes.

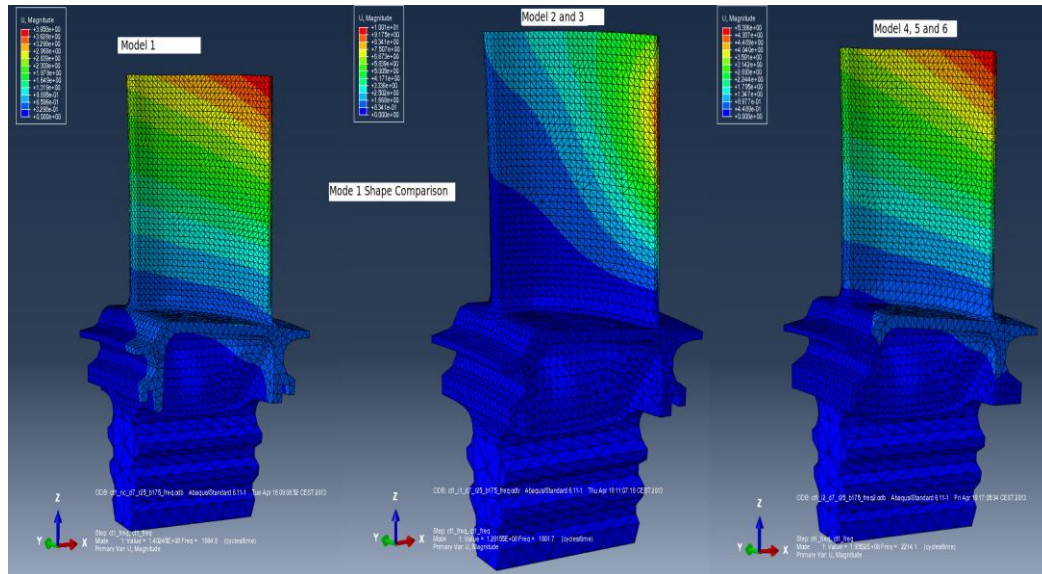
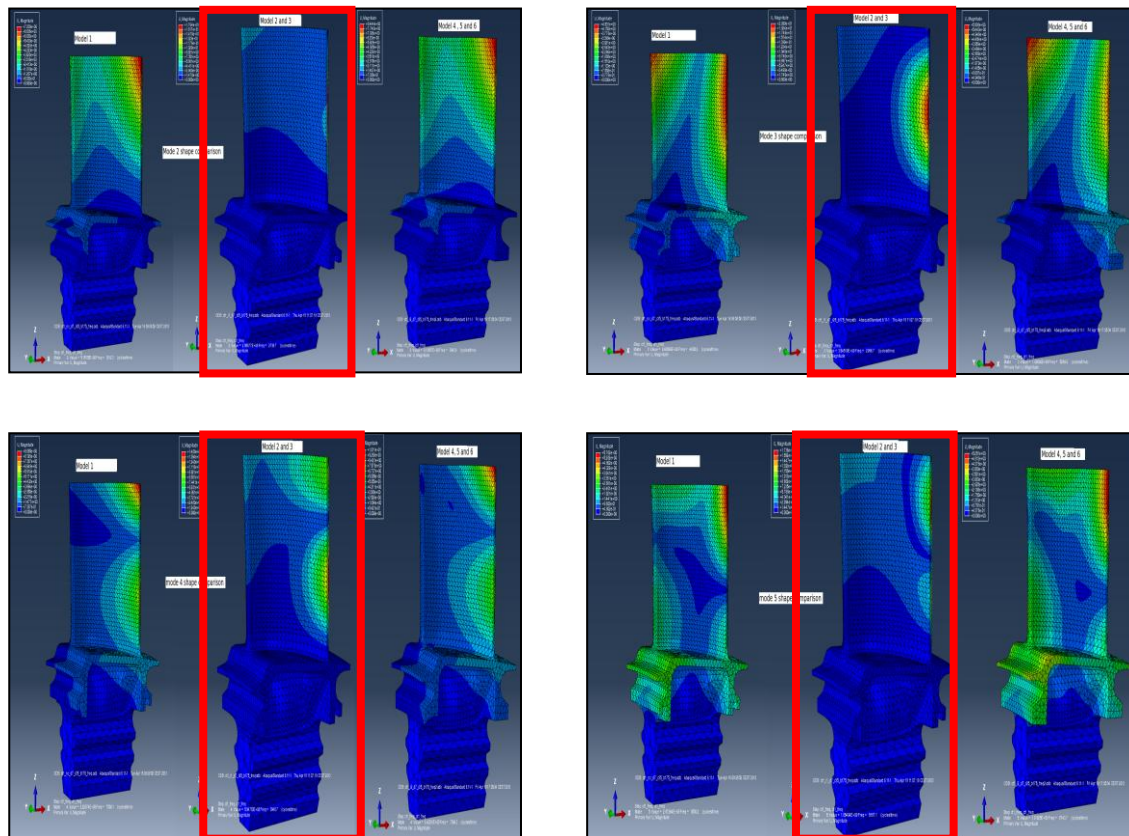


Figure 6.9 Mode 1 from the modal analysis



Models 2 and 3 → No Cooling Matrix

Figure 6.10 Mode 2 to Mode 5 from the modal analysis; CT1

6.2.6 Mass Scaling

As observed before, the mode shapes are well described by the non-cooling model but the frequencies are generally underestimated. The differences of the

models in frequency depend on the model deviations in mass and stiffness. One parameter that could be corrected is the density, so that the mass of the cooled and the non-cooled model is the same. A simple manner to derive a new density could be done by knowing the ratio of the blade volume, as explained in equations 6.1 to 6.3.

$$M_{\text{model1}} = M_{\text{model6}} \quad (6.1)$$

$$\rho_{\text{model1}} * V_{\text{model1}} = \rho_{\text{model6}} * V_{\text{model6}} \quad (6.2)$$

$$\rho_{\text{model1}} = (\rho_{\text{model6}} * V_{\text{model6}}) / V_{\text{model1}} \quad (6.3)$$

The corrected density of model 1 is determined and included in the solver deck and then the modal analysis is re-run in Abaqus. The volume of the geometries is taken from the NX model.

The frequency variation with model 6 as reference is plotted in Figure 6.11. In this case an unadjusted model 1 (no cooling) and a model 1 with new density (or mass scaled) are compared. It is obvious that the frequencies of all the modes are shifted down. With this shift, the first three modes are closer to the zero line (more accurate) but modes 4 and 5 become farther apart. One could say that modes 1, 2 and 3 are globally mass dominated. However, once the modes become more localized, then the global density change does not correlate in a positive manner. One can then think on a local change of the density depending on the real geometry difference vs. the simplified model. For example, it could be inferred that the mass near the trailing edge region should not be removed.

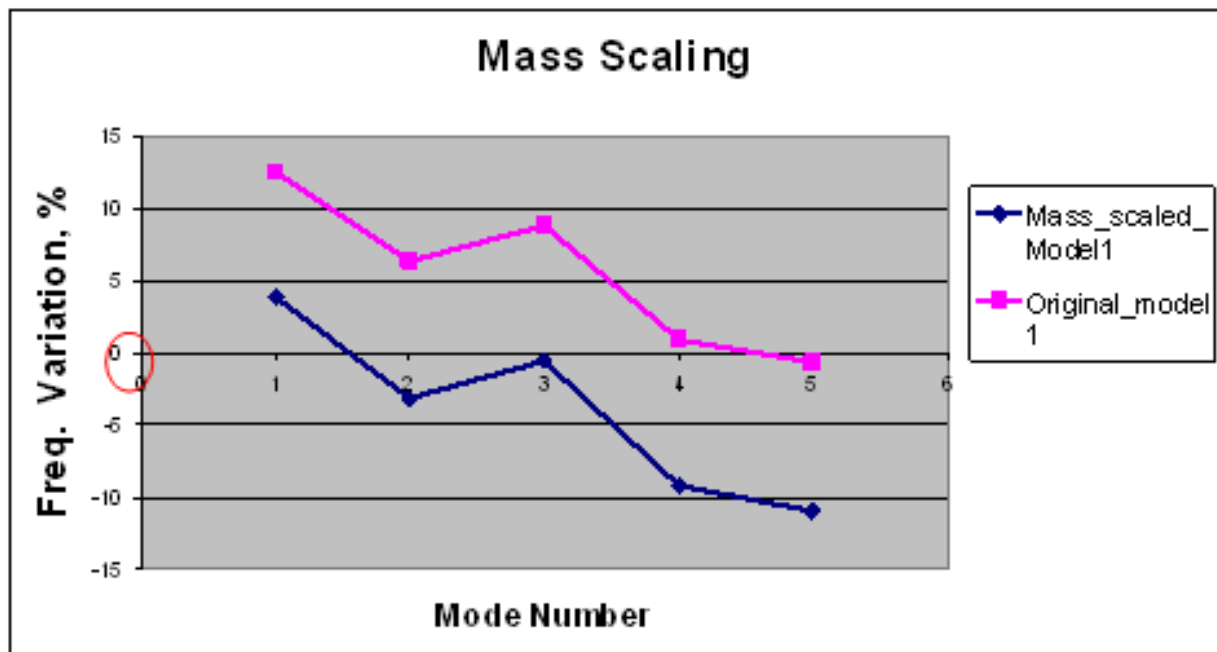


Figure 6.11 Mass scaling on CT1

The best solution from the mass scaling process is that an optimization of distributed density modifications could provide better result.

6.3 CT2 Modal Analysis

For the second stage turbine blade models, the loads are implemented in a similar manner as in CT1, but with data related to CT2. All the loads are implemented in this model, but the values are different. In this modal analysis, there is no experimentation with different loading conditions. It is simulated with the full loading condition and after that mass scaling was practiced in the model with no cooling core. The material that is implemented in the CT2 modal analysis is a single crystal alloy. In the case of single crystal alloy, a crystal orientation vector has to be defined and used for all the elements in the mesh.

6.3.1 Full Modal Analysis

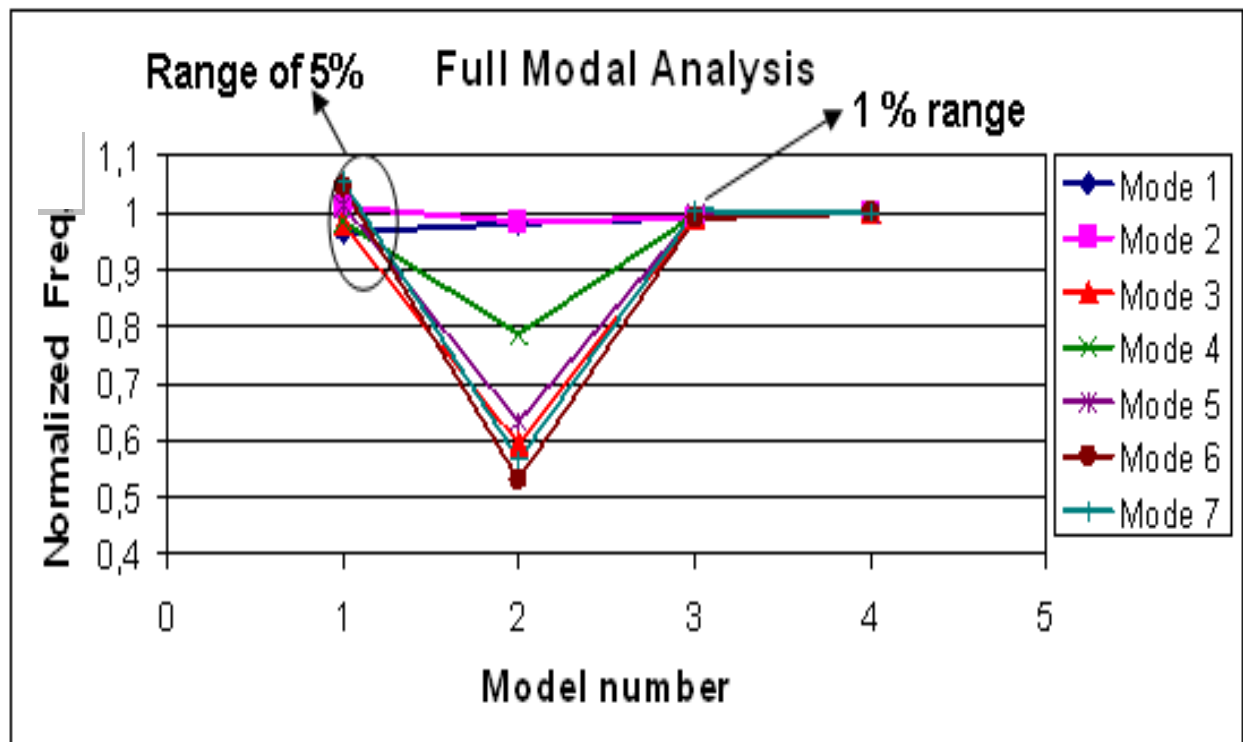


Figure 6.12 Full modal analysis results with respect to model number

The 4 different models are plotted with their respective modal frequencies in Figure 6.12. It is shown that models 3 and 4 can be considered converged models with a maximum difference with the reference model (6) within the range of 1%. Model 2 (ribs and no trailing edge cutback) is not in sync with the rest of the models. Model 1 (no cooling) shows a difference of around 5% for all the first 7 modes when compared to the converged model. This frequency range was attained in CT1 only after the mass scaling. So, this is one of the surprising features exhibited by the modal analysis of CT2. The difference in size of the models can be observed in Figure 6.13, where the number of elements is included. It is clear that model 3 is almost one-third of the size of model 4 but with only a difference of 1% in the modal frequencies. This clearly shows the potential of the FE size reduction for the dynamics check in an early stage of the design.

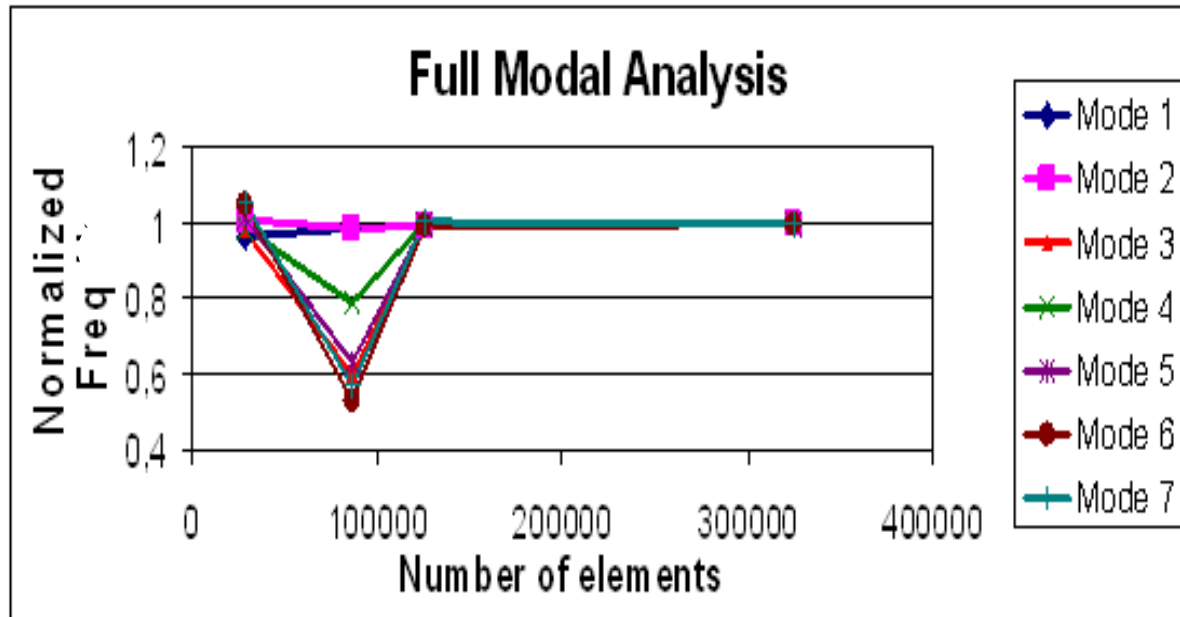


Figure 6.13 Full Modal Analysis result with respect to number of elements

6.3.2 Mode Shape Comparison

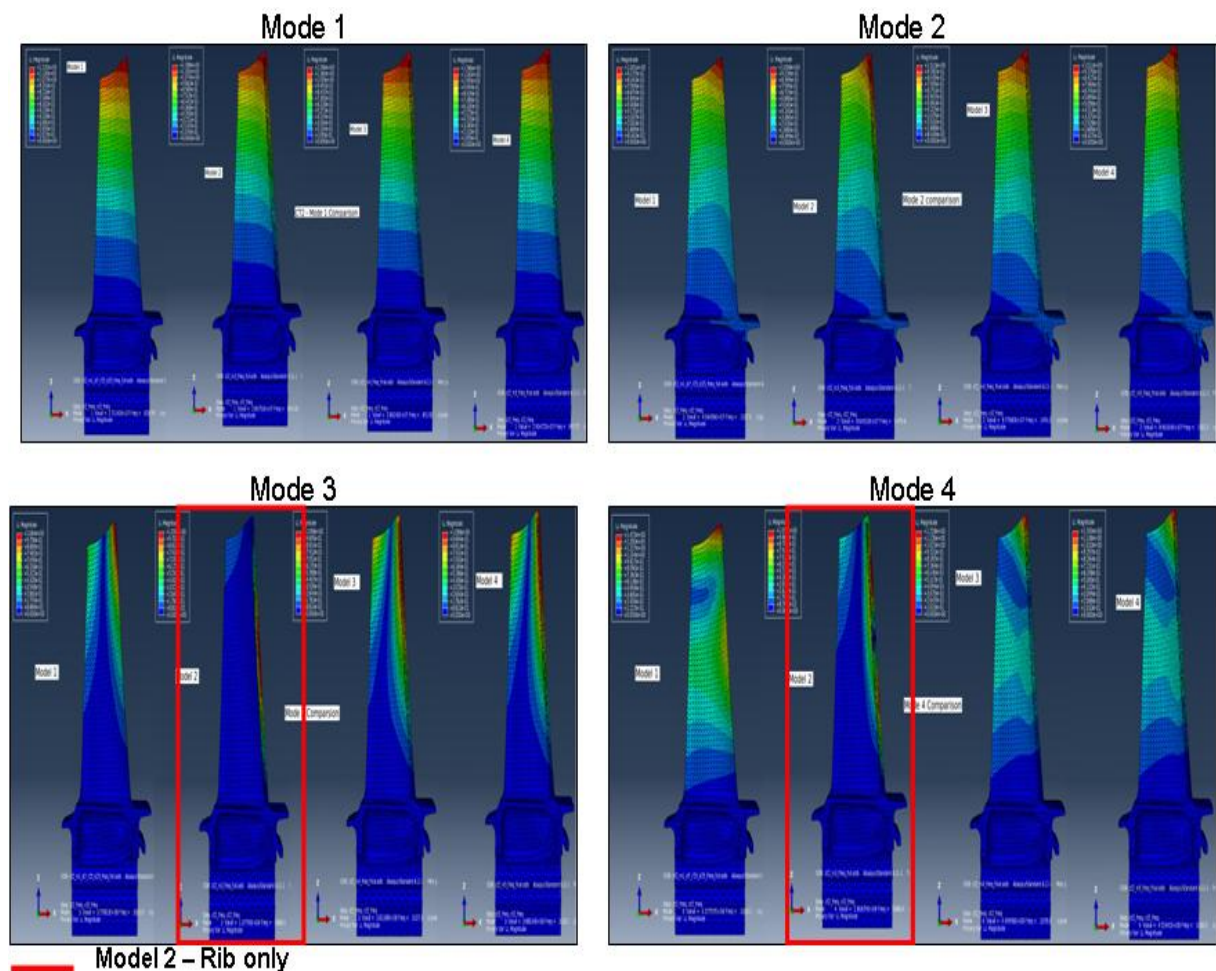


Figure 6.14 Mode 1 to 4 from full modal analysis results; models 1 to 4 from left to right

- The mode shape comparison between the models is presented in Figure 6.14 and Figure 6.15. Model 2, having the worst accuracy in frequency is

highlighted. It can be seen that mode shapes 1 and 2 are predicted well by all the models, with only a slight difference in model 2. However, the comparison of higher mode shapes (3 to 7) highlights the difficulty for model 2 to predict the mode shapes correctly. Instead, with this model, modes are mainly localized to the trailing edge. This is somewhat expected, since for this case the blade does not include the trailing edge cutback structures and consequently there is no support in the trailing edge. This results in an excessively flexible trailing edge region., which is obvious in mode shape 7 (Figure 6.15). The structural weakening in this critical section causes localized mode shapes and also lower frequencies than for the real geometry.

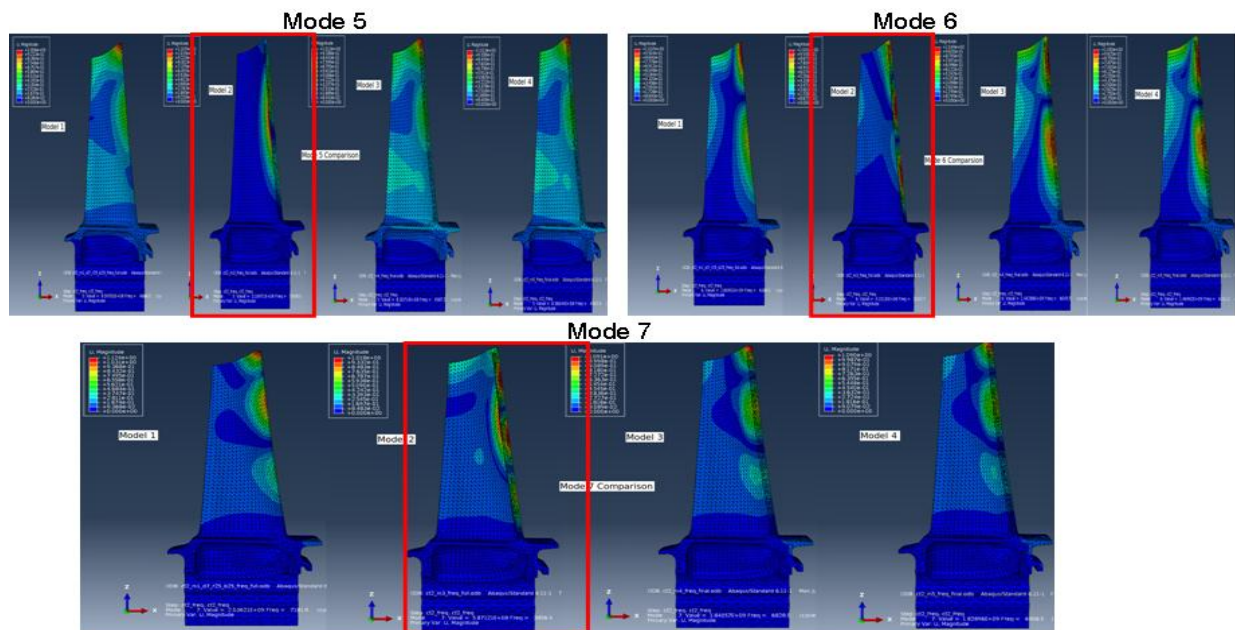


Figure 6.15 Mode shapes 5 to 7 for CT2; models 1 to 4 from left to right

6.3.3 Mass Scaling

Mass scaling is implemented in the CT2 model 1 which has no cooling core. The motive of mass scaling is to study if the modal frequencies would be closer to the converged modal frequencies for the different modes. To achieve this, the density has to be corrected in a similar approach as presented for CT1. In the case of CT2, the mass scaling made the results move farther away from the zero line (Figure 6.16). The original model 1 was already in the frequency range of 5 percent. The mass scaled model 1 moved to a frequency range of 15 percent. Hence, mass scaling is not useful in the case of CT2. This might be due to the fact that in the mass scaling global change of density is introduced into the model which does not provide reasonable results.

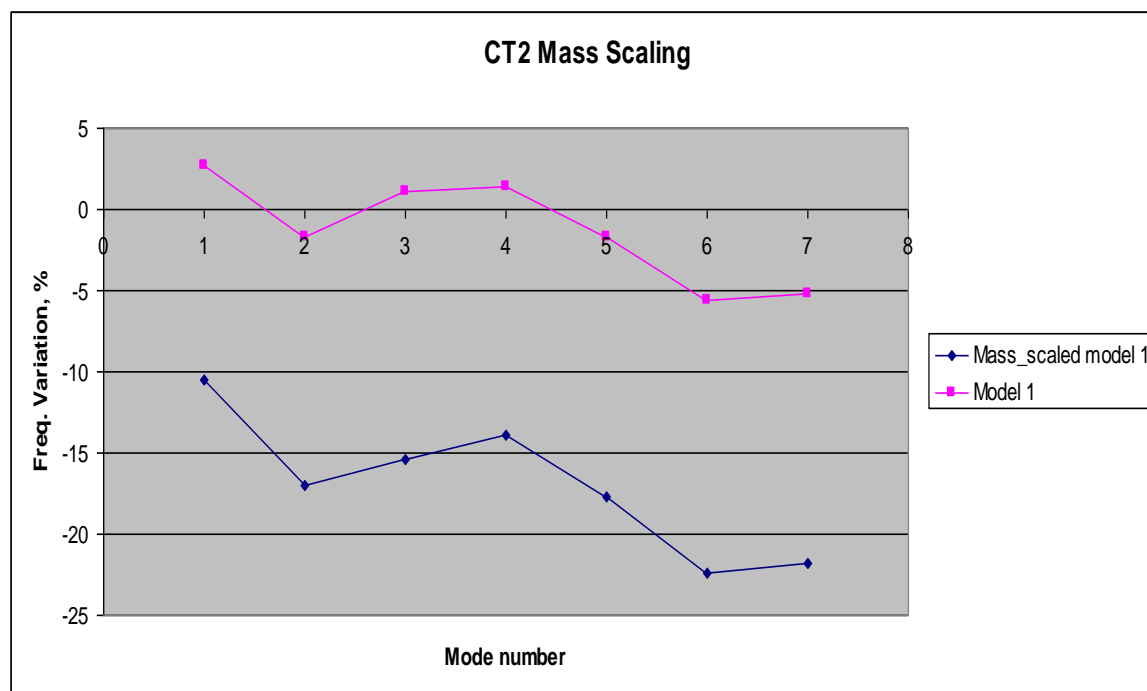


Figure 6.16 Mass scaling results of CT2

7 SUMMARY AND CONCLUSION

A parametric study has been performed in order to understand the effects of internal cooling-related geometrical features on the dynamic analysis of cooled turbine blades. Two distinct cooled blades have been considered for the analyses. One of the blades considered represents a typical cooled design of the first stage rotor blade of a compressor turbine. This blade included as key features the cooling matrix and film cooling. The other blade considered was a typical second stage rotor blade of a compressor turbine. This blade's key cooling features were the ribs and the trailing cutback.

It has been shown that for both blades the presence of turbulators is not required for the dynamic analyses. The frequencies obtained for models without this feature resulted in practically the same frequency and mode shapes as the full model. This is important to note, since the meshing of these details is highly time consuming and also the size of the mesh can be reduced in some cases by a factor of 3.

Especially for the first stage blade, the film cooling holes also represent a detail which does not have a large effect on the prediction of the modal frequencies for first five modes ($<0.2\%$).

The most relevant cooling core features with respect to the dynamics are the cooling matrix, the ribs and the trailing cutback. These features play an important role on the stiffness of the blade and thus the final modal frequencies.

On the other hand, one key observation is that the non-cooled model (solid blade) represents all the lower mode shapes for both blades in a good manner. The shape of the modes is fairly close to that of the fully detailed geometry. The frequency difference obtained for such model was in a range of $\sim 10\%$ for the first stage blade and $\sim 5\%$ for the second stage blade. This observation is quite positive, since not modeling the cooling core at all makes the mesh process substantially easier and also the mesh sizes could be reduced up to a factor of 10. These models could allow quick frequency checks in the very first stages of the design. Additionally, it is brought forward the possibility to improve the accuracy of the solid blade model by changes in density. In the present report, only a global density change was assessed to compensate for the added mass of the solid model. However, it is here proposed to apply localized density changes depending on the geometrical features of each blade.

As a summary of the principal models used in this report that exhibit acceptable performance, Figure 7.1 and Figure 7.2 are included, showcasing the improvement in size depending on included features.

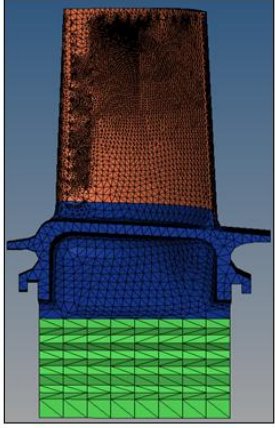
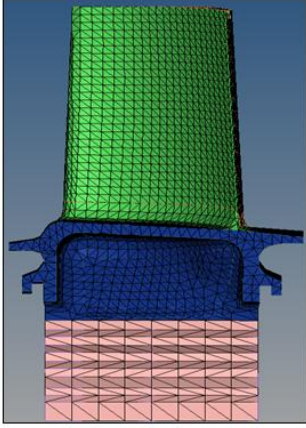
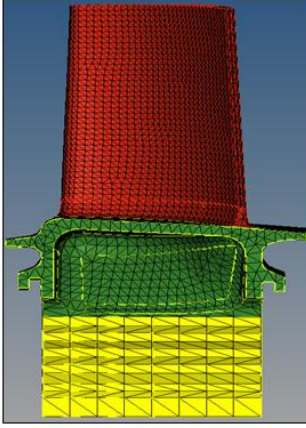
		
Complete cooling model (Model 6)	Simplified cooling model (Model 4)	No cooling model (Model 1)
~860 000 nodes	~ 30 % of original model	~10 % of original model

Figure 7.1 Comparison of CT1 turbine blade models

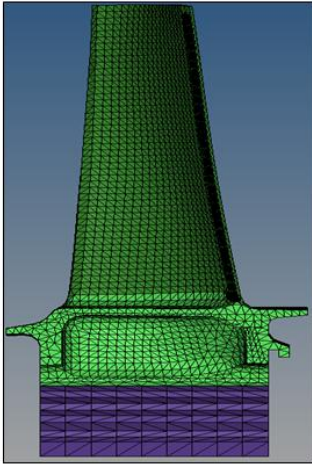
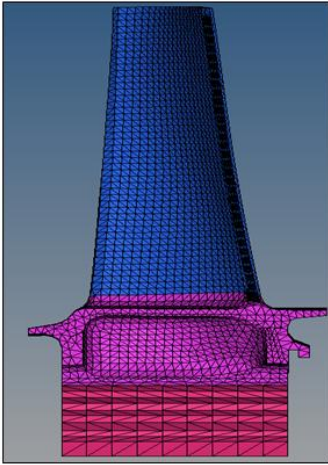
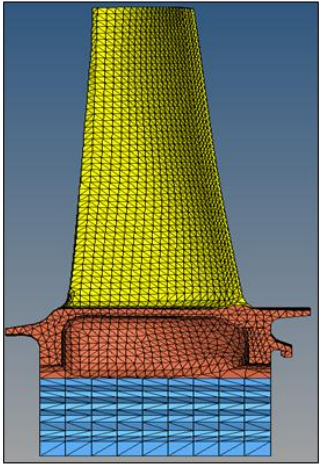
		
Complete cooling model (Model 4)	Simplified Cooling model (Model 3)	No cooling model (Model 1)
~870 000 nodes	~25 % of original model	~10 % of original model

Figure 7.2 Comparison of CT2 turbine cooled blade models

7.1 Future work

This project provides an insight into the influence of different cooling features in the estimation of modal frequencies for two different test cases. This can be implemented in the cooled turbine blades also of other engines.

It is proposed to study local changes of density and possibly stiffness in the non-cooled model in order to obtain improved accuracy with respect to the fully detailed cooled model.

A further reduction in time on the dynamics check can be achieved by the implementation of reduced order modeling, where the 3d Finite Element mesh would not be generated. A schematic of this process is presented in Figure 7.3, where the blade sections would be represented by reduced degrees of freedom. A process like this would highly increase the possibilities of necessary loops in the design chain, allowing sufficient iterations with the aerodynamic and cooling groups.

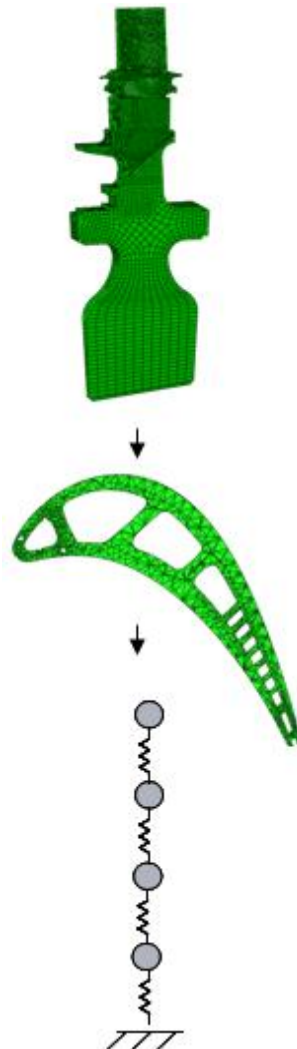


Figure 7.3 Future objectives in a flow chart

8 REFERENCES

Saravanamuttoo H.I.H, Rogers G.F.C, Cohen H., 2001

“Gas Turbine Theory”

Pearson Publication, ISBN-13: 978-0-13-015847-5

Hellberg A., 2011

“SGT-750, 37 MW Gas Turbine 11-IAGT-305”

19th symposium on Industrial applications of gas turbine, Alberta, Canada, 17-19 October 2011

Ganesan V., 2010

“ Gas Turbine”

Pearson publication, ISBN -13: 978-0-07-068192-7

Lakshminarayana.B, 1996

“Turbine Cooling and Heat Transfer,” Fluid Dynamics and Heat Transfer of Turbomachinery, John Wiley, New York, 1996, pp. 597-721; M.G. Dunn, “Convection Heat Transfer and Aerodynamics in Axial Flow Turbines,” ASME Journal of Turbomachinery. 123 no.4 (2001):.637-686.

Je-Chin Han, Wright L.M., 2013

“Enhanced Internal Cooling of Turbine Blade and Vanes”

National energy technology laboratory turbine handbook, 2013

Horbach.T, Schulz.A, Bauer H.J, 2011

“Trailing Edge Film Cooling of Gas Turbine Airfoils – External Cooling Performance of Various Internal Pin Fin Configurations”

Journal of Turbomachinery , 133 no 4 (2011):, 041-006

Sundberg .J, 2005

“Heat Transfer Correlation for Gas Turbine Cooling”

Dissertation in Linkoping University on the work on Siemens, Finspang

Barkanov E., 2001

“Introduction to the Finite Element Method”

Institute of Materials and Structures, Faculty of Engineering, Riga Technical University

Vogt D.,2005

“Experimental Investigation of Three-Dimensional Mechanisms in Low-Pressure Turbine Flutter”

Doctoral thesis dissertation, KTH, Sweden, ISBN-05: 91-7178-034-3

Mayorca M.A., 2011

“Numerical Methods for Turbomachinery Aeromechanical Predictions”

Doctoral thesis dissertation, KTH, Sweden, ISBN-11: 978-91-7501-135-6

Laumert B., Martensson H., Fransson T., 2002

"Investigation of Unsteady Aerodynamic Blade Excitation Mechanisms in a Transonic Turbine Stage Part1: Phenomenological Identification and Classification"

ASME Journal of Turbomachinery, 124 (2002): 419-428.

Dello J., 2013

"Frequency Evaluation of Steam Turbine Bladed Disk"

Dresser-Rand, Wellsville, NY, USA

Castanier M.P., Pierre C., 2006

"Modeling and Analysis of Mistuned Bladed Disk Vibration: Status and Emerging Directions"

Journal of Propulsion and Power 22 No 2 (2006) March-April edition

Rojkov O., 2007

"Strategy for Turbine Blade Solid Meshing using Hypermesh"

Presentation made in Siemens Industrial Turbomachinery AB, Sweden

Analysis User's manual, SIMULIA, 2013

ABAQUS, CAE Tool, Version 6.12

9 APPENDIX A: GUIDELINES IN CREATING MESHES FOR COOLED TURBINES IN HYPERMESH VER12.0 AND MAKING IT COMPATIBLE FOR ABAQUS VER6.12

9.1 Starting with Hypermesh

Before working with Hypermesh, the geometry that has to be imported into Hypermesh has to be checked in NX for any modifications to be updated and the file format that has been saved in NX is UG (Uni-graphics) format.

1. A working directory for the HM files must be created, so that the HM files can be saved in that directory.
2. Right Click in the Desktop > Open terminal > hm12.
3. Hypermesh ver12.0 will open and a dialog box **User Profiles** opens. In that dialog box, In the Application box, **Abaqus** is selected and in the scroll down option in the right will be activated as soon as Abaqus is selected. In the scroll down option, **Standard3D** option is selected.
4. Uncheck the switch **Always show at start-up** and click **Ok**

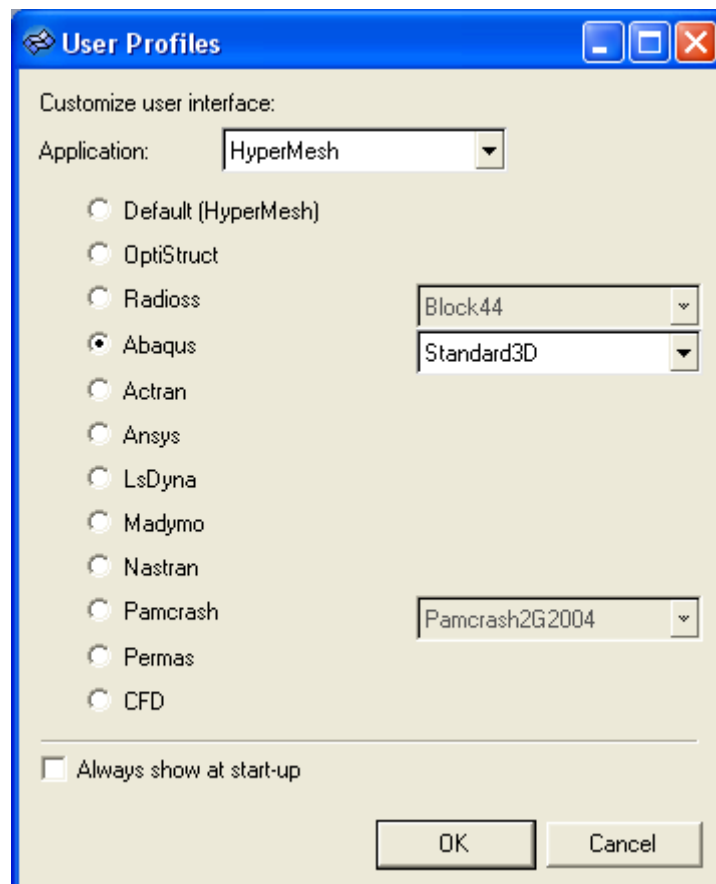


Figure 9.1 User Profile Option at the start up of Hypermesh

9.2 Importing geometry

The simplified geometry to be meshed in Hypermesh is generated in NX. The directory of the geometry is required to import the geometry in to Hypermesh.

1. Open **File** menu > Click **Import** option > Click **Geometry** option.
2. In the **Import** Menu displayed on the left side of the screen, select **UG** in the scroll down menu for file type.
3. Browse for the file to be imported and add it to the file selection box.
4. In the import options box, the **Scale factor** is taken as 1 and **Cleanup tol** menu is selected as **Manual** and the value is 0.01
5. Select the switch option **Use native reader** and click **Import**.

Note: The Cleanup tol option is the cleanup tolerance that is used while importing the UG file into Hypermesh and the units used for the cleaning operation is in millimeters.

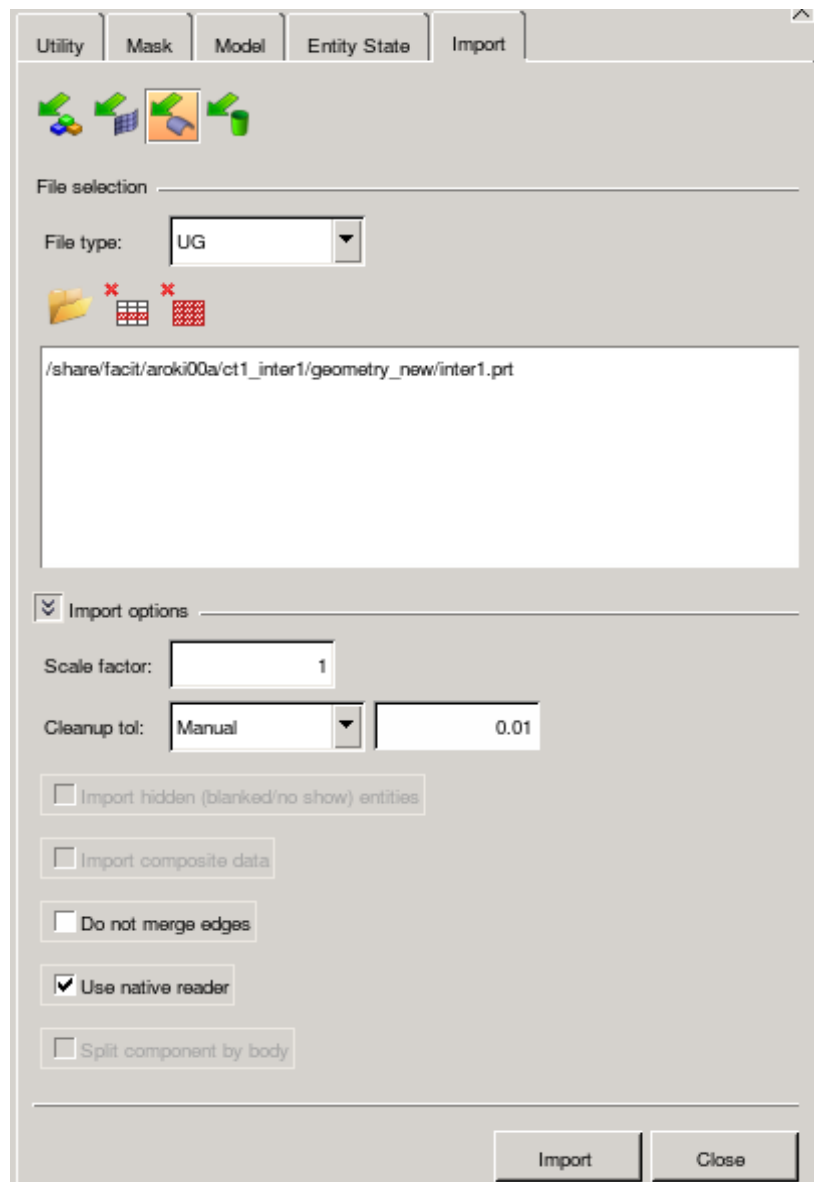


Figure 9.2 Import Menu in Hypermesh

A pop up menu appears after the import button is pressed. In the **UG Part Browser** pop up menu, click **Ok**. Make sure that the **Include invisible geometry** option is unchecked.

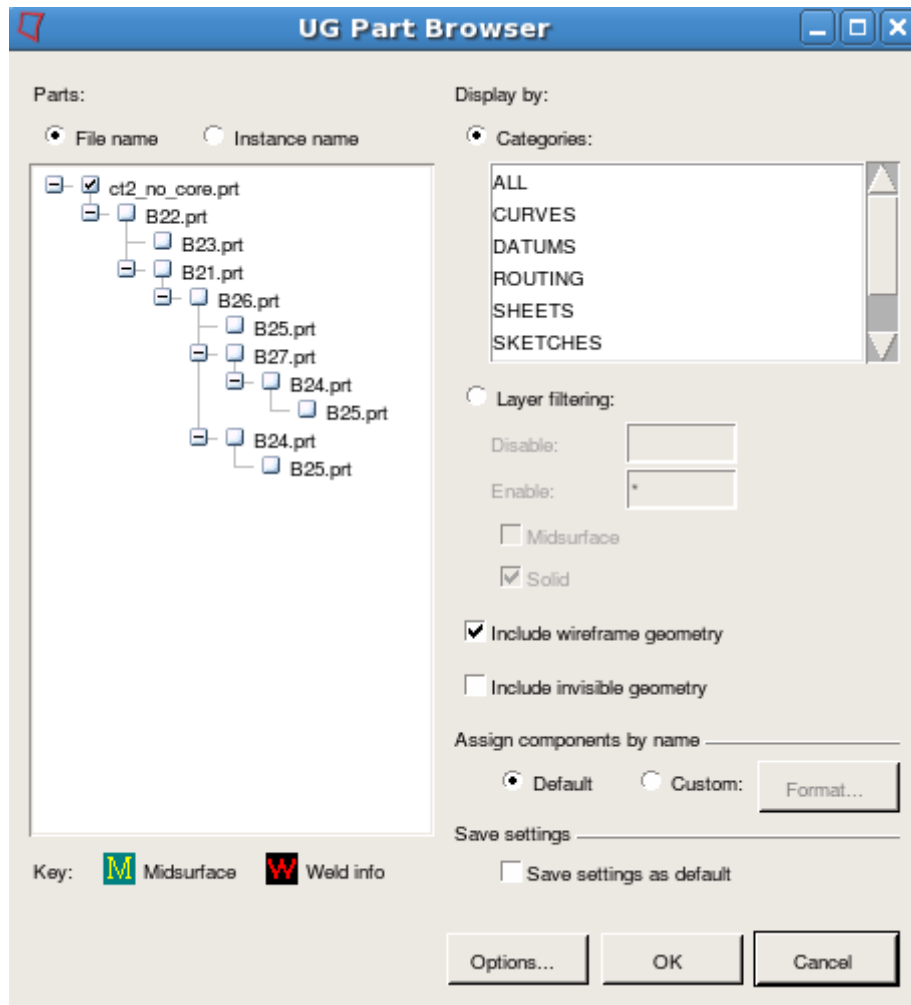


Figure 9.3 UG part browser menu in Hypermesh

9.3 Geometry Cleanup

The Cleaning up of geometry is critical for meshing. If this is not done, then, meshing complex shapes will be difficult and time-consuming.

9.3.1 Suppress unwanted edges

The edges that is not necessary for meshing in the geometry can be suppressed without altering the shape of the geometry.

1. In the lower part of the screen, select **Geom** option.
2. In the Geom option, select the option **Quick edit**.
3. In the Quick edit option , Press the button **line(s)** next to **toggle edge** option. See Figure 9.4 Quick edit option in Hypermesh
4. The edges that have to be suppressed can be selected by left clicking on the edge. In case of releasing an edge, right click on the edge at this option.

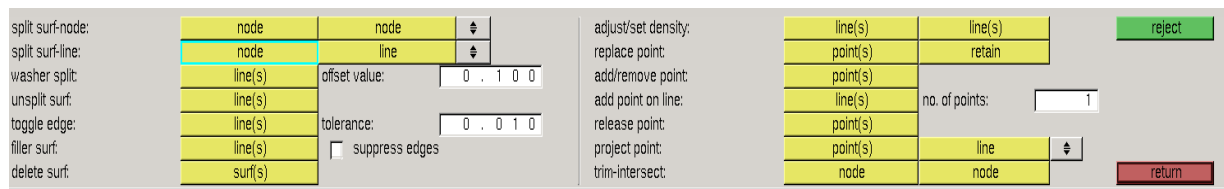


Figure 9.4 Quick edit option in Hypermesh

9.3.2 Removing Fillets in the geometry

The fillets are complex shapes that use a lot of elements in the meshing process. In the case of modal analysis, smaller fillets can usually be removed.

1. In the Geom option, select the **defeature** option.
2. In the defeature menu, select the option **surf fillets**. Now, you click the lines that are surrounding the fillets in the geometry and as all the sides enclosing the fillet are selected. Click **find**. See Figure 9.5 Defeature option in Hypermesh
3. Then, the filleted surface to be removed will be highlighted in white. Click **remove** to remove the fillet.

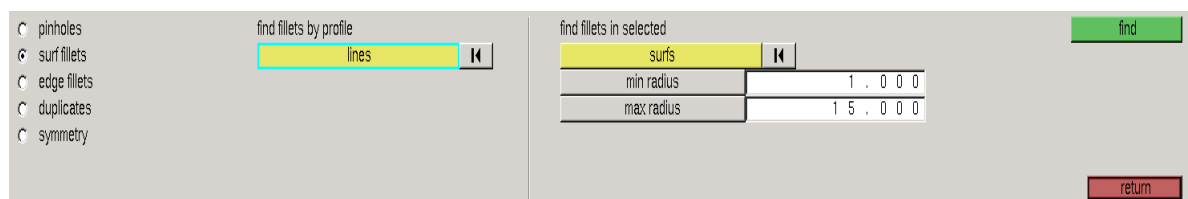


Figure 9.5 Defeature option in Hypermesh

9.3.3 Splitting Surface or Additional trim

Splitting surfaces or trimming surfaces are useful in simplifying geometry and also in creation of components for shell coating meshes. The Additional trim is useful in meshing of cylindrical or tubular components.

1. In the Geom option, select the **Quick edit** option.
2. In the Quick edit menu, **split surf-line** option is used to trim or split surfaces. See Figure 9.4 Quick edit option in Hypermesh
3. The node is used as the starting point for the trimming and a line is selected perpendicular to the trimming surface.
4. Sometimes, **split surf-node** option is used and it uses the node-node definition method to trim a surface.

9.4 Creation of components

The components are necessary for creation of shell coating elements. 3d tetra meshes can be created by two methods:

- Volume tetra method and
- Tetra mesh method.

The Volume tetra method does not require a shell coating mesh, but, requires only an enclosed solid with minimum geometrical complexity.

The tetra mesh method uses an enclosed shell coating mesh to generate tetra meshes within the enclosed shell coating. This method is useful in creating mesh for complex structures.

The shell coating elements can be created only if the volume is closed, in order to create closed volumes for the shell coating elements, new surfaces are created.

9.4.1 Creating Surfaces

Creation of surfaces with common edges is useful for creating and separating components. The **Split surf-line** command is used to trim surfaces.

An example is the creation of the disk surface with creation of a new surface with common edges. New edges that enclose the surface are created with the use of the split surf-line command. **Geom > Surface > Spline-filler** method is used to create the surface and all the edges enclosing the surface are selected. Make sure that the switch **Auto create** is unchecked.

In Figure 9.6 Surface creation in Hypermesh, the right side shows the disk with the surface of common edges.

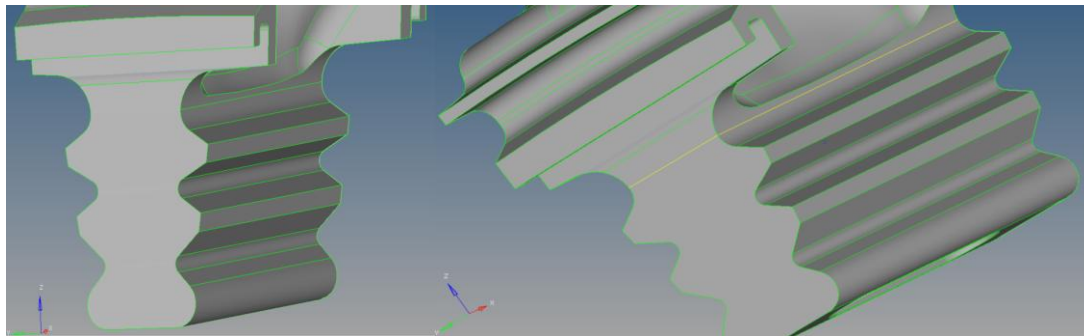


Figure 9.6 Surface creation in Hypermesh

In case of models with a lot of internal surfaces, the **Surface edit** command is useful. Go to **Geom > Surface edit > trim with surfs/plane** option.

9.4.2 Mask / Unmask entities

In order to view or work with the internal surfaces of the model without deleting the outer surface, a masking operation is used. The **Mask** icon on the left side of the screen is pressed and the outer surfaces can be hidden for editing internal surfaces.

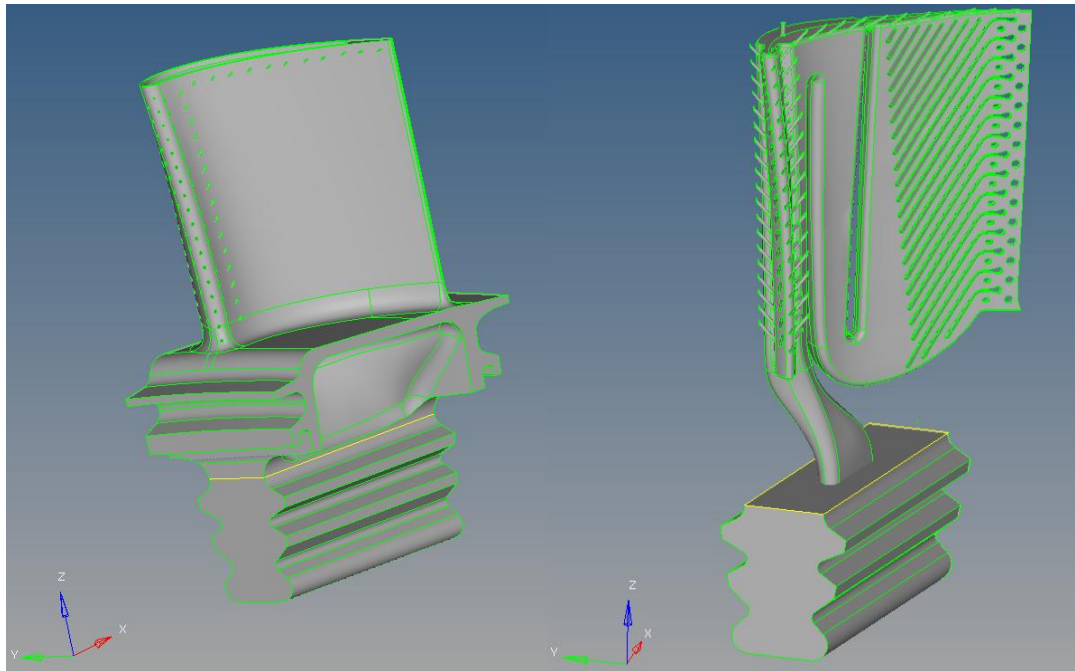


Figure 9.7 Masking entities of a model

In Figure 9.7 Masking entities of a model, the right side has the outer surfaces of the airfoil being masked, to show the internal cooling profile. Now, the trim with surfs/ plane command is used to separate the fir tree part from the rest of the model.

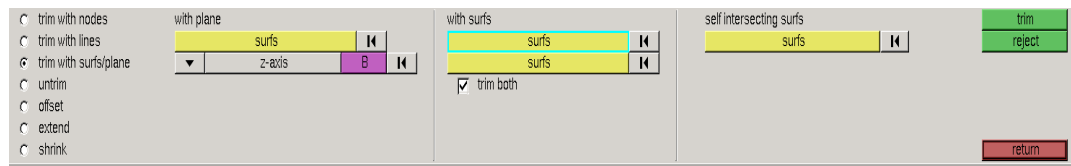


Figure 9.8 Surface edit option in Hypermesh

In Figure 9.8 Surface edit option in Hypermesh, the right side for the trim with surfs/plane, check the switch **trim both** option and select the newly created surface first and then click the surfaces that have to be trimmed in the second option. Click **trim** option and you will get the left side of the Figure 9.9 Component creation in Hypermesh.9

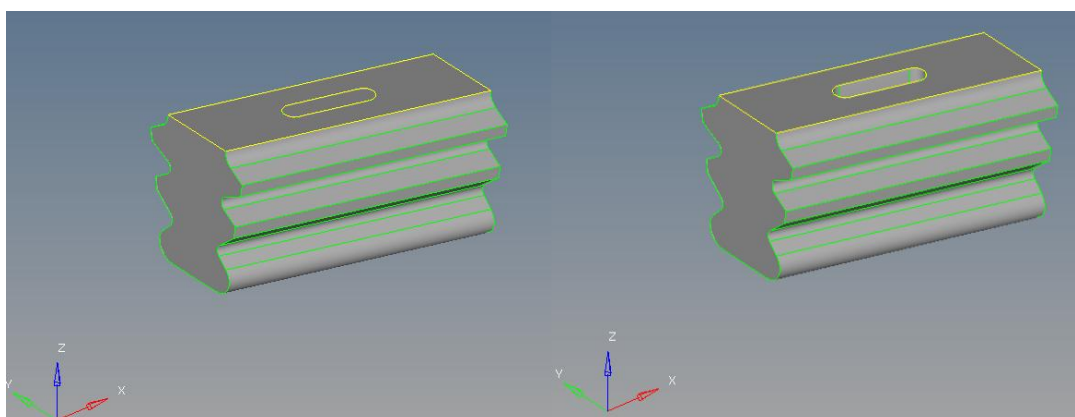


Figure 9.9 Component creation in Hypermesh

In the left side of Figure 9.9 Component creation in Hypermesh, the disk component is created and separated from the rest of the model. But, there is an internal surface that is not necessary and it is deleted by clicking **Geometry > Delete> Surfaces**.

Now, the surfaces that are displayed in Figure 9.8 Surface edit option in Hypermesh have to be moved to a new component and that can be done by going to **Tools > Organize > surfs > displayed > move**. Do not use the option **copy** as it will have this surface retained in the previous component as well.

Note: The components that are created for 2d shell coating meshes should start with “^” symbol so that the component will not be exported to the solver deck files.

9.5 2d Mesh creation

For creating shell coating mesh, **2d** option is selected from the bottom of the screen and then, **automesh** is selected. The automesh dialog box is as in Figure 9.10 Automesh option for 2d mesh in Hypermesh

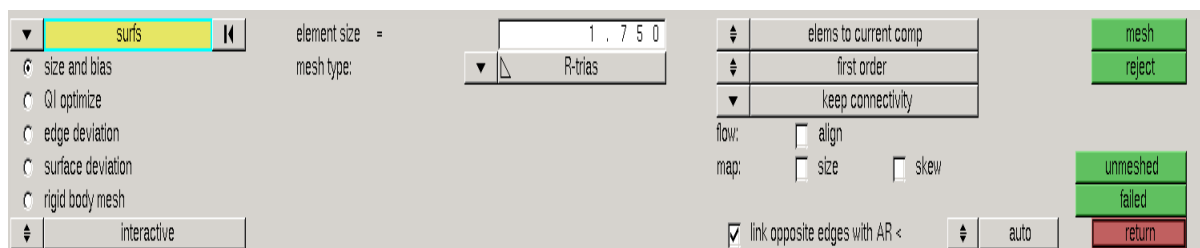


Figure 9.10 Automesh option for 2d mesh in Hypermesh

The above mentioned dialog box contains the different methods of generating shell coating elements. **Size and bias** method is the simplest by denoting the element size and biasing the deviation of the element.

- The size of the element to be generated is specified in the box **element size**.
- **Mesh type** scroll down menu contains the different element types that are available for shell coating elements. **R-trias** is selected to generate good tetra 3d meshes.
- **Elems to current comp** option is used to create the elements for the current selected component. The component can be made current by right clicking on the component available at the **Model** menu on the left side of the screen and selecting **Make current** option.
- **Second order** option is available in the scroll down menu and it is used to create the second order trias or quad elements accordingly with the mid side nodes in the elements.
- **Keep connectivity** option is used to keep connectivity with the neighboring and the connected components to the current component while generating the shell coating elements.
- Make sure that the options **align** , **size** and **skew** are switched off.
- Select the surfaces to be meshed by selecting the **surfs** option and click **mesh** to see the generated mesh for further modifications.

The **interactive** mode of meshing is used to override the automesh feature and provides control over the mesh density, biasing and other parameters while meshing. This is an intermediate phase between the automesh feature and the final mesh. See Figure 9.11 Interactive mesh mode in Hypermesh

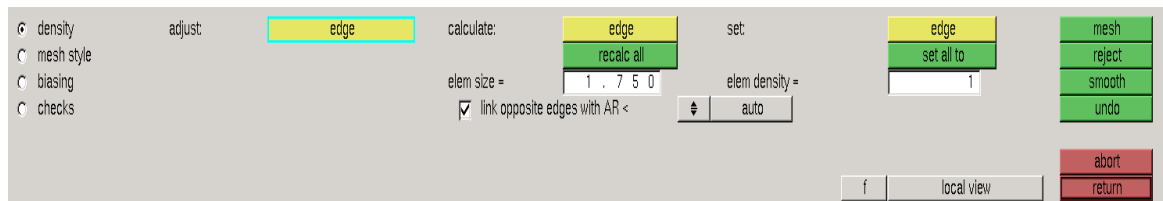


Figure 9.11 Interactive mesh mode in Hypermesh

- **Density** option is used to control the element size of the overall mesh elements as well as the number of elements to be available at each edge. The number of elements in the edge can be increased by left-clicking on the number displayed on each edge and decreased by right-clicking on the number displayed.
- **Mesh style** option is used to change the element type, the mapping of the elements in the mesh. Make sure that the options **skew**, **smoothing**, **size** and **align** options are unchecked.
- **Check** option can be used to do an initial element check of the 2d mesh and adjust the density or the mesh style according to the result of the element check.

9.6 Element Check of 2d mesh

Once the 2d meshes are generated for all the partitions or components in a model, the elements have to undergo a series of element checks, so that, they produce good, consistent 3d tetrahedral elements that are compatible with the Abaqus solver.

9.6.1 Minimum angle check

Go to **Tools > Check elems > 2d** and the **min angle** option is used to display the mesh elements that are below the specified angle. The minimum angle requirement for the Abaqus solver is 10 degrees.

In case of elements that are below the minimum angle requirement, the **save failed** option is used to save the elements that don't fit the criteria. See Figure 9.12 Element check option in Hypermesh

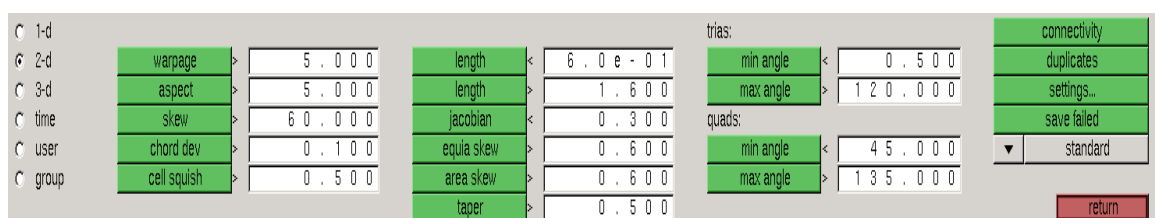


Figure 9.12 Element check option in Hypermesh

- Once the elements are saved, the elements can be displayed by clicking **Mask icon> elems > retrieve > Mask > Reverse**. Delete these elements by clicking **delete > elems > displayed > delete entities**.
- Unmask all the elements and click **tool > edges > comp > displayed** and then click **free edges** option on the right, to visualise the free edges in the model.
- The nodes available in the free edges can be numbered by going in to **tools> numbers > nodes > displayed > on**.

Note: Never use the option **all** for deleting or masking elements for working in the current component, because using the option all will activate even the components that have been hidden.

Shell element can be repaired by using the **edit element, replace** and **split/combine** commands available under the option **2d** in the bottom part of the screen. In Figure 9.13 Replacing node with another node by using replace command, the repairing of elements that are having small minimum angles is done by using the **replace** command to replace the nodes.

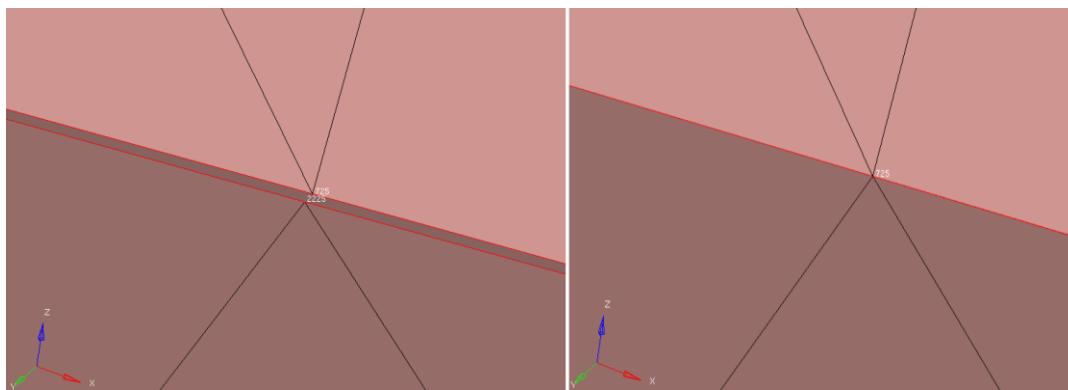


Figure 9.13 Replacing node with another node by using replace command

9.6.2 Free edges

The Model should be checked for free edges every time an operation is made on the elements, because the 3d tetra meshes will not be formed unless the shell coating elements are enclosed. The free edges can be checked by going to **Tools > edges > comps > displayed** and clicking **free edges** on the right side.

The free edges will be highlighted in red colour in the screen and if there are no free edges, then the **^edges** component will not be created on the Model menu. The free edges are formed due to a lot of reasons and some of them are:

- When the edges are released, they form as free edges.
- The overlapping of shell elements in different components.
- The shell elements which are not enclosed will have free edges.

Identify the root cause of the free edges, to eliminate them in a simple way.

9.6.3 Jacobian

The Jacobian of the element is mainly dependent on how skewed the element is. So, if the element satisfies the minimum angle criteria, then, the Jacobian will not be an issue. The Jacobian can be checked by going to **Tools > check elems > 2d > Jacobian** option. For further reference, refer to Figure 9.12 Element check option in Hypermesh

The Jacobian that is required should not be less than 0.5 for it to be compatible with the Abaqus solver.

9.6.4 Penetration

The penetration of the elements is critical in the development of 3d tetra meshes. The presence of penetrated elements in the shell coating elements will not allow the generation of 3d tetra mesh as the meshing process will be stopped due to the input mesh for 3d tetra being self-intersecting.

Go to **Tools > Penetration > elems > displayed** and click **check** on the right side. If there are elements showing intersection or penetration, then, they are formed due to overlapping of shell elements within the component or between two components. In Figure 9.14 Penetration menu in Hypermesh, the intersecting and the penetrating elements will be displayed by left clicking on those options.

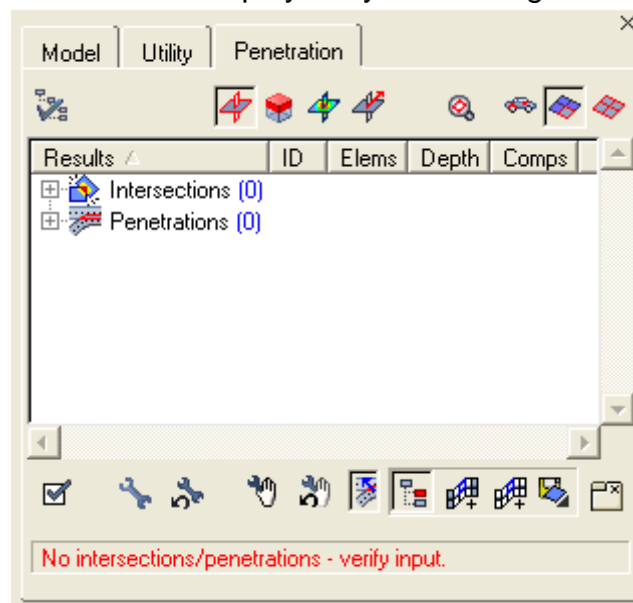


Figure 9.14 Penetration menu in Hypermesh

9.7 Creation of 3d tetra mesh

The 3d tetra mesh is easier when all the 2d shell coating meshes are checked. The partition of the shell coating meshes is used to generate the 3d tetra volume mesh. By clicking **3d > tetramesh > Tetra mesh**

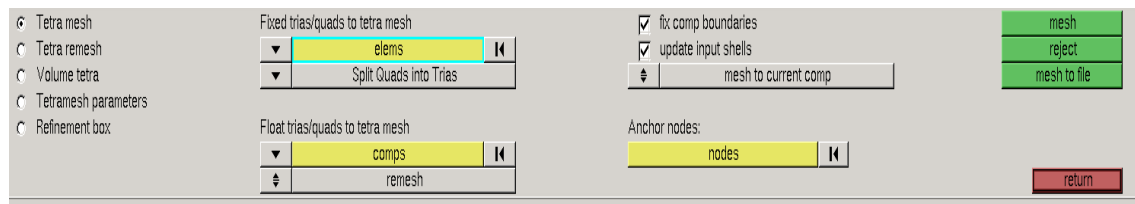


Figure 9.15 tetramesh option in Hypermesh

In Figure 9.15 tetramesh option in Hypermesh, the elems option is used to convert the quad shell mesh into triangular elements and check the switches **fix comp boundaries** and **update input shells**. Click **mesh** to mesh the 3d tetra mesh.

Mesh to current comp option is used to create the 3d tetra elements and save them to the current component.

Note: The common surfaces between partitions should have the elements being included for creating 3d tetra mesh, otherwise the 3d tetra mesh will not be created; exiting with the error **the shell elements are not enclosed**.

9.8 Quality tetra check

Location: **Tool -> check elems -> 3d** menu in the bottom panel.

The most important check, which corresponds to ABAQUS **Quality measure**, is **vol skew**. The ABAQUS value and Hypermesh value are related as

$$\text{vol skew} = 1 - \text{Quality measure}$$

For example, if we want to limit quality measure to 1.E-5 in ABAQUS then HM volume skew is to be set as $1 - 1.E-5 = 0.99999$.

If there are elements that do not fit this criteria, then the elements will be found overlapping each other or having a very small skewed volume almost like a 2d shell coating mesh.

9.9 Creation of Element / Node sets

The element and node sets that are required for loading, boundary conditions and contact interaction are created by going to **Analysis > entity sets**



Figure 9.16 Entity set option in Hypermesh

The entity sets can be created for either elements or nodes and the nodes can be arranged in an orderly or random manner as well.

9.10 Scaling

Scaling down is an important operation to be done as the Model that has been imported into Hypermesh was in millimetres and in Abaqus, all the parameters are considered in SI units and hence, the model has to be scaled down to meters.

Location: **Tools > Scale> elems**

Click on the option **elems** and **displayed** to scale down all the 3d tetra meshes into meters. In Figure 9.17 Scaling option in Hypermesh, the **x scale** , **y scale** and **z scale** values are registered as 0.001 to convert the model from millimetres to meters.

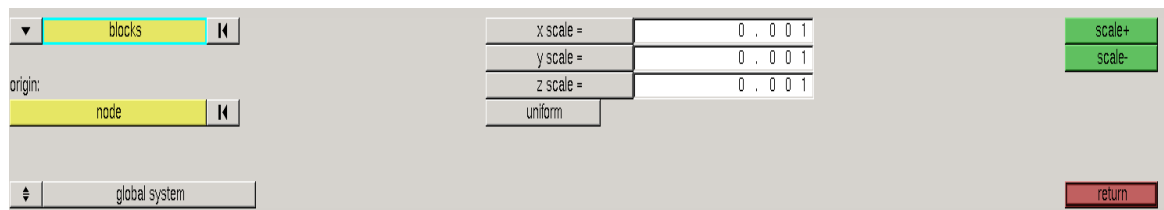


Figure 9.17 Scaling option in Hypermesh

Note: The scaling down operation should be done only when the entity sets and the 3d tetra elements are created. Do not scale down before the entity sets are created.

9.11 Loading Conditions and constraint definition

In the Hypermesh menu bar, since the solver is Abaqus, the preferences are set to Abaqus. In order to change or select the appropriate preferences, go to **Preferences -> User Profile**. In the preferences pop-up menu, select the appropriate solver.

In selecting the initial condition, in this case, the temperature and fixed constraints are used. Since the creation of the element and node sets are already mentioned, the next step will be the generation of the load collectors to incorporate the loadings in the model.

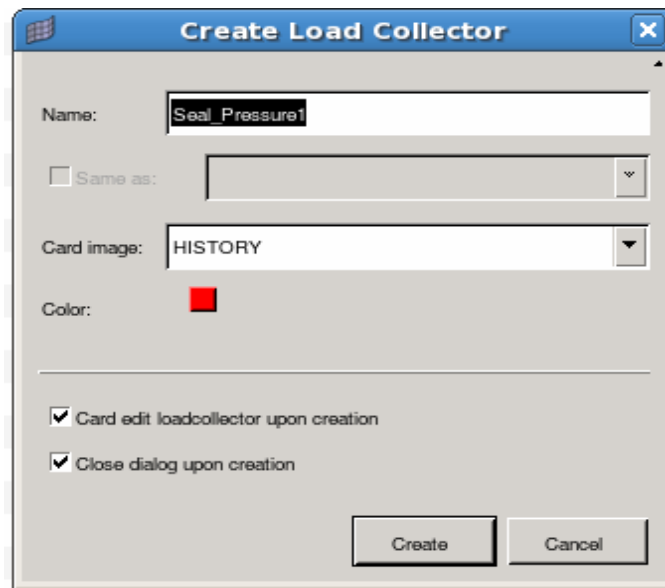


Figure 9.18 Load collector pop up menu in Hypermesh

Create a load collector to which the initial conditions are assigned. Right click in the model browser and go to **Create -> load collector**. The Load collector pop-up menu appears and in that menu, enter a name for the load collector. In the card image scroll down menu, choose initial condition and check options card edit load collector upon creation and close dialog upon creation and finally, click create.

Since the solver is Abaqus in this case, the Load step browser pop up menu is used to control and see the overall load conditions. Go to **Tools -> Load step browser**

In the menu, select initial condition and click edit, to open the initial condition pop up menu. Select boundary on the left hand side of the menu, to create boundaries for the initial condition. The entity set is already created before scaling down. Select the entity set to which the boundary condition is to be applied. In the Boundary condition box, the node sets have to be assigned.

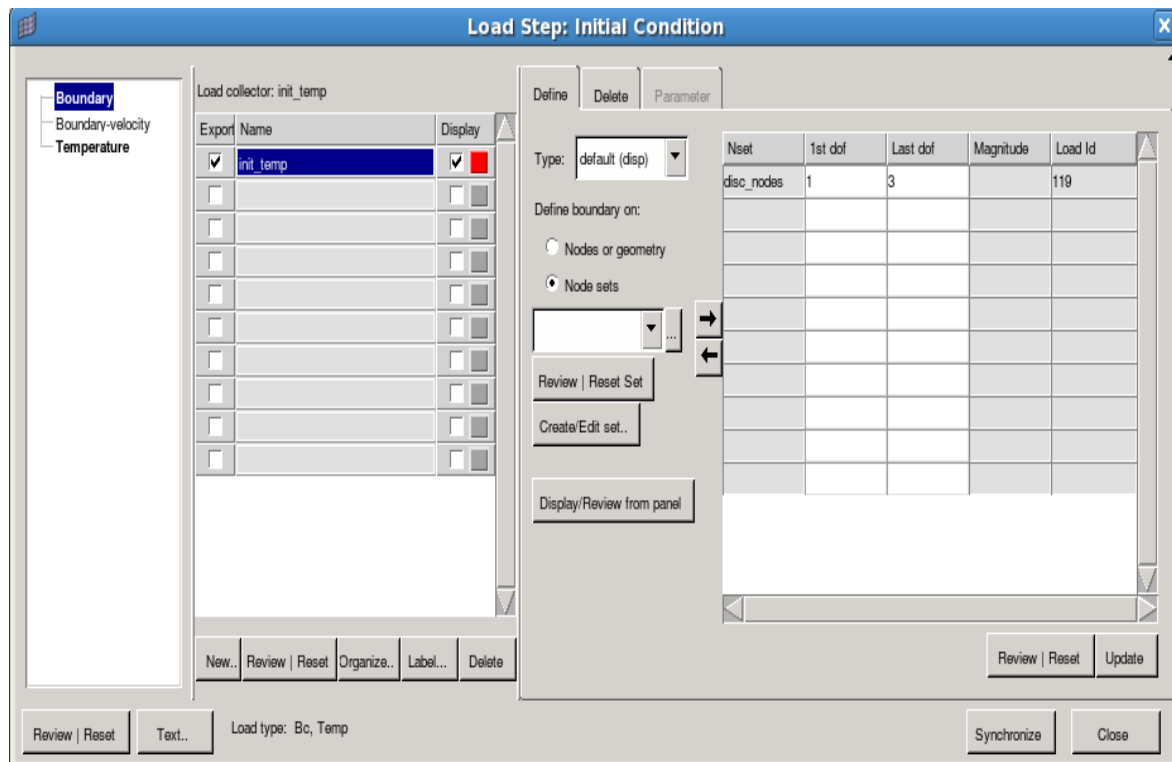


Figure 9.19 Initial conditions browser in Hypermesh

On the right hand side of the initial condition browser, there are columns mentioned as Nset which means the node set to which the boundary has to be assigned. The column 1st dof is used to describe the degree of freedom or the axis that has to be implemented in the boundary condition and the last dof column is to provide the maximum number of axis that has to be involved in that particular boundary condition. For example, in a condition of keeping a particular node set fixed, the 1st dof option will be set to 1 and the last dof option will be set to 3 to suppress motion in all three directions. In the initial conditions, the magnitude is mentioned as zero by default. The load condition is assigned automatically when you click update. In a similar manner, the temperature constraint can be done. Click the temperature option on the left side of the browser. On the right side, define the element sets to which the temperature constraint should be assigned.

The loads that are being implemented in this model are:

- Temperature profile from an output file from Abaqus
- Seal pressure and
- Centrifugal force

9.11.1 Pressure definition

The pressure profile is implemented in the model on the seal region for this case. The direction of the pressure is in the radial direction. First, a load collector has to be created or assigned to have the seal pressure parameters in it. The procedure for creating a load collector is discussed earlier. The only difference is that in the scroll down menu for card image, select history. This option is used to use the load collector for load steps rather than that of the initial condition. Go to **Analysis -> Pressure**.

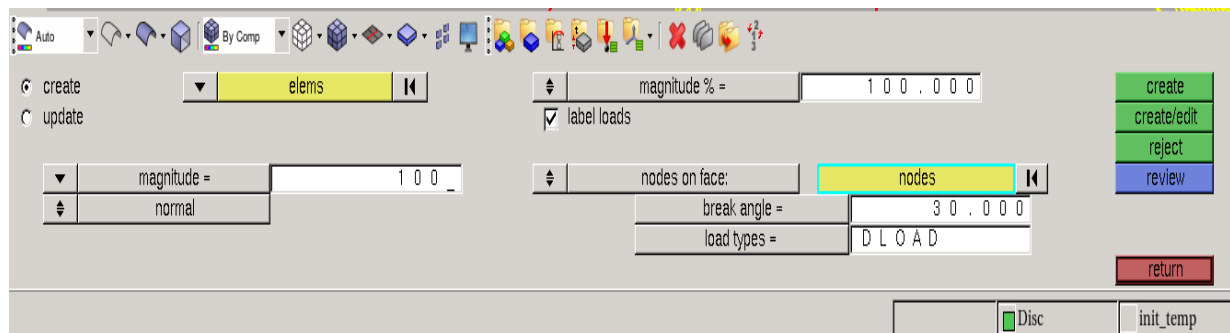


Figure 9.20 Pressure menu browser in Hypermesh

In the pressure menu browser, the elements to which the pressure has to be implemented are to be selected and in the magnitude option, the pressure value is entered. The node on face is the option where the face at which the loading acts is defined and the nodes are selected from the selected elements in such a way that the face is defined properly and precisely. Click on the option 'create' to create the pressure profile.

Note: Once the Pressure is created, it is important to activate the created loading condition into the analysis. It is done by checking the load collector in the load step created in the load step browser.

9.11.2 Centrifugal force definition

The centrifugal force is the force exerted on the model at a particular operating speed. The load collector is created with the card image represented as history. The load step is initially generated before defining the load collector with the loading parameters. For creating a load step, go to Tools -> Load step browser. The load step browser opens and in the name column, click the box below the initial condition and click edit to enter the name of the newly formed load step. In order to edit the parameters in the load step, click the load step and then click edit.

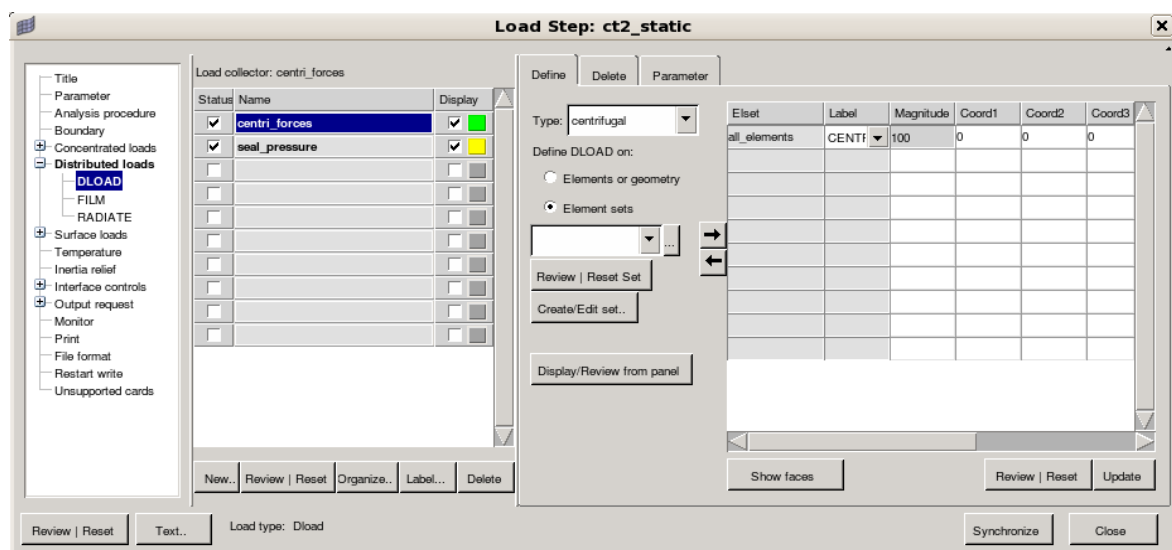


Figure 9.21 Centrifugal loading option in Hypermesh

In the load step browser, the centrifugal loading option is under the DLOAD option of the Abaqus solver. Click on the load collector to which the loading should be implemented and on the right side of the browser, the element set is defined with

the value and the direction at which the loading is implemented on the model. Since the loading is centrifugal, the rotation axis of the model is mentioned with the help of the 'coord' options in the browser and click update to include the loading in to the load step.

9.11.3 Temperature profile definition

The temperature profile definition is easier to implement directly in the input file of the Abaqus solver. The temperature profile is an Abaqus output file in this case. If it is a CFD result, then, another method is used to implement the temperature profile from a CFD result.

Some of the options that have been incorporated in the temperature profile definition are as follows:

- The **interpolate** option is used when the mesh in the output file is different from the present model.
- The **absolute exterior tolerance** option is used in relation to the interpolate option and set this parameter equal to the absolute value (given in the units used in the model) by which nodes of the current model may lie outside the region of the model in the output database specified by the FILE parameter'
- The word FILE is used to define the path of the temperature profile that is used in the model.

Note: The Temperature profile is included in the model by following the syntax of the example below. The asterisk symbol is used to indicate any input parameter in the model which is compatible to the Abaqus solver.

```
*TEMPERATURE, FILE =mgtxCT2_stat,INTERPOLATE,ABSOLUTE EXTERIOR  
TOLERANCE=0.02
```

9.12 Exporting to Abaqus

The model generated is transferred as an Abaqus input file. Ensure that all the parameters and components that have to be included in the solver deck are active. Go to **File-> Export-> Solver deck**

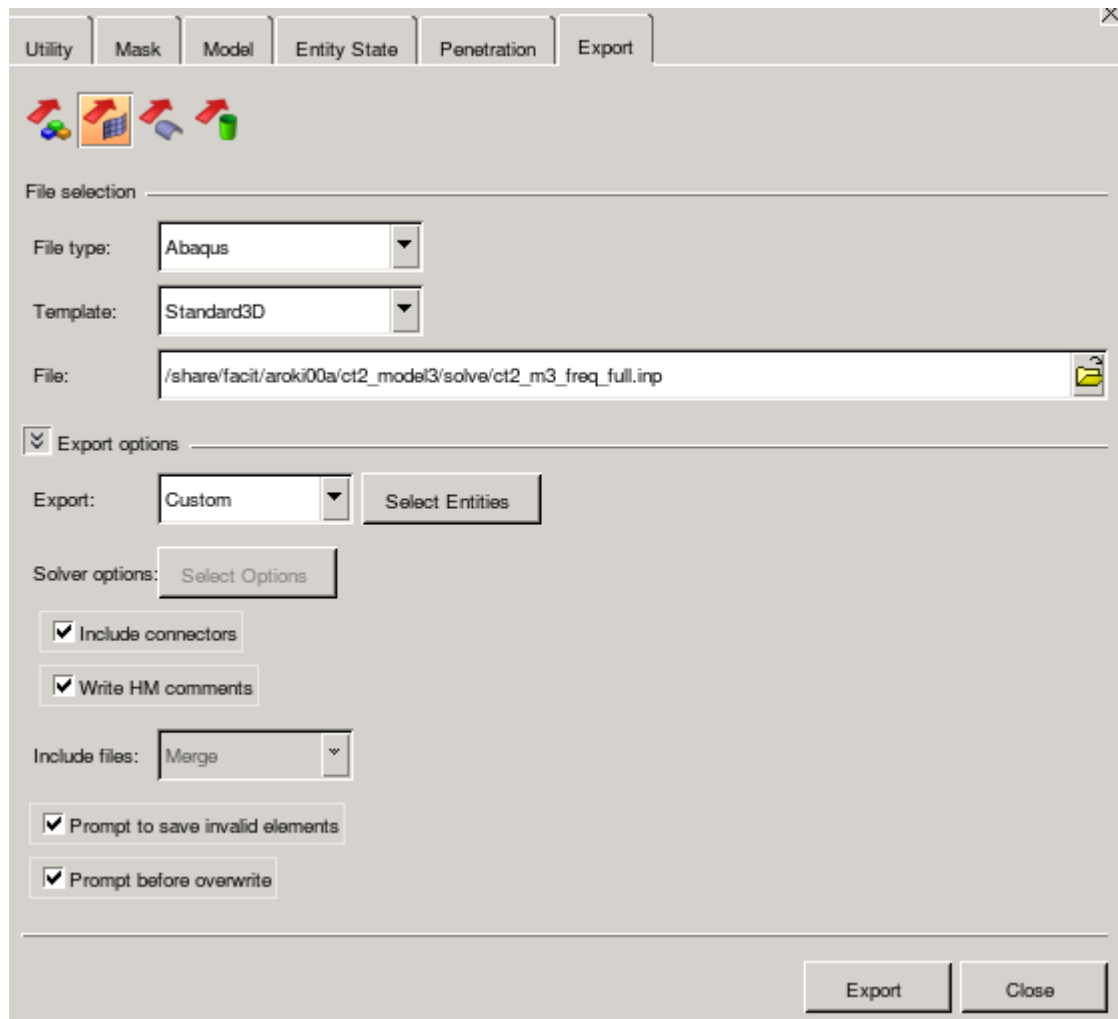


Figure 9.22 Export browser in Hypermesh

In the Solver deck browser, Select the file type scroll down menu as Abaqus and the template is Standard 3d and the path of the file is defined in the file scroll down menu and the export options are opened to view more options. The input file can be customized by selecting the custom option in the export scroll down option. Then, the entities that are required to be exported are kept active in the entity browser. Check all the options mentioned below which are include connectors, Write HM comments, Prompt to save invalid elements and Prompt before overwrite. Click export to export the solver deck into the mentioned path and the file extension will be .inp in the case of the above mentioned example.

10 APPENDIX B: RESULTS OF MESH SENSITIVITY ANALYSIS

10.1 Mode 2 – Root Optimization

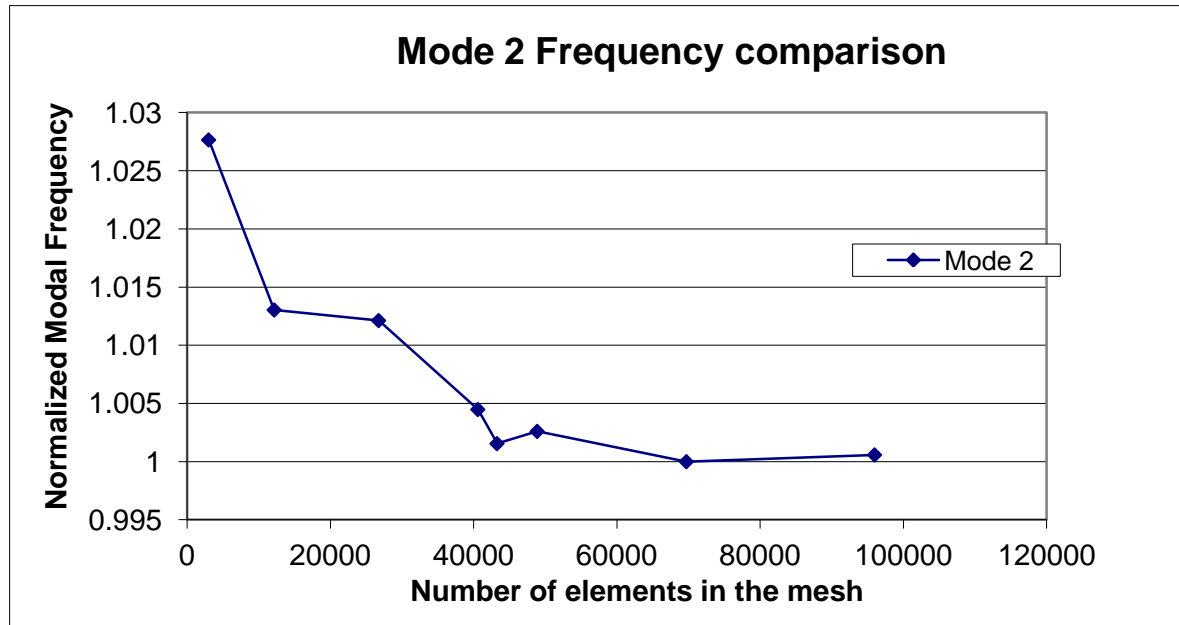


Figure 10.1 Mode 2 root optimization process

10.2 Mode 3 – Root Optimization

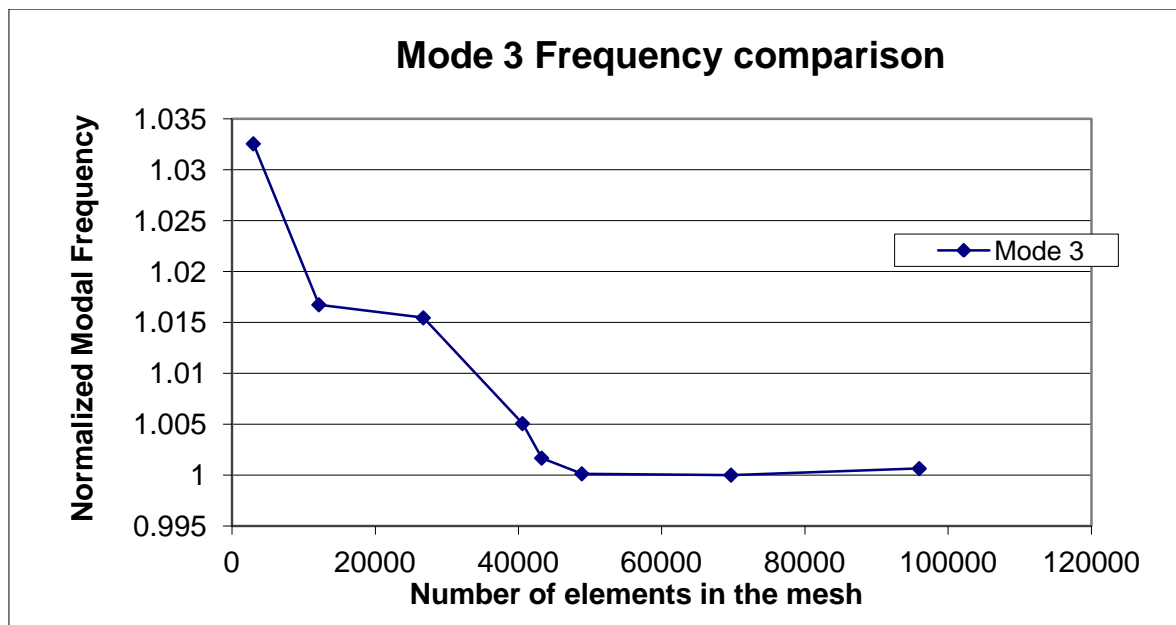


Figure 10.2 Mode 3 root optimization process

10.3 Mode 4 – Root Optimization

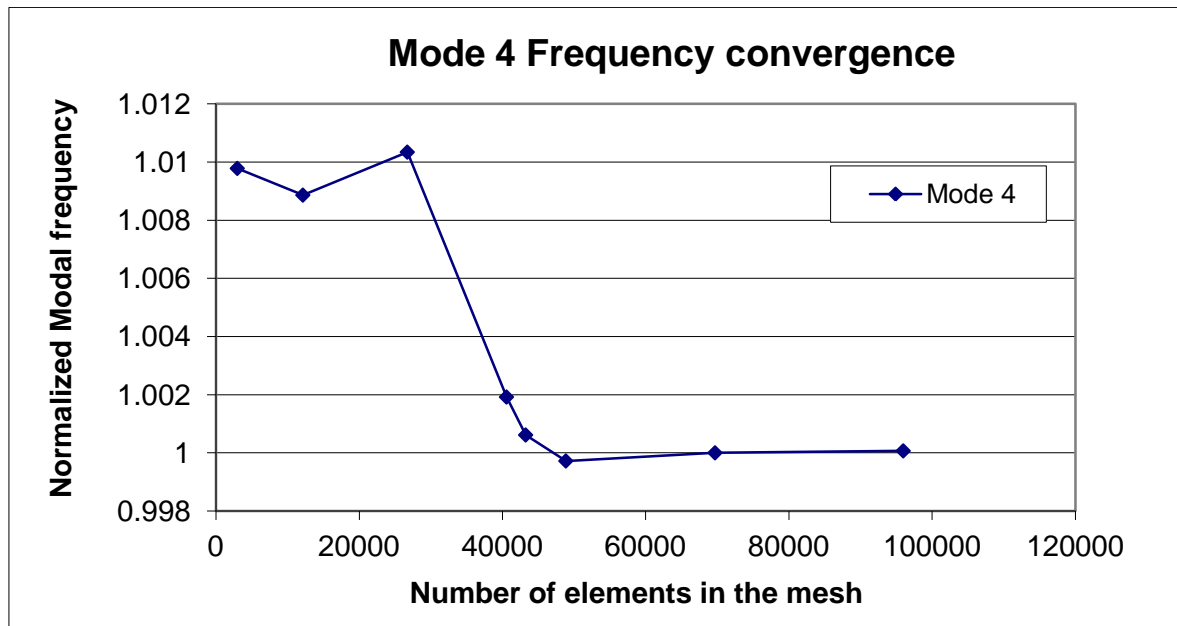


Figure 10.3 Mode 4 root optimization process

10.4 Mode 5 - Root Optimization

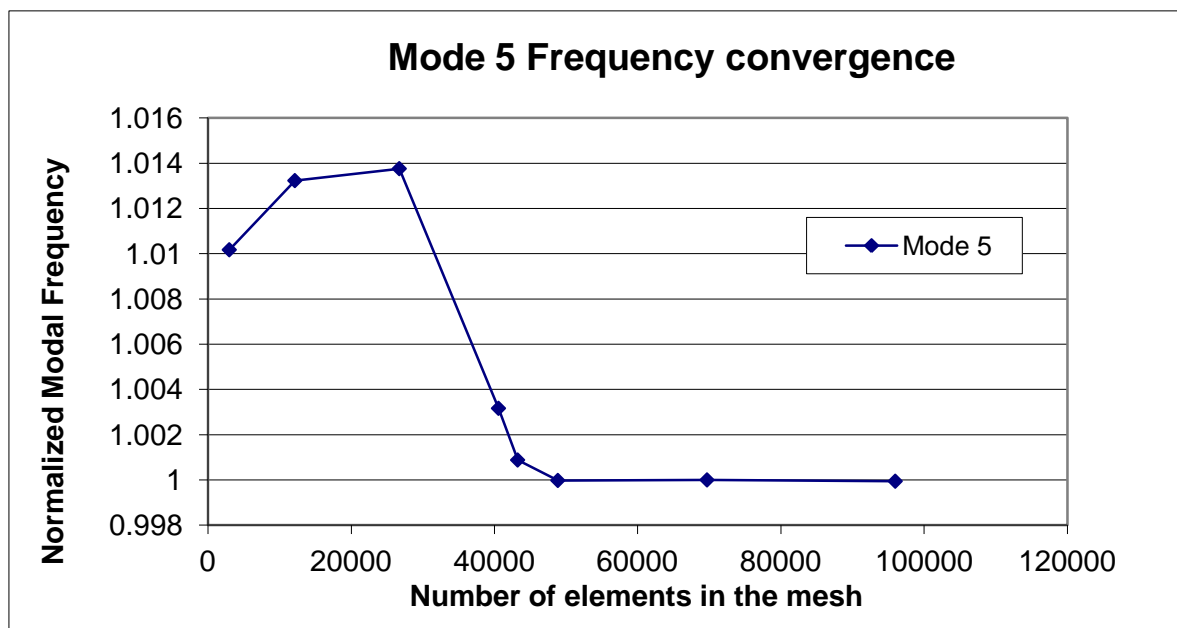


Figure 10.4 Mode 5 root optimization process

Dept of Energy Technology
Div of Heat and Power Technology
Royal Institute of Technology



SE-100 44 Stockholm, Sweden